Supporting Information for:

Supramolecular Control of Azobenzene Switching on Nanoparticles

Zonglin Chu,[†] Yanxiao Han,[‡] Tong Bian,[†] Soumen De,[†] Petr Král,[‡,§] and Rafal Klajn*[,†]

[†]Department of Organic Chemistry, Weizmann Institute of Science, Rehovot 76100, Israel

[‡]Department of Chemistry, University of Illinois at Chicago, Chicago, IL 60607, USA

[§]Department of Physics, Department of Biopharmaceutical Sciences, University of Illinois at Chicago, Chicago, IL 60607, USA

Table of contents

1. Materials and methods

All chemicals were of analytical grade and were used as received. ^{1}H and ^{13}C NMR spectra were recorded on a Bruker Avance III 400 MHz or a Bruker Avance III HD 500 MHz NMR spectrometer. Chemical shifts (δ) in the ^{1}H NMR spectra are reported in parts per million (ppm) downfield from TMS (0.00 ppm) or relative to residual solvent resonances (3.31 ppm for methanol-d_4, 7.26 ppm for $CDCl_3$, 2.05 ppm for acetone-d_6, 4.79 ppm for D_2O, and 2.50 ppm for DMSO-d_6). Multiplicities in the ^{1}H NMR spectra are reported as "s" (singlet), "d" (doublet), "t" (triplet), and "m" (multiplet). Chemical shifts (δ) in the ^{13}C NMR spectra are reported in ppm relative to TMS (0.00 ppm) or relative to residual solvent resonances (49.00 ppm for methanol-d_4, 77.16 ppm for $CDCl_3$, 29.84 ppm for acetone-d_6, and 39.52 ppm for DMSO-d_6). Electrospray ionization mass spectrometry (ESI-MS) measurements were carried out on a Waters Micromass Q-TOF spectrometer. Transmission electron microscopy (TEM) was performed on a JEOL JEM-2100 microscope operating at 200 kV. UV/Vis absorption spectra were recorded with a Shimadzu UV-2700 spectrophotometer. Free-radical thioacetylation reactions were carried out using an LZC-ORG photoreactor (Luzchem Research, Inc.) equipped with eight UVB lamps (wavelength range 280–315 nm; total intensity ~1 $mW \cdot cm^{-2}$). For photoirradiation experiments, a 365 nm UVP UVGL-25 lamp (light intensity ~0.7 $mW \cdot cm^{-2}$) and a Prizmatix Mic-LED 460 nm LED (collimated LED power of ~215 mW) were used as the UV and blue light sources, respectively.

2. Synthesis and characterization of thiolated azobenzenes **A1**–**A6**

2.1. Thiolated azobenzene **A1**

11-(4-(phenyldiazenyl)phenoxy)undecane-1-thiol (**A1**) was synthesized based on a previously reported literature procedure.[1]

2.2. Thiolated azobenzene **A2**

3-(2-(2-(2-(4-(phenyldiazenyl)phenoxy)ethoxy)ethoxy)ethoxy)propane-1-thiol (**A2**) was synthesized based on a previously reported literature procedure.[2]

2.3. Thiolated azobenzene **A3**

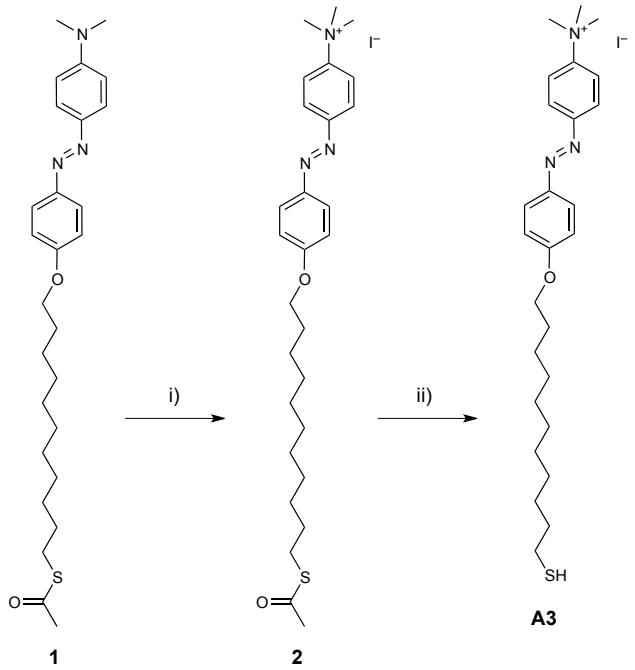

Scheme S1. Synthetic route for ligand **A3**. Reagents and conditions: i) CH_3I, 50 ºC, 4 d, quantitative; ii) HCl/MeOH, reflux, 6 h, quantitative.

***S*-(11-(4-((4-(dimethylamino)phenyl)diazenyl)phenoxy)undecyl) ethanethioate** (**1**) was synthesized based on a previously reported literature procedure.[3]

4-((4-((11-(acetylthio)undecyl)oxy)phenyl)diazenyl)-*N,N,N*-trimethylbenzenaminium iodide (**2**): Methyl iodide (1.5 mL; 3.42 g; 24.1 mmol) was mixed with **1** (85.0 mg; 0.18 mmol) and the mixture was refluxed (50 ºC) for 4 days. Then, the residual methyl iodide was evaporated *in vacuo* and the residue was triturated with diethyl ether to afford **2** in a quantitative yield.

^{1}H NMR (500 MHz, methanol-d_4): δ = 8.11–8.07 (m, 4H), 7.97–7.95 (m, 2H), 7.11–7.09 (t, 2H), 4.11 (t, 2H), 3.74 (s, 9H), 2.86 (t, 2H), 2.29 (s, 3H), 1.86–1.80 (m, 2H), 1.58–1.48 (m, 4H), 1.37–1.32 (m, 12H). **^{13}C NMR** (100 MHz, methanol-d_4): δ = 197.63, 164.35, 154.53, 149.07, 147.96, 126.42, 125.00, 122.40, 116.07, 69.59, 57.84, 30.75, 30.62, 30.55, 30.54, 30.49, 30.41, 30.25, 30.18, 29.85, 29.78, 27.07. **HRMS** calcd for $C_{28}H_{42}N_3O_2S$ $[M - I]^+$, m/z = 484.2998; found, 484.2998.

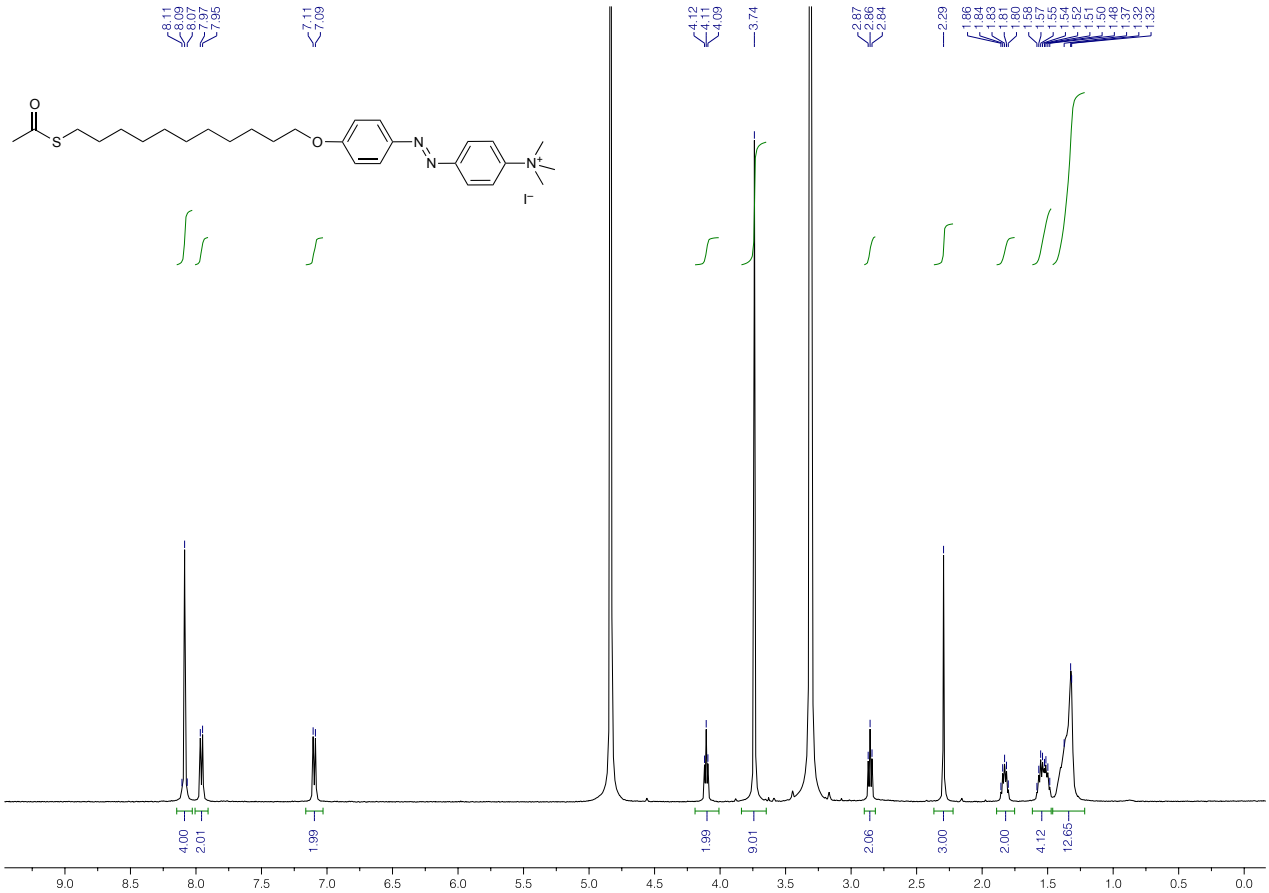

Figure S1. ^{1}H NMR spectrum of **2** (500 MHz, methanol-d_4).

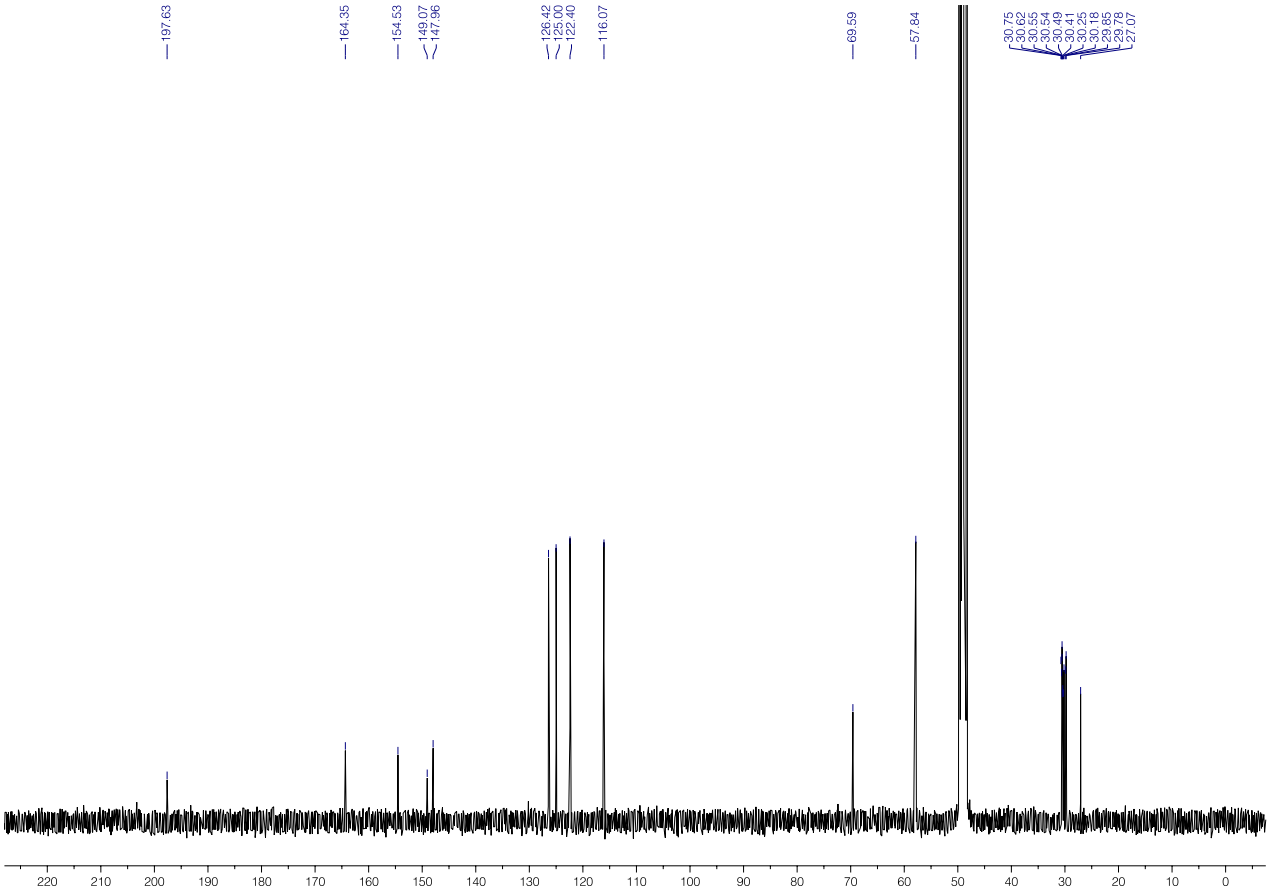

Figure S2. ^{13}C NMR spectrum of **2** (100 MHz, methanol-d_4).

4-((4-((11-mercaptoundecyl)oxy)phenyl)diazenyl)-*N*,*N*,*N*-trimethylbenzenaminium iodide (**A3**): Compound **2** (61.2 mg; 0.1 mmol) was placed in a Schlenk flask equipped with a magnetic stirring bar and a reflux condenser. The flask was purged with nitrogen and charged with degassed methanol (2.0 mL), followed by 50 µL of 1.25 M HCl solution in methanol. The resulting mixture was refluxed for 6 h. Then, the reaction mixture was cooled down to room temperature and the solvent was evaporated *in vacuo* to afford **A3** in a quantitative yield.

^{1}H NMR (500 MHz, methanol-d_4): δ = 8.12–8.06 (m, 2H), 7.97–7.84 (m, 2H), 7.31–7.23 (m, 2H), 7.11–7.03 (m, 2H), 4.11–3.98 (m, 2H), 3.74–3.63 (m, 9H), 2.68 (t, 2H), 1.86–1.74 (m, 2H), 1.71–1.64 (m, 2H), 1.51–1.33 (m, 14H). **^{13}C NMR** (125 MHz, methanol-d_4): δ = 164.33, 154.51, 149.10, 147.97, 126.42, 125.01, 122.43, 116.06, 69.59, 57.85, 39.81, 30.63, 30.60, 30.57, 30.50, 30.44, 30.27, 30.19, 29.41, 27.10. **HRMS** calcd for $C_{26}H_{40}N_3OS$ $[M - I]^+$, m/z = 442.2892; found, 442.2884.

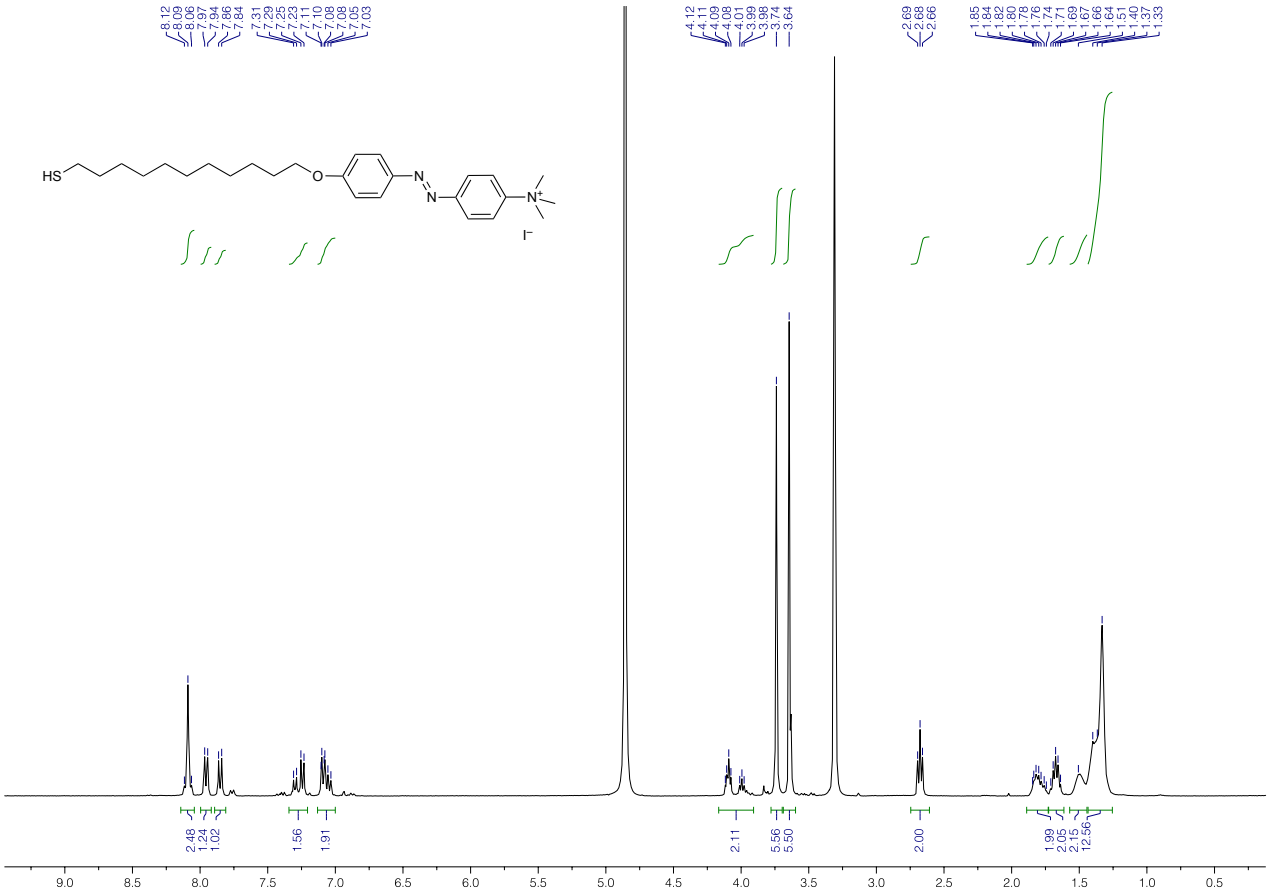

Figure S3. ^{1}H NMR spectrum of **A3** (500 MHz, methanol-d_4).

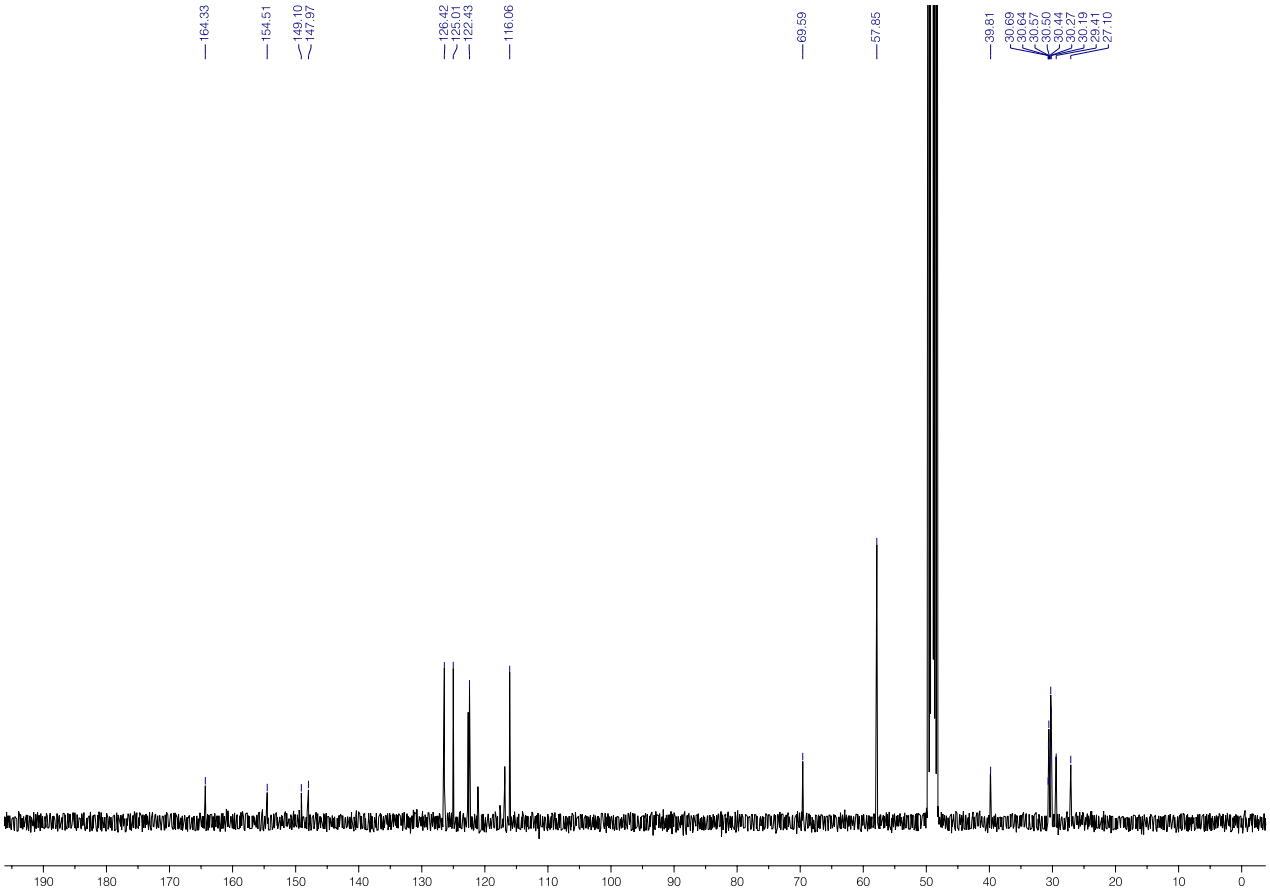

Figure S4. ^{13}C NMR spectrum of **A3** (125 MHz, methanol-d_4).

2.4. Thiolated azobenzene **A4**

3-(4-(phenyldiazenyl)phenoxy)propane-1-thiol (**A4**) was synthesized based on a previously reported literature procedure.[2]

2.5. Thiolated azobenzene **A5**

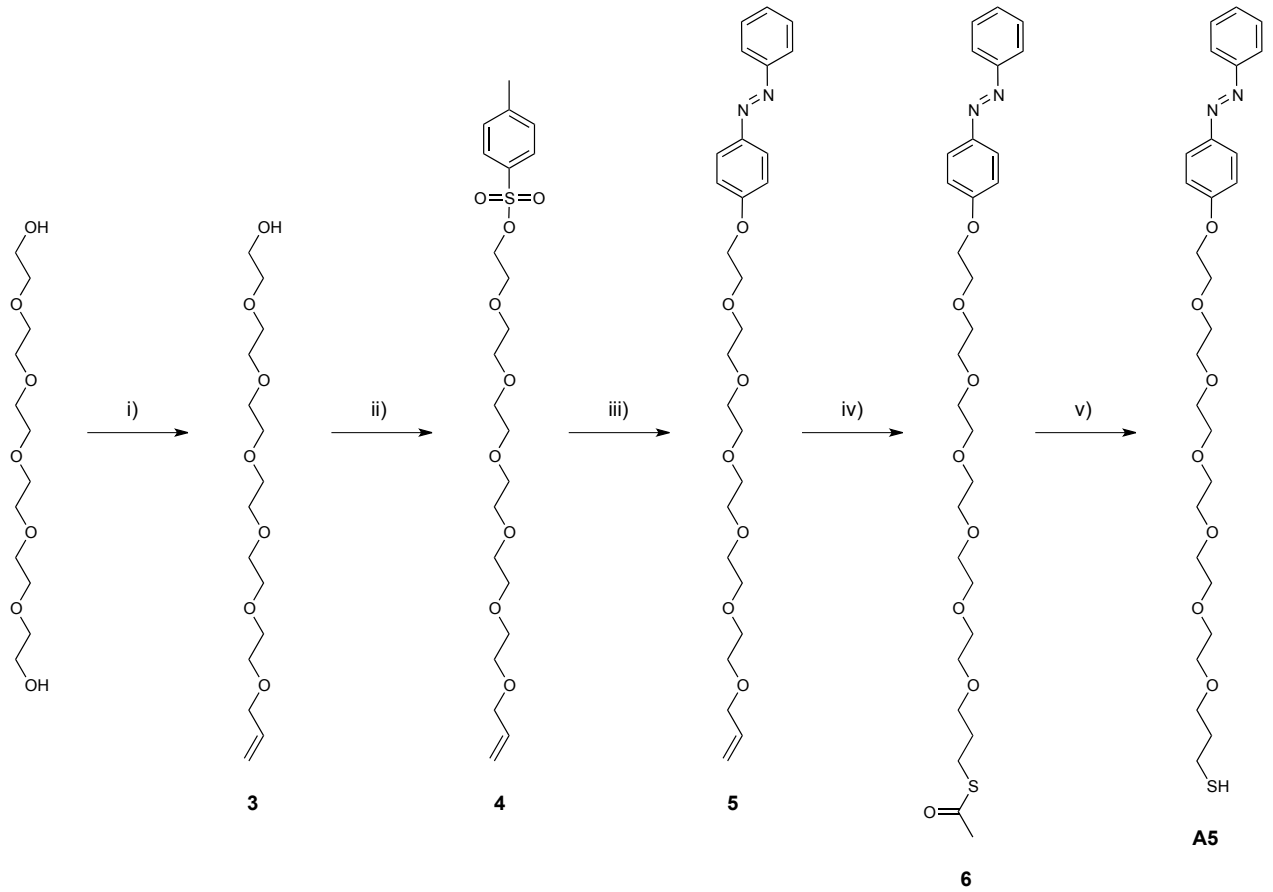

Scheme S2. Synthetic route for ligand **A5**. Reagents and conditions: i) NaOH/H_2O, allyl bromide, 100 ºC, 15 min, 82%; ii) Et_3N, TsCl, DCM, RT, overnight, 88%; iii) ^{t}BuOK, 4-hydroxyazobenzene, THF, reflux, overnight, 90%; iv) AIBN, CH_3COSH, toluene, reflux, 6 h, 84%; v) HCl/MeOH, reflux, 2 h, quantitative.

3,6,9,12,15,18-hexaoxahenicos-20-en-1-ol (**3**): Hexaethylene glycol (11.60 g; 41.09 mmol) was mixed with a solution of NaOH (0.44 g; 11.00 mmol) in water (0.5 mL). The solution was stirred at 100 ºC for 30 min, followed by the addition of allyl bromide (1.21 g; 10.00 mmol). After 15 min, the reaction mixture was cooled to room temperature and 100 mL of CH_2Cl_2 was added. The organic phase was washed with brine (70 mL × 5), dried over $MgSO_4$, filtered, and concentrated *in vacuo* to afford 2.65 g of **3** (yield = 82%).

^{1}H NMR (400 MHz, $CDCl_3$): δ = 5.96–5.87 (m, 1H), 5.30–5.16 (m, 2H), 4.03–4.01 (m, 2H), 3.74–3.72 (m, 2H), 3.68–3.65 (m, 18H), 3.623.59 (m, 4H). **^{13}C NMR** (100 MHz, $CDCl_3$): δ = 134.92, 117.26, 72.70, 72.39, 70.95, 70.77, 70.68, 70.46, 69.57, 61.90.

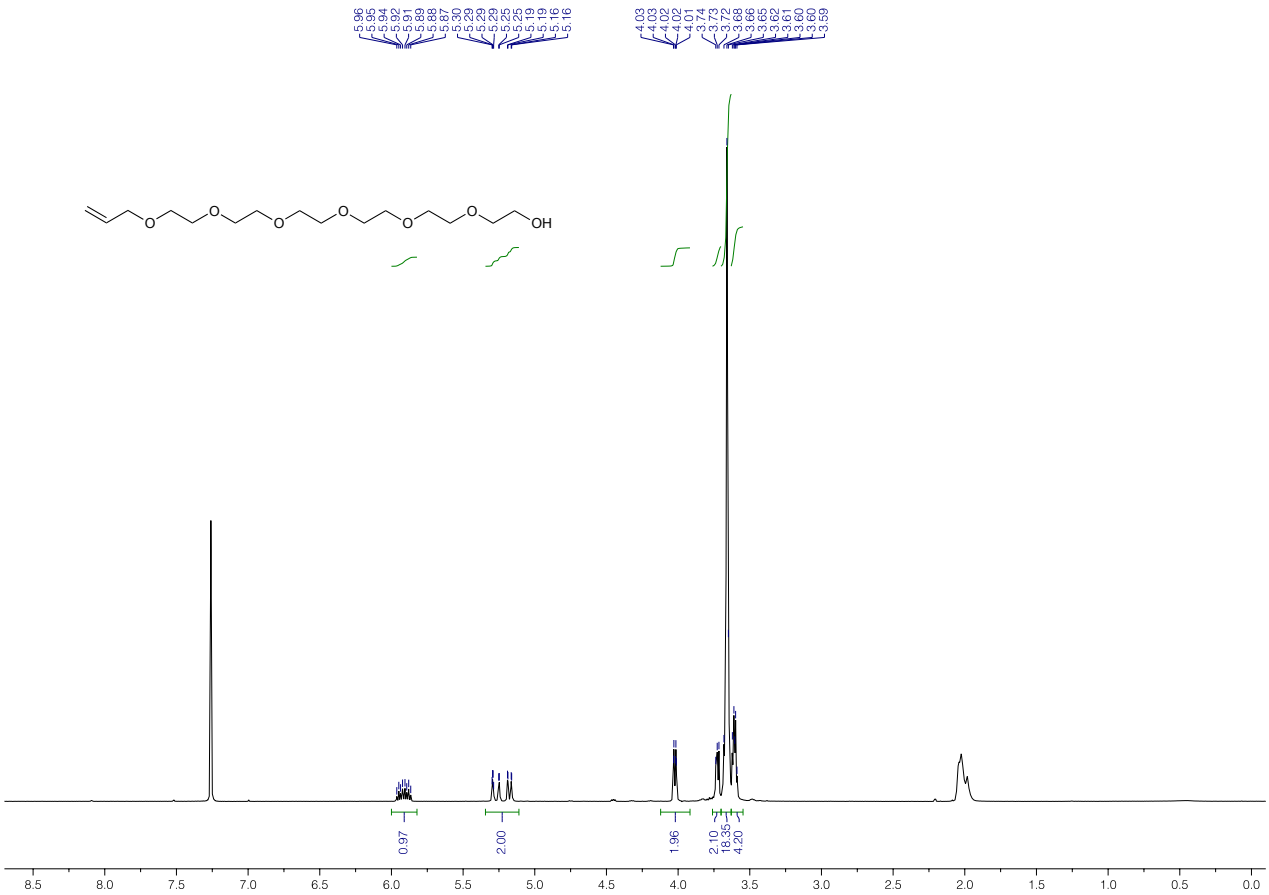

Figure S5. ^{1}H NMR spectrum of **3** (400 MHz, $CDCl_3$).

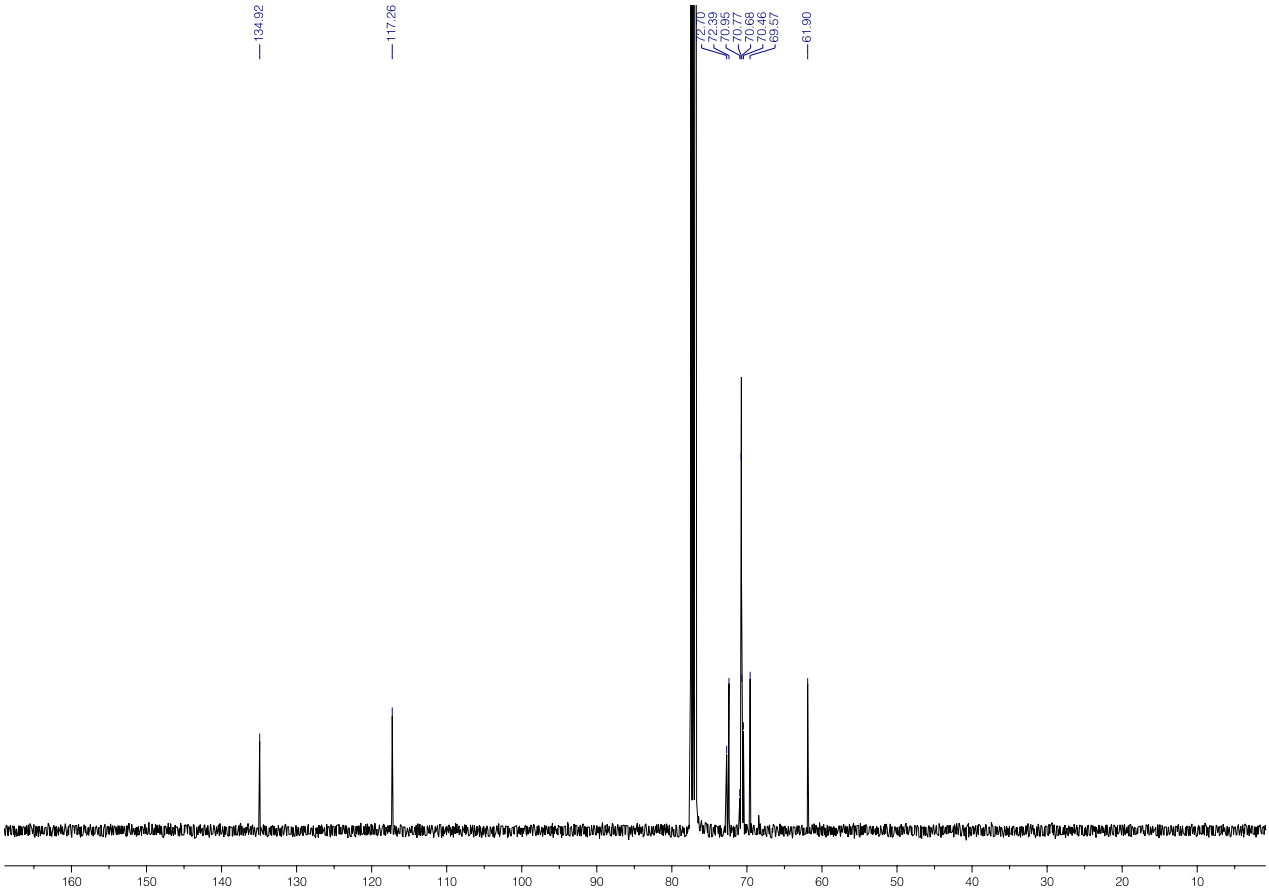

Figure S6. ^{13}C NMR spectrum of **3** (100 MHz, $CDCl_3$).

3,6,9,12,15,18-hexaoxahenicos-20-en-1-yl 4-methylbenzenesulfonate (**4**): To a stirred solution of **3** (2.48 g; 7.69 mmol) in DCM (25 mL) containing Et_3N (1.93 mL; 1.40 g; 13.85 mmol) was added dropwise a solution of TsCl (1.76 g; 9.23 mmol) in DCM (20 mL) at 0 ºC. The reaction mixture was stirred at room temperature overnight. Then, 100 mL of statured $NaHCO_3$ solution in water was added. The crude product was extracted with DCM (100 mL) and the organic layer was washed with brine (100 mL × 4). The organic phase was dried over $MgSO_4$ and concentrated *in vacuo*. The crude product was purified by silica gel column chromatography (eluent: from $CHCl_3$ to EtOAc/MeOH = 9/1) to afford 3.21 g of **4** (yield = 88%).

^{1}H NMR (400 MHz, $CDCl_3$): δ = 7.80–7.78 (d, 2H), 7.35–7.33 (d, 2H), 5.96–5.86 (m, 1H), 5.29–5.16 (m, 2H), 4.15 (t, 2H), 4.02–4.01 (d, 2H), 3.69–3.58 (m, 22H), 2.44 (s, 3H). **^{13}C NMR** (100 MHz, $CDCl_3$): δ = 144.91, 134.90, 133.16, 129.95, 128.12, 117.24, 72.38, 70.89, 70.76, 70.72, 70.70, 70.66, 69.57, 69.37, 68.83, 27.79.

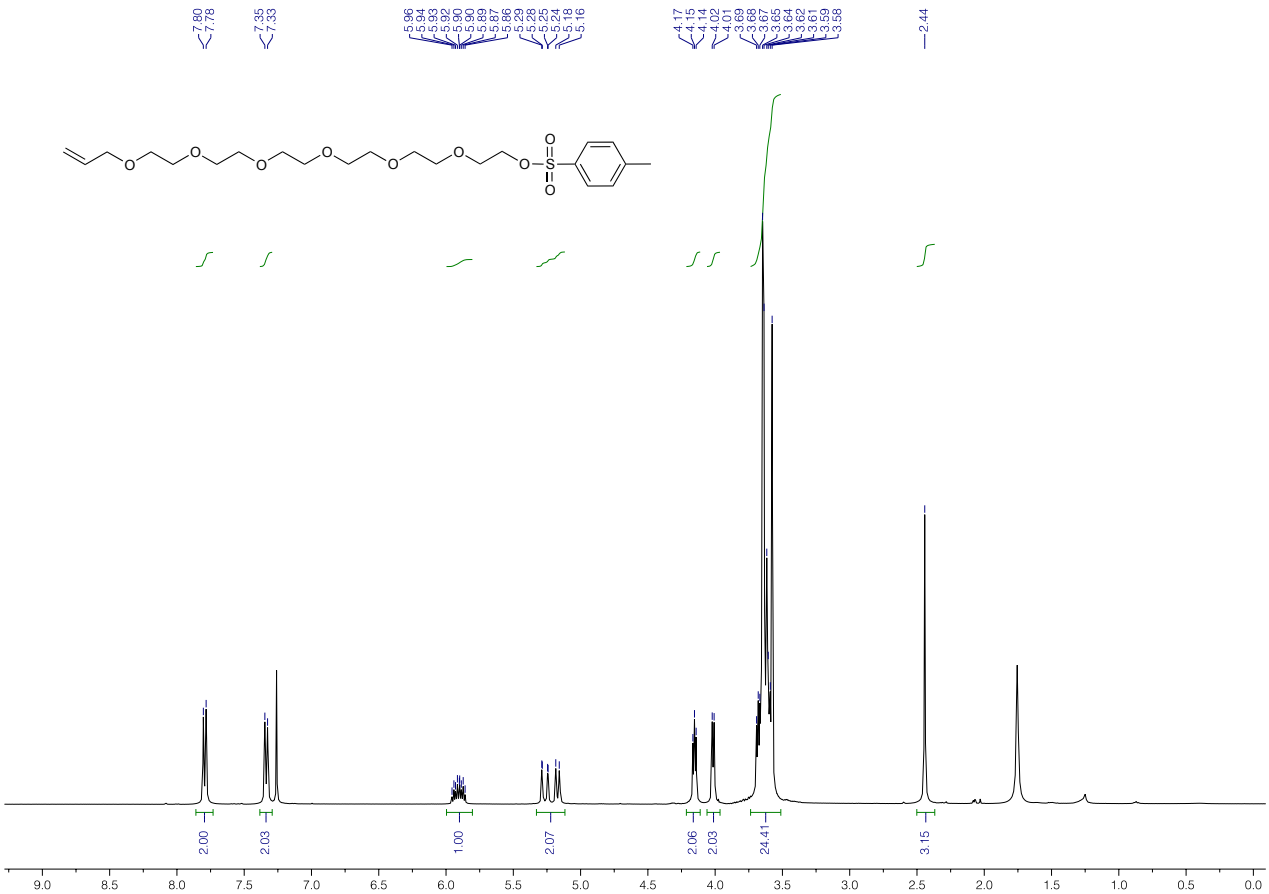

Figure S7. ^{1}H NMR spectrum of **4** (400 MHz, $CDCl_3$).

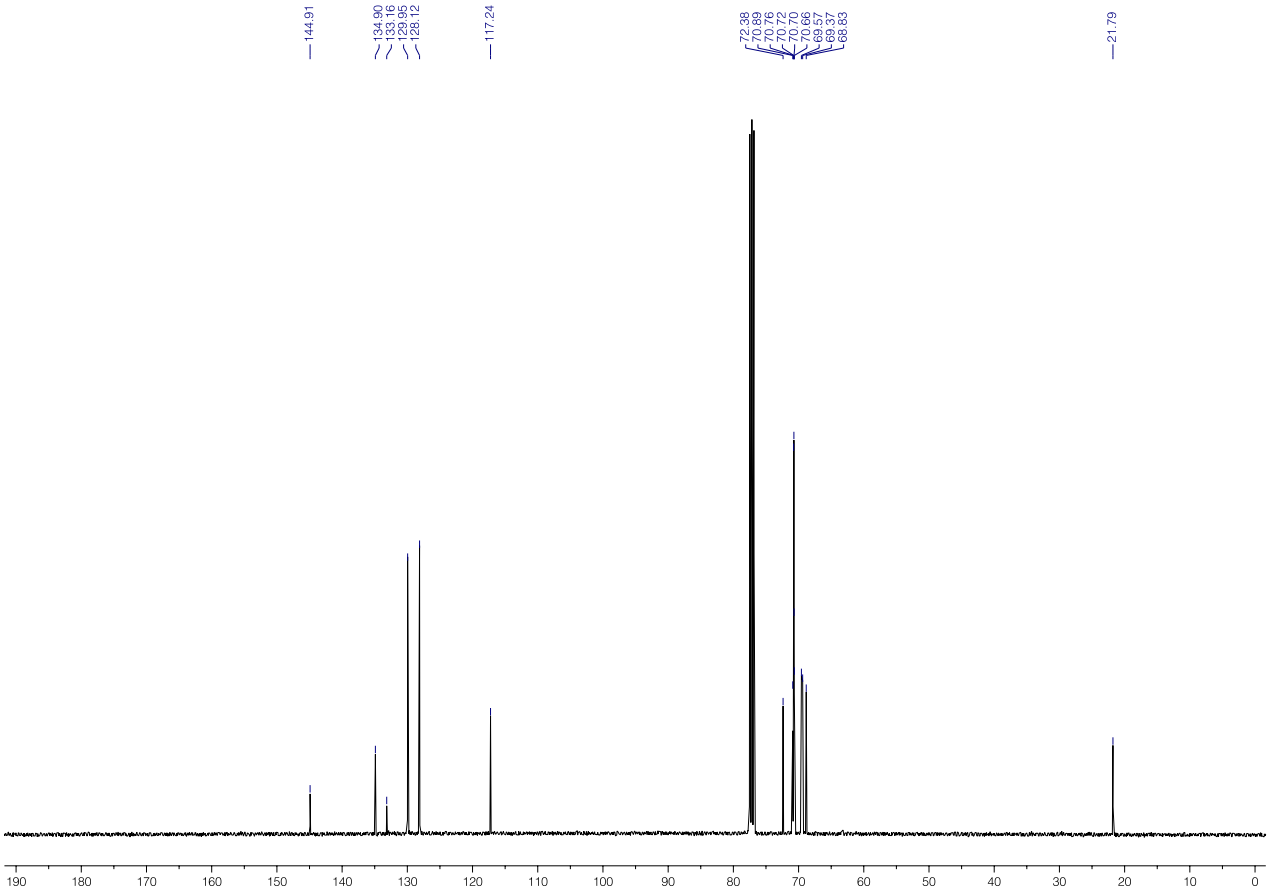

Figure S8. ^{13}C NMR spectrum of **4** (100 MHz, $CDCl_3$).

1-(4-(3,6,9,12,15,18-hexaoxahenicos-20-en-1-yloxy)phenyl)-2-phenyldiazene (**5**): Solid 4-hydroxyazobenzene (0.87 g; 4.39 mmol) and potassium *tert*-butoxide (0.54 g; 4.81 mmol) were placed in a Schlenk flask equipped with a magnetic stirring bar and a reflux condenser. The flask was evacuated and purged with nitrogen and then dry THF (20 mL) was added. The resulting solution was heated to reflux. Then, **4** (1.90 g; 4.0 mmol), dissolved in THF (10 mL) was added dropwise and the reaction mixture was refluxed overnight. Then, the mixture was cooled down to room temperature and the solvent was removed *in vacuo*. The resulting residue was dissolved in 150 mL of DCM and washed with brine (100 mL × 2). The organic layer was collected, the solvent was removed *in vacuo*, and the residue was purified by silica gel column chromatography (eluent: from $CHCl_3$ to $CHCl_3$/EtOAc = 2/1) to afford 1.81 g of **5** (yield = 90%).

^{1}H NMR (400 MHz, $CDCl_3$): δ = 7.92–7.86 (m, 4H), 7.52–7.41 (m, 3H), 7.04–7.02 (d, 2H), 5.96–5.86 (m, 1H), 5.29–5.16 (m, 2H), 4.22 (t, 2H), 4.02–4.01 (d, 2H), 3.90 (t, 2H), 3.76–3.73 (m, 2H), 3.70–3.64 (m, 16H), 3.60–3.58 (m, 2H). **^{13}C NMR** (100 MHz, $CDCl_3$): δ = 161.42, 152.89, 147.21, 134.91, 130.49, 129.15, 124.83, 122.68, 117.22, 114.97, 72.37, 71.05, 70.79, 70.77, 70.73, 69.77, 69.57, 67.88. **HRMS** calcd for $C_{27}H_{38}N_2NaO_7$ $[M + Na]^+$, m/z = 525.2577; found, 525.2579.

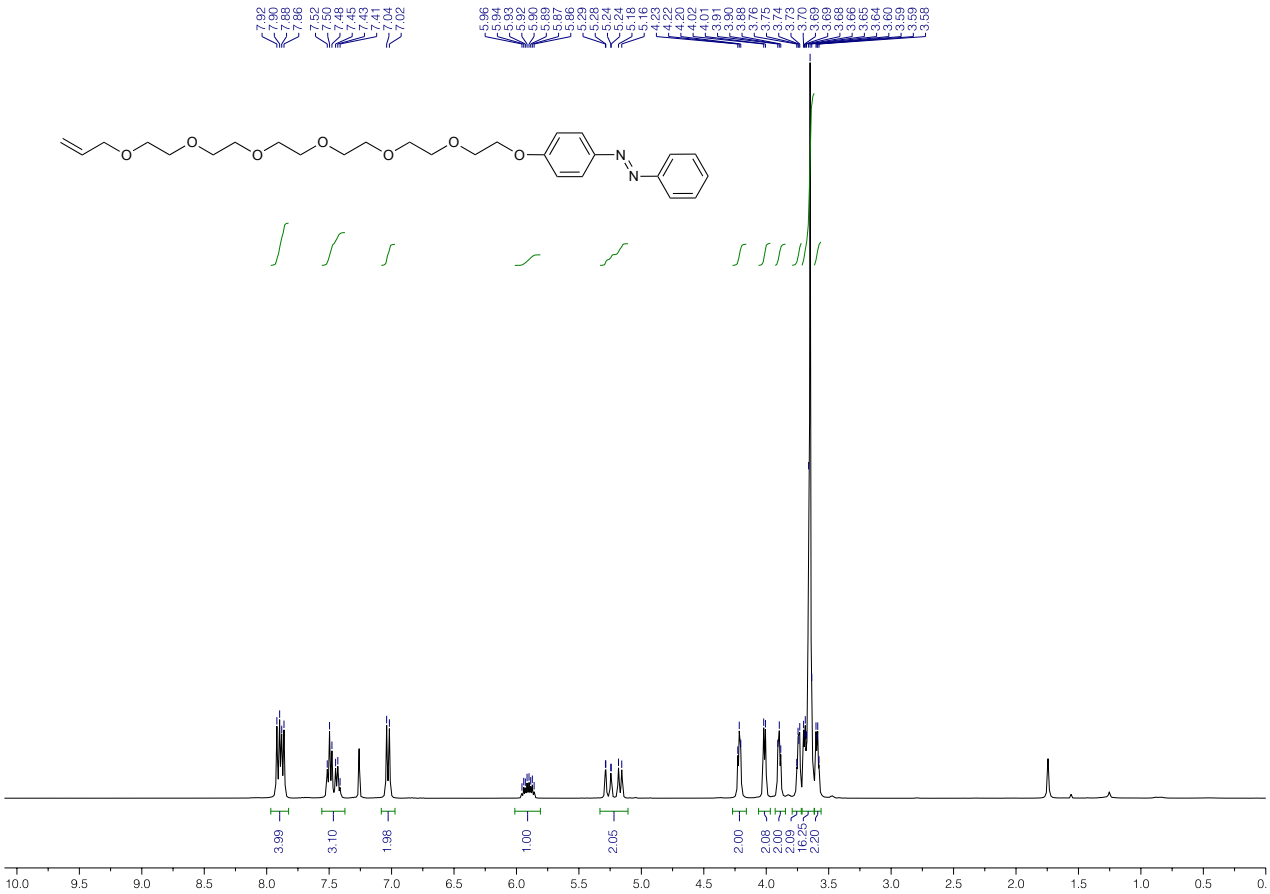

Figure S9. ^{1}H NMR spectrum of **5** (400 MHz, $CDCl_3$).

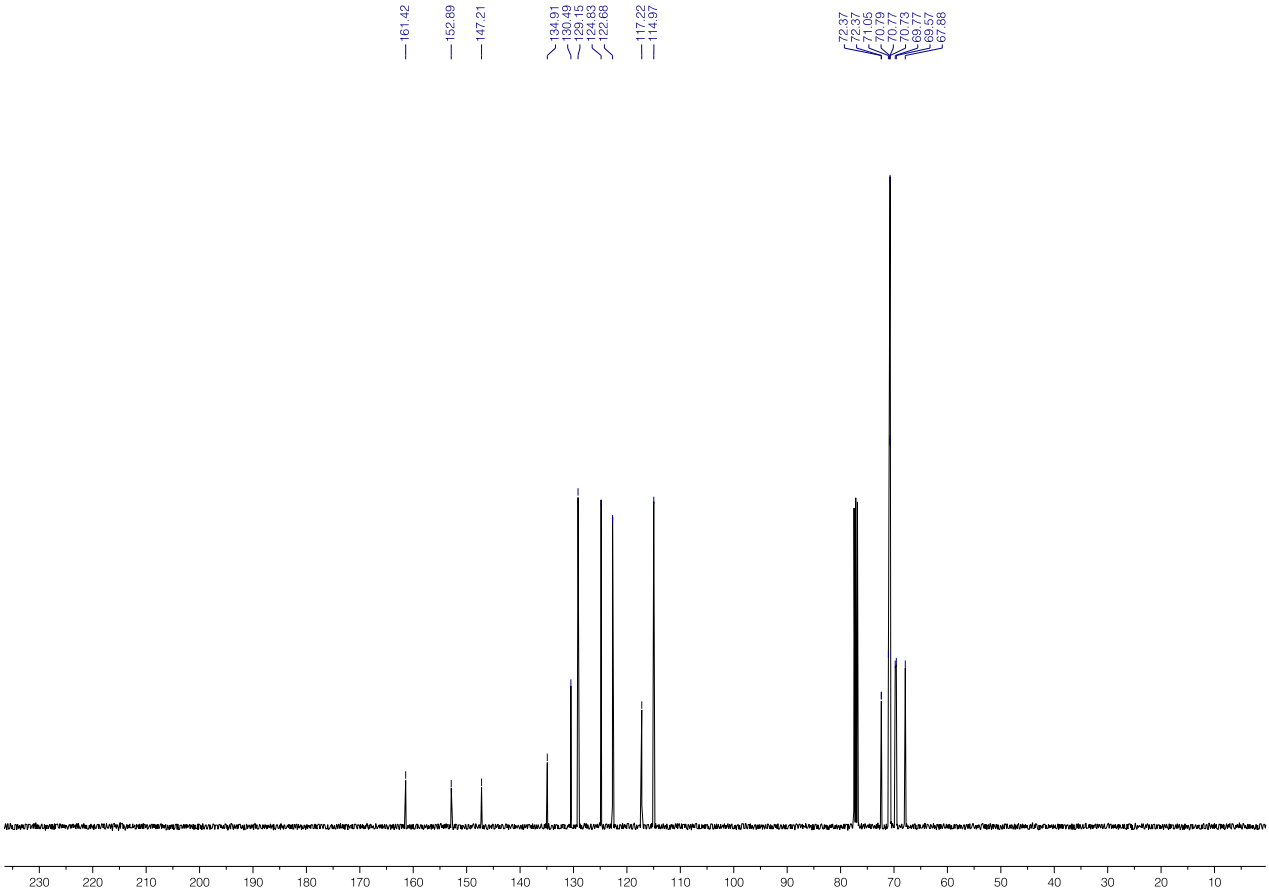

Figure S10. ^{13}C NMR spectrum of **5** (100 MHz, $CDCl_3$).

***S*-(1-(4-(phenyldiazenyl)phenoxy)-3,6,9,12,15,18-hexaoxahenicosan-21-yl) ethanethioate** (**6**): A solution of **5** (1.26 g; 2.50 mmol), AIBN (0.50 mmol; 82 mg) and thioacetic acid (700 µL; 0.76 g; 10.0 mmol) in 15 mL toluene was bubbled with N_2 for 15 min before heating to reflux under nitrogen atmosphere. After 6 hours, the reaction mixture was allowed to cool down to room temperature. The solvent was removed *in vacuo* and the resulting crude product was purified by silica gel column chromatography (eluent: from hexane/EtOAc = 4/1 to hexane/EtOAc = 1/2) to afford 1.22 g of **6** (yield = 84%).

^{1}H NMR (400 MHz, $CDCl_3$): δ = 7.92–7.86 (m, 4H), 7.51–7.41 (m, 3H), 7.04–7.02 (d, 2H), 4.22 (t, 2H), 3.89 (t, 2H), 3.75–3.73 (m, 2H), 3.70–3.61 (m, 16H), 3.58–3.55 (m, 2H), 3.49 (t, 2H), 2.94 (t, 2H), 2.31 (s, 3H), 1.88–1.81 (m, 2H). **^{13}C NMR** (100 MHz, $CDCl_3$): δ = 195.99, 161.41, 152.88, 147.21, 130.49, 129.15, 124.83, 122.68, 114.97, 71.05, 70.79, 70.76, 70.73, 70.70, 70.35, 69.77, 69.72, 67.88, 30.76, 29.71, 26.13. **HRMS** calcd for $C_{29}H_{42}N_2NaO_8S$ $[M + Na]^+$, m/z = 601.2560; found, 601.2566.

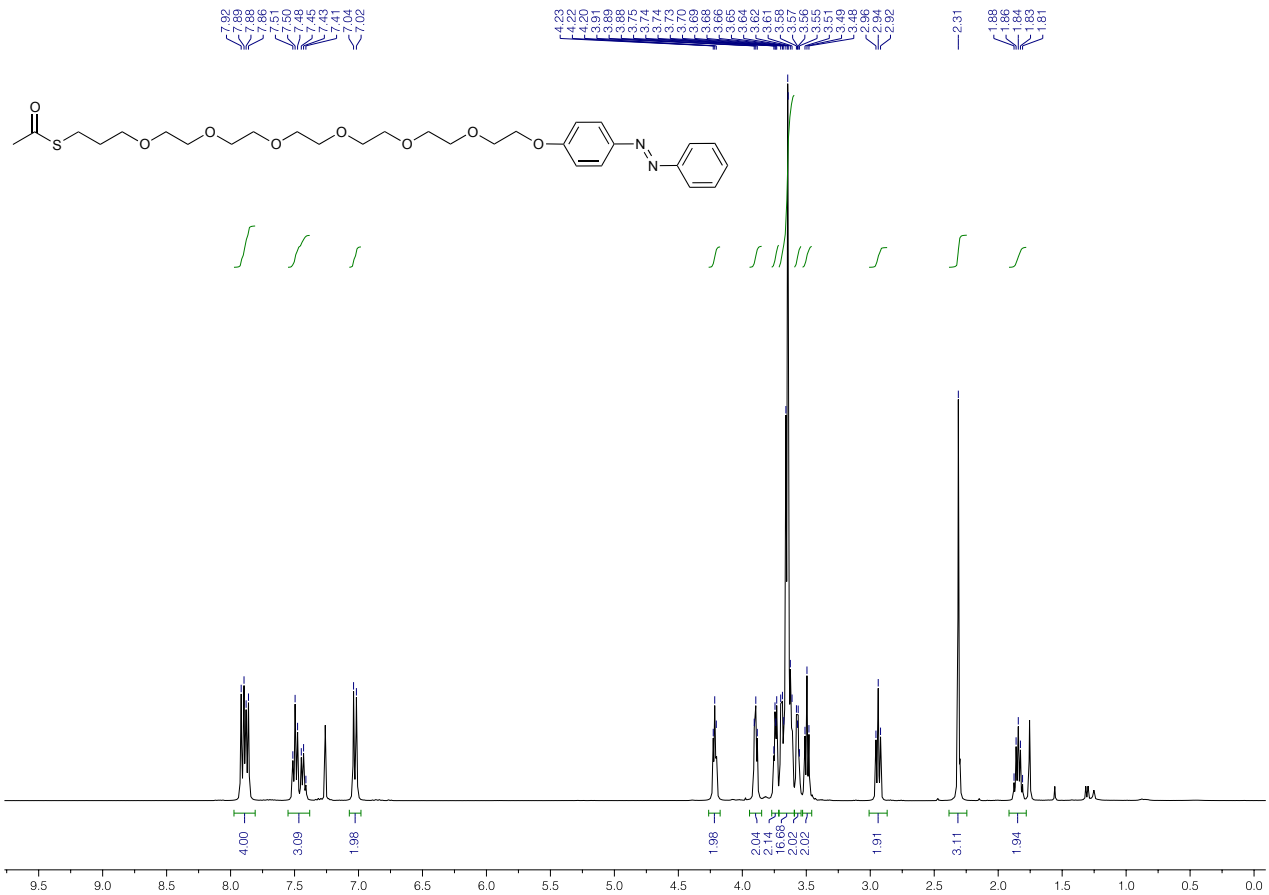

Figure S11. ^{1}H NMR spectrum of **6** (400 MHz, $CDCl_3$).

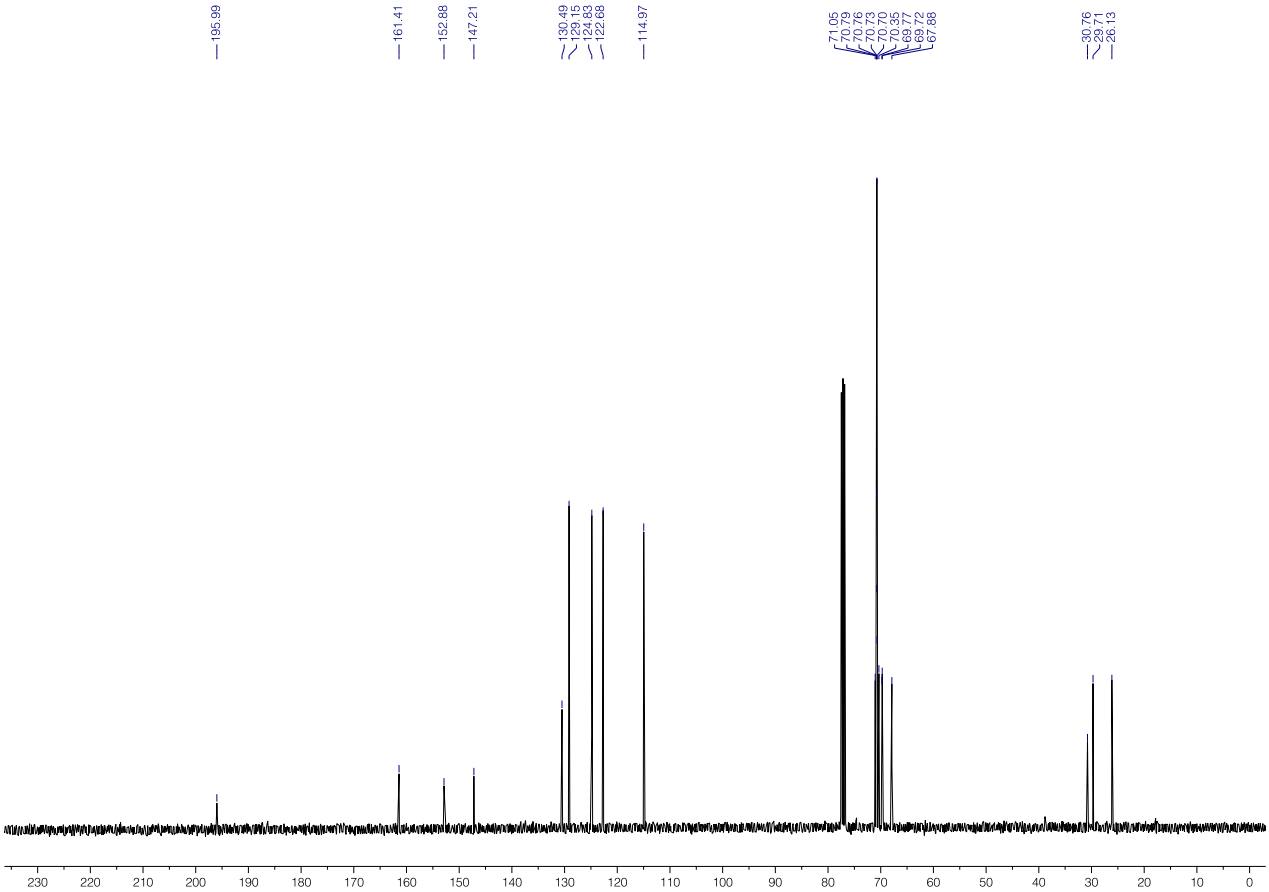

Figure S12. ^{13}C NMR spectrum of **6** (100 MHz, $CDCl_3$).

1-(4-(phenyldiazenyl)phenoxy)-3,6,9,12,15,18-hexaoxahenicosane-21-thiol (**A5**): Compound **6** (199 mg; 0.50 mmol) was placed in a Schlenk flask equipped with a magnetic stirring bar and a reflux condenser. The flask was purged with nitrogen and degassed methanol (7 mL) was added, followed by 3.0 mL of 1.25 M methanolic HCl. The resulting mixture was refluxed for 2 h. Then, the mixture was cooled down to room temperature and the solvent was evaporated *in vacuo* to afford **A5** in a quantitative yield.

^{1}H NMR (400 MHz, $CDCl_3$): δ = 7.92–7.86 (m, 4H), 7.52–7.42 (m, 3H), 7.04–7.02 (d, 2H), 4.22 (t, 2H), 3.90 (t, 2H), 3.75–3.54 (m, 22H), 2.64–2.59 (q, 2H), 1.90–1.84 (m, 2H), 1.37 (t, 1H). **^{13}C NMR** (100 MHz, $CDCl_3$): δ = 161.45, 152.87, 147.20, 130.52, 129.17, 124.87, 122.70, 115.00, 71.06, 70.80, 70.75, 70.38, 69.80, 69.27, 67.93, 35.50, 33.88, 29.29, 21.59. **HRMS** calcd for $C_{27}H_{40}N_2NaO_7S$ $[M + Na]^+$, m/z = 559.2454; found, 559.2462.

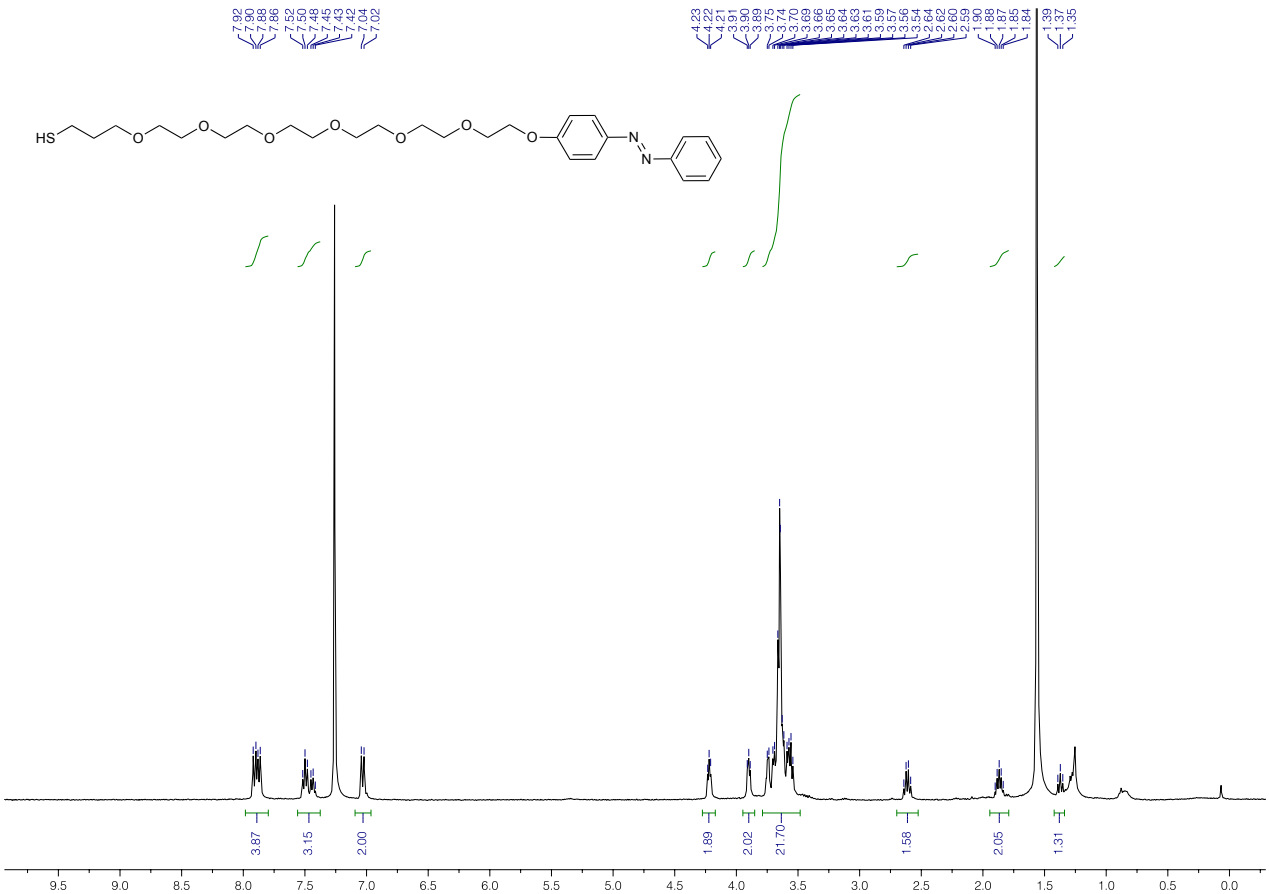

Figure S13. ^{1}H NMR spectrum of **A5** (400 MHz, $CDCl_3$).

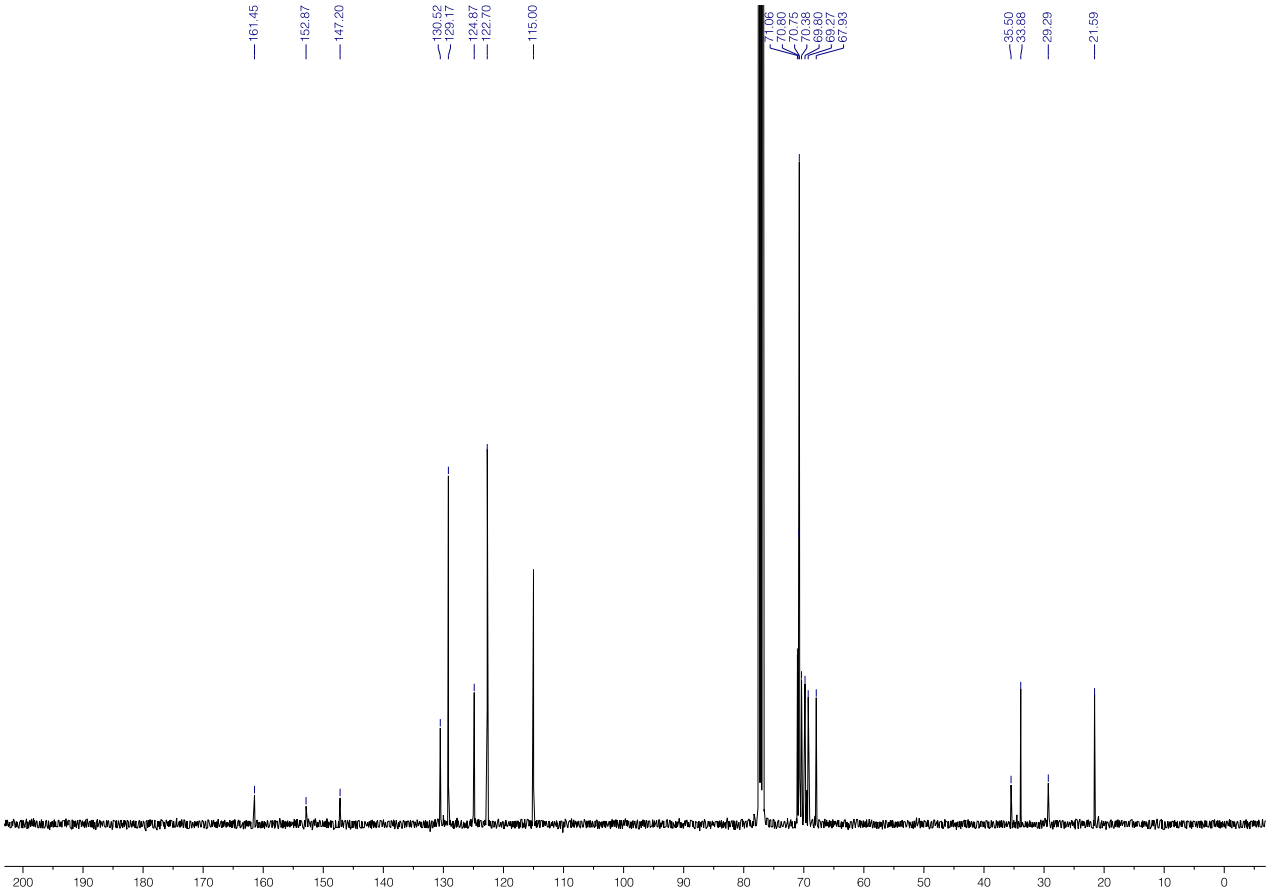

Figure S14. ^{13}C NMR spectrum of **A5** (100 MHz, $CDCl_3$).

2.6. Thiolated azobenzene **A6**

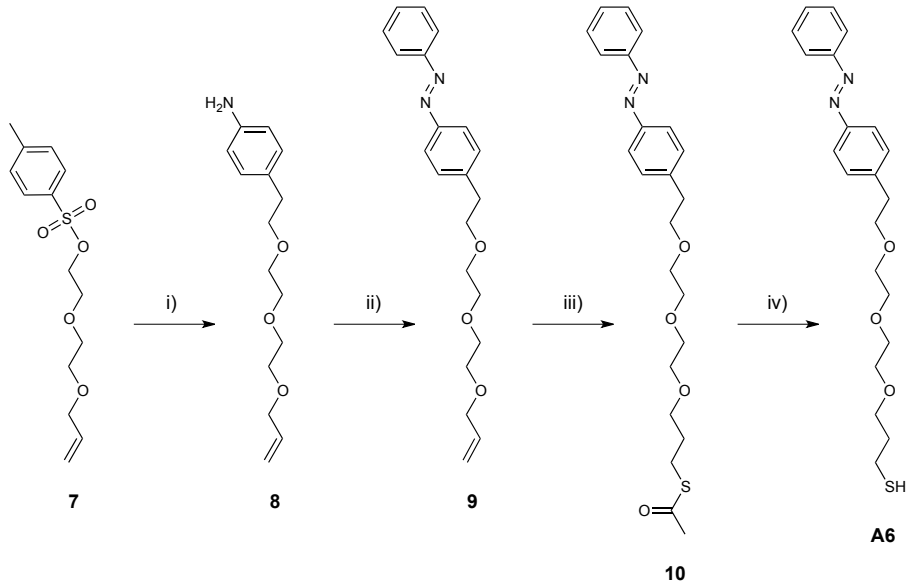

Scheme S3. Synthetic route for ligand **A6**. Reagents and conditions: i) ^{t}BuOK, 2-(4-aminophenyl)ethyl alcohol, THF, RT, overnight, 60%; ii) nitrosobenzene, CH_3COOH, DCM, RT, overnight, quantitative; iii) CH_3COSH, DCM, UVB, 2 d, 78%; iv) HCl/MeOH, reflux, 2 h, quantitative.

4-(2-(2-(2-(allyloxy)ethoxy)ethoxy)ethyl)aniline (**8**). Compound **7** (Ref. 4) was synthesized in two steps following the same protocol as compound **4**, but using di(ethylene glycol), as opposed to hexa(ethylene glycol), as the starting material. A solution of **7** (330 mg; 1.10 mmol) in 5 mL of dry THF was slowly added to a stirred mixture of 2-(4-aminophenyl)ethyl alcohol (137 mg; 1.00 mmol) and potassium *tert*-butoxide (123 mg; 1.10 mmol) under nitrogen atmosphere and the resulting reaction mixture was stirred overnight at room temperature under nitrogen atmosphere. Then, the mixture was placed in a separating funnel containing EtOAc (100 mL) and washed with water (50 mL) and brine (50 mL). The organic layer was collected, dried over $MgSO_4$ and concentrated *in vacuo*. The crude was purified by silica gel column chromatography (eluent: Hexane/EtOAc from 9/1 to 1/1) to afford 160 mg of **8** (yield = 60%).

^{1}H NMR (400 MHz, $CDCl_3$): δ = 6.93 (d, 2H), 6.58 (d, 2H), 5.94–5.84 (m, 1H), 5.26 (d, 1H), 5.11 (d, 1H), 4.40 (bs, 2H), 3.98 (d, 2H), 3.58–3.53 (m, 10H), 2.68 (t, 2H). **^{13}C NMR** (100 MHz, $CDCl_3$): δ = 136.43, 130.25, 127.93, 120.11, 116.23, 115.23, 73.45, 72.96, 72.40, 71.29, 70.94, 70.39, 36.24. **HRMS** calcd for $C_{15}H_{23}NNaO_3$ $[M + Na]^+$, m/z = 288.1576; found, 288.1572.

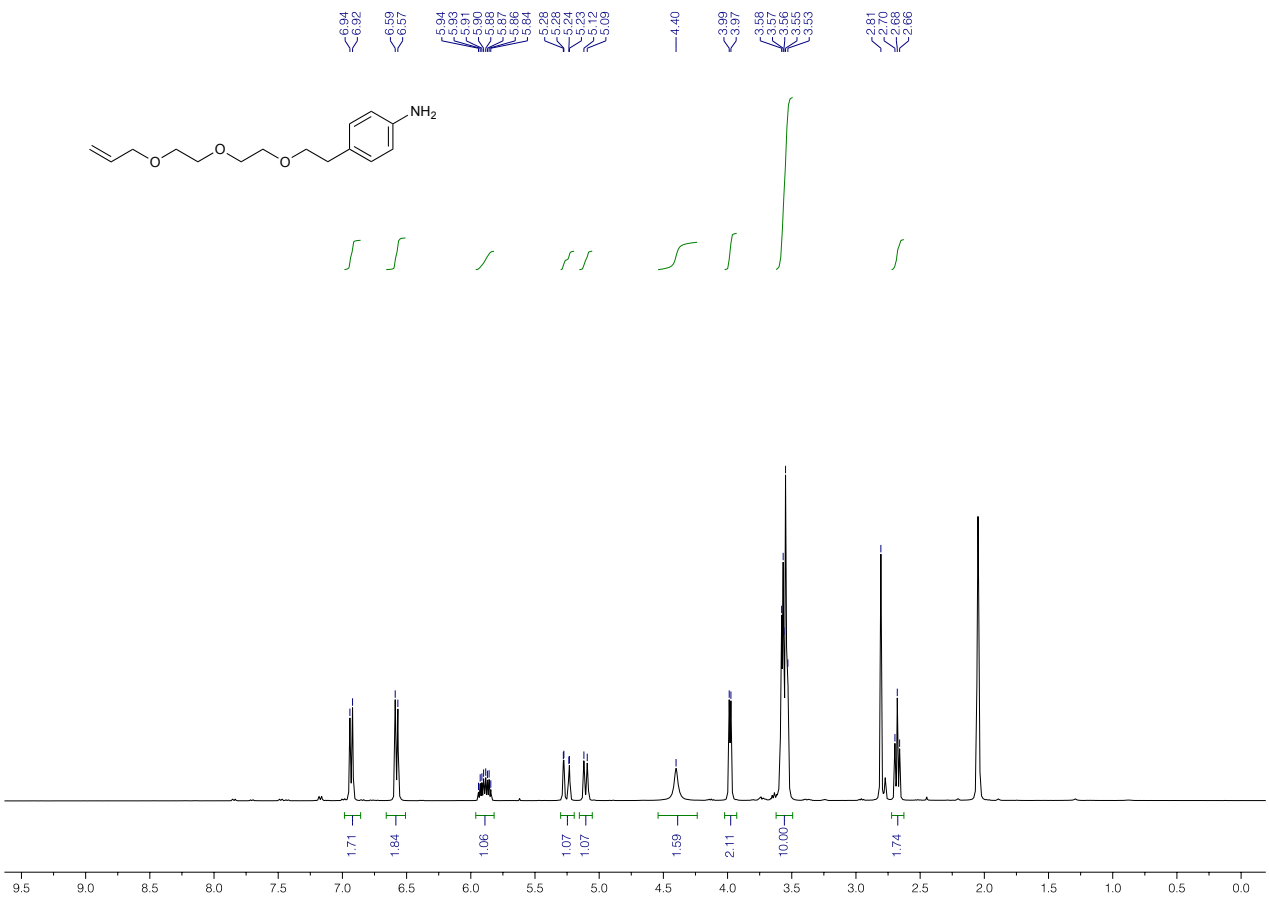

Figure S15. ^{1}H NMR spectrum of **8** (400 MHz, acetone-d_6).

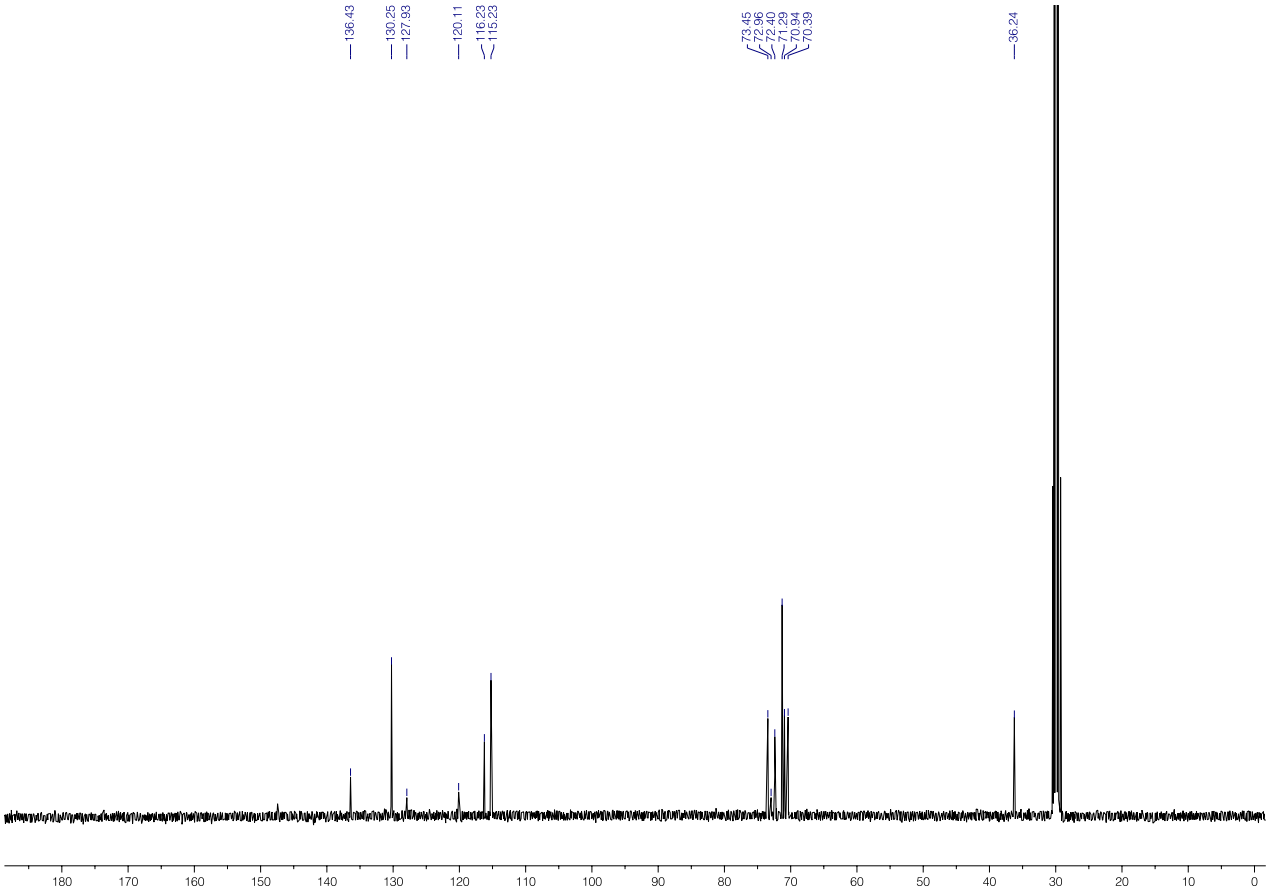

Figure S16. ^{13}C NMR spectrum of **8** (100 MHz, acetone-d_6).

1-(4-(2-(2-(2-(allyloxy)ethoxy)ethoxy)ethyl)phenyl)-2-phenyldiazene (**9**). To a solution of nitrosobenzene (60.5 mg; 0.565 mmol) in DCM (0.5 mL), a solution of **8** (150 mg; 0.565 mmol) in DCM (2 mL) was introduced, followed by the addition of acetic acid (177 μL). The reaction mixture was stirred overnight under nitrogen atmosphere at room temperature. Then, the reaction mixture was diluted with 100 mL of EtOAc and washed with a 1 M NaOH solution (30 mL × 3), saturated $NaHCO_3$ solution (30 mL × 2), and brine (30 mL × 2). The organic phase was dried over $MgSO_4$ and concentrated *in vacuo* to afford **9** in a quantitative yield.

^{1}H NMR (400 MHz, $CDCl_3$): δ = 7.90 (d, 2H), 7.85 (d, 2H), 7.53–7.44 (m, 3H), 7.37 (d, 2H), 5.96–5.87 (m, 1H), 5.27 (d, 1H), 5.17 (d, 1H), 4.02 (d, 2H), 3.74 (t, 2H), 3.66–3.64 (m, 6H), 3.61–3.58 (m, 2H), 2.98 (t, 2H). **^{13}C NMR** (100 MHz, $CDCl_3$): δ = 152.88, 151.42, 142.73, 134.93, 130.93, 129.80, 129.21, 123.03, 122.90, 117.26, 72.41, 72.06, 70.85, 70.80, 70.55, 69.61, 36.34. **HRMS** calcd for $C_{21}H_{26}N_2NaO_3$ $[M + Na]^+$, m/z = 377.1841; found, 377.1829.

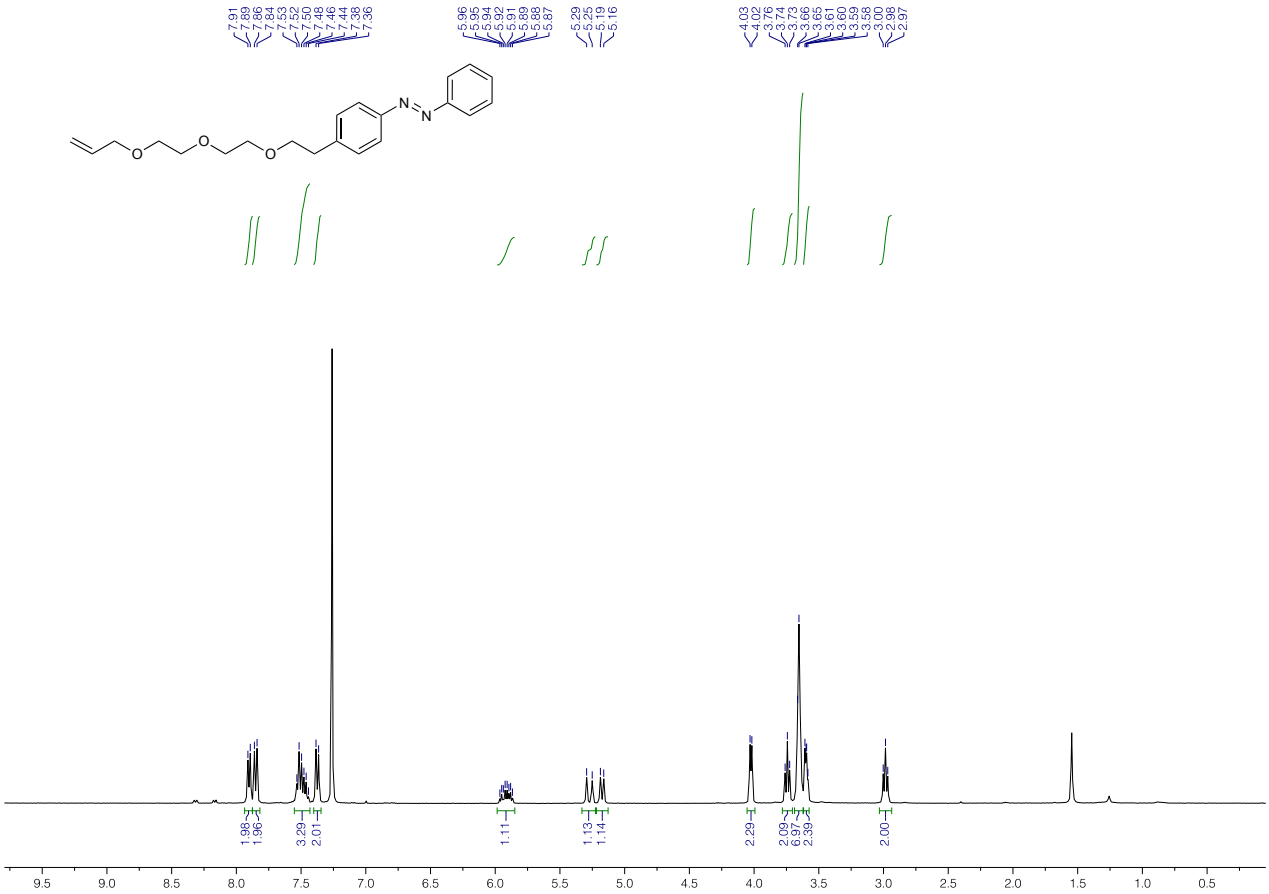

Figure S17. ^{1}H NMR spectrum of **9** (400 MHz, $CDCl_3$).

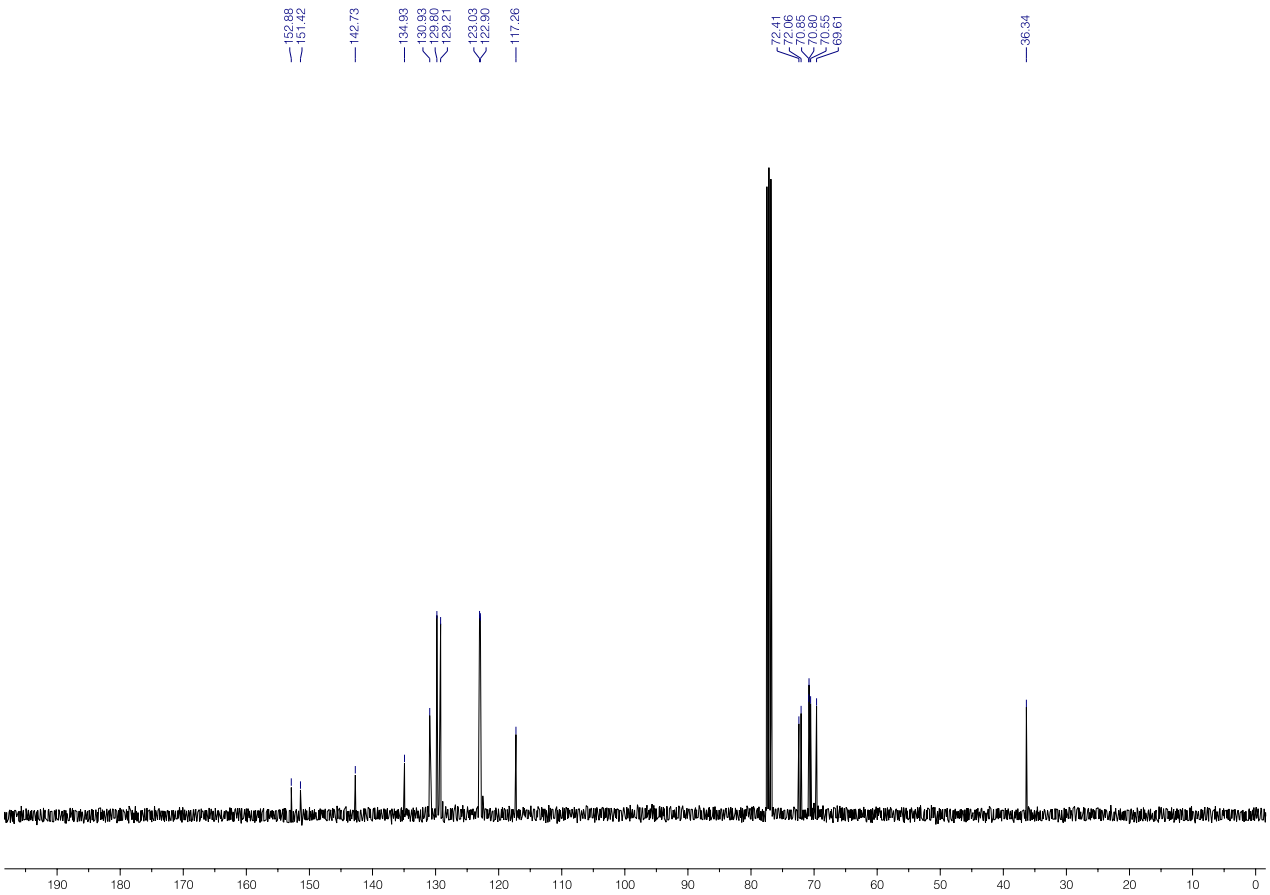

Figure S18. ^{13}C NMR spectrum of **9** (100 MHz, $CDCl_3$).

***S*-(3-(2-(2-(4-(phenyldiazenyl)phenethoxy)ethoxy)ethoxy)propyl) ethanethioate** (**10**): A solution of **9** (200 mg; 0.56 mmol) and thioacetic acid (139 μL; 150 mg; 1.98 mmol) in DCM (5 mL) was stirred at room temperature under UVB light for 2 days. Then, the reaction mixture was diluted with 100 mL of DCM and washed with a saturated solution of $NaHCO_3$ (30 mL × 2). The organic phase was collected, dried over $MgSO_4$, and concentrated *in vacuo*. The crude product was purified by silica gel column chromatography (eluent: hexane/EtOAc = 9/1 → 1/1) to afford 190 mg of **10** (yield = 78%).

^{1}H NMR (500 MHz, $CDCl_3$): δ = 7.90 (d, 2H), 7.85 (d, 2H), 7.51 (t, 2H), 7.48–7.45 (m, 1H), 7.37 (d, 2H), 3.74 (t, 2H), 3.66–3.62 (m, 6H), 3.58–3.56 (m, 2H), 3.51 (t, 2H), 2.98 (t, 2H), 2.94 (t, 2H), 2.31 (s, 3H), 1.88–1.82 (m, 2H). **^{13}C NMR** (125 MHz, $CDCl_3$): δ = 196.03, 152.87, 151.42, 142.72, 130.93, 129.80, 129.21, 123.03, 122.90, 72.07, 70.78 (2 C), 70.56, 70.40, 69.75, 36.34, 30.77, 29.72, 26.15. **HRMS** calcd for $C_{23}H_{30}N_2NaO_4S$ $[M + Na]^+$, m/z = 453.1824; found, 453.1821.

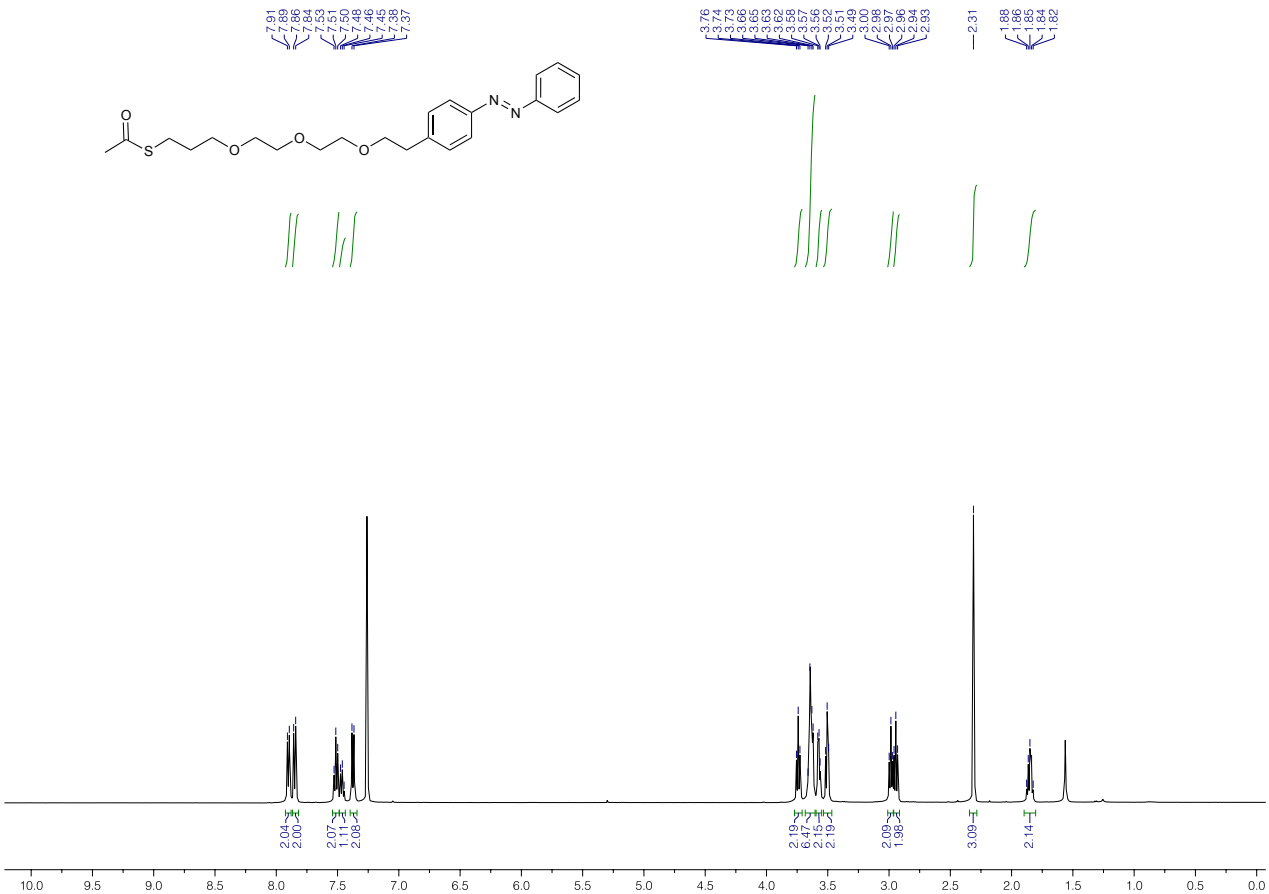

Figure S19. ^{1}H NMR spectrum of **10** (500 MHz, $CDCl_3$).

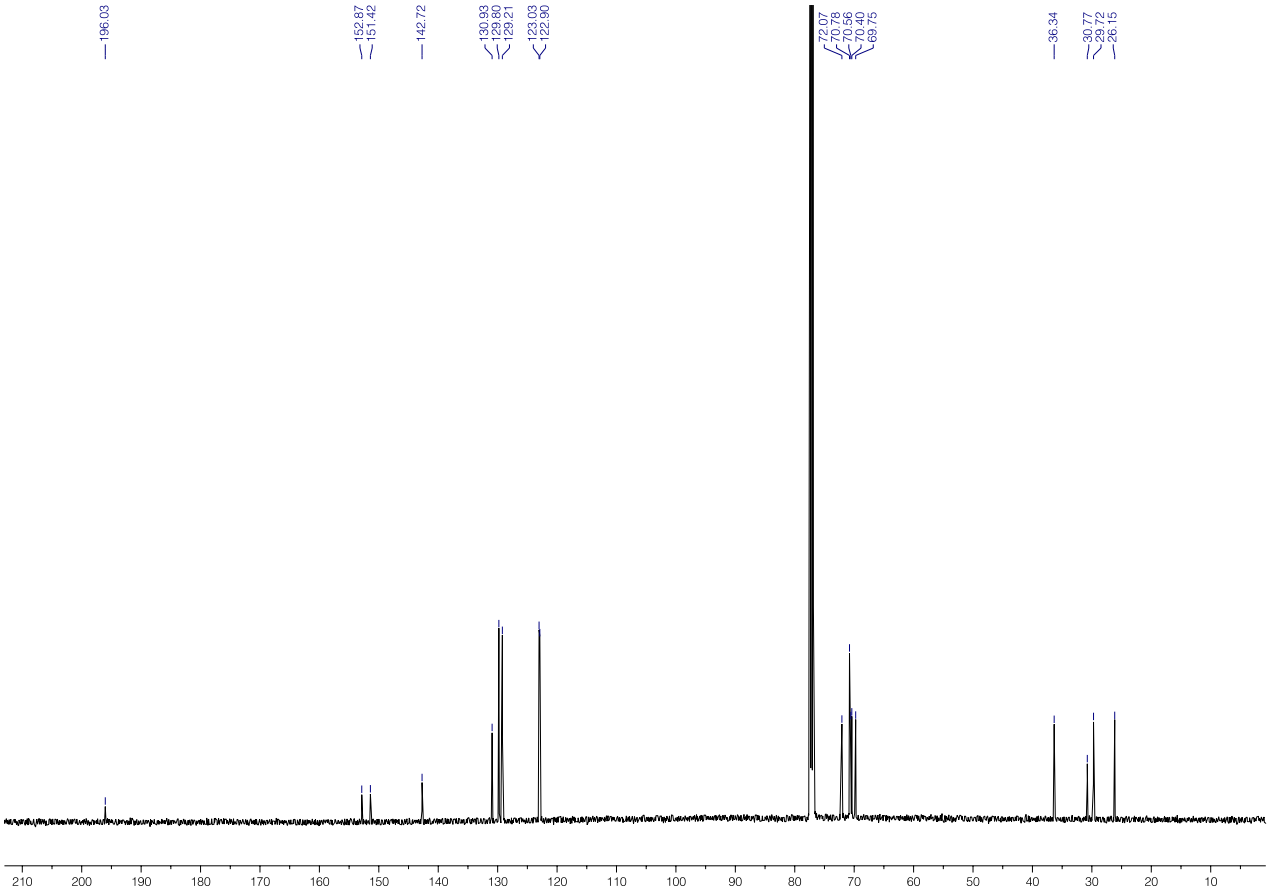

Figure S20. ^{13}C NMR spectrum of **10** (125 MHz, $CDCl_3$).

3-(2-(2-(4-(phenyldiazenyl)phenethoxy)ethoxy)ethoxy)propane-1-thiol (**A6**). Compound **10** was deprotected following the procedure identical to compound **A5** to afford **A6** quantitatively.

^{1}H NMR (500 MHz, $CDCl_3$): δ = 7.90 (d, 2H), 7.85 (d, 2H), 7.51 (t, 2H), 7.48–7.45 (m, 1H), 7.37 (d, 2H), 3.74 (t, 2H), 3.64–3.62 (m, 6H), 3.59–3.54 (m, 4H), 2.99 (t, 2H), 2.61 (q, 2H), 1.90–1.84 (m, 2H), 1.37 (t, 1H). **^{13}C NMR** (125 MHz, $CDCl_3$): δ = 152.87, 151.42, 142.73, 130.95, 129.81, 129.22, 123.04, 122.91, 72.07, 70.79 (2 C), 70.58, 70.42, 69.28, 36.35, 33.89, 21.60. **HRMS** calcd for $C_{21}H_{28}N_2NaO_3S$ $[M + Na]^+$, m/z = 411.1718; found, 411.1716.

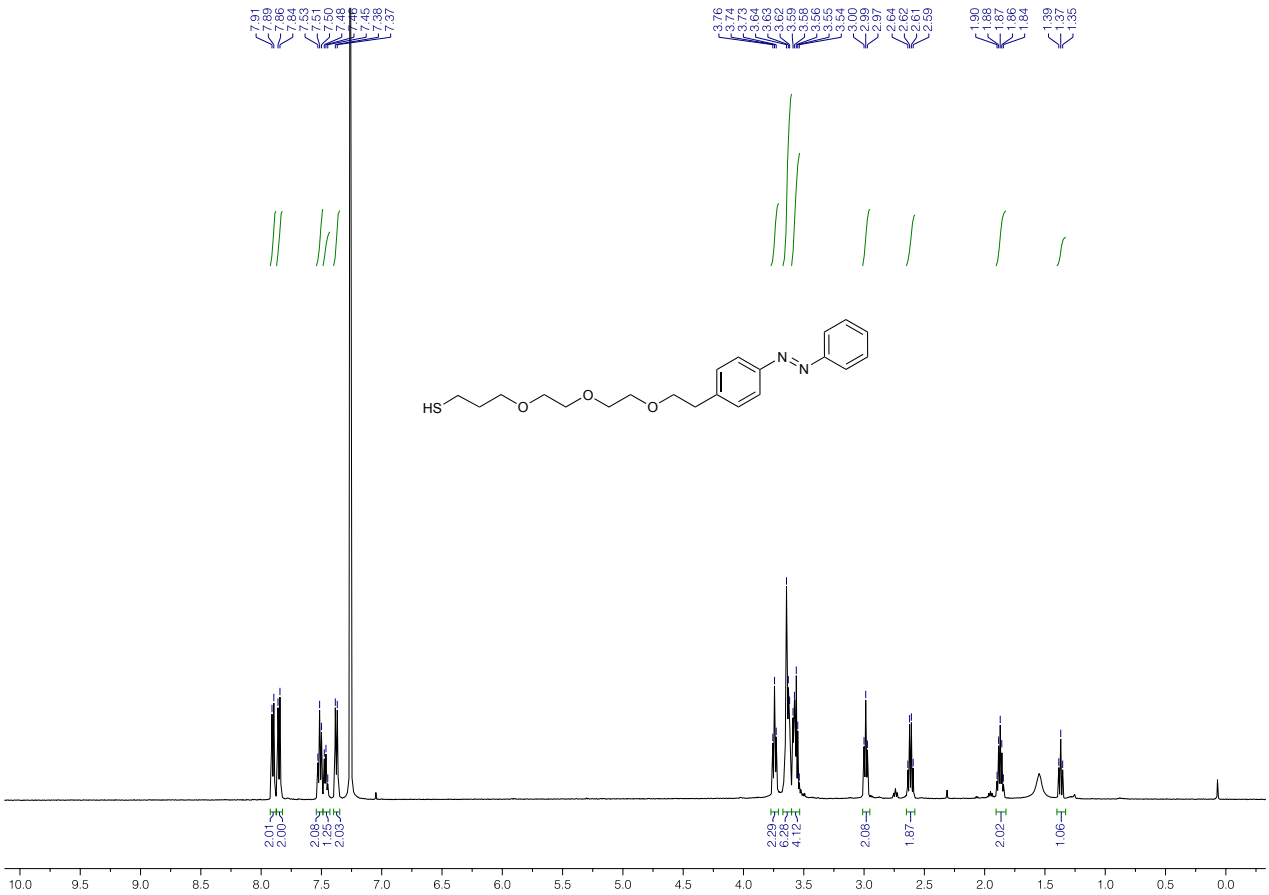

Figure S21. ^{1}H NMR spectrum of **A6** (500 MHz, $CDCl_3$).

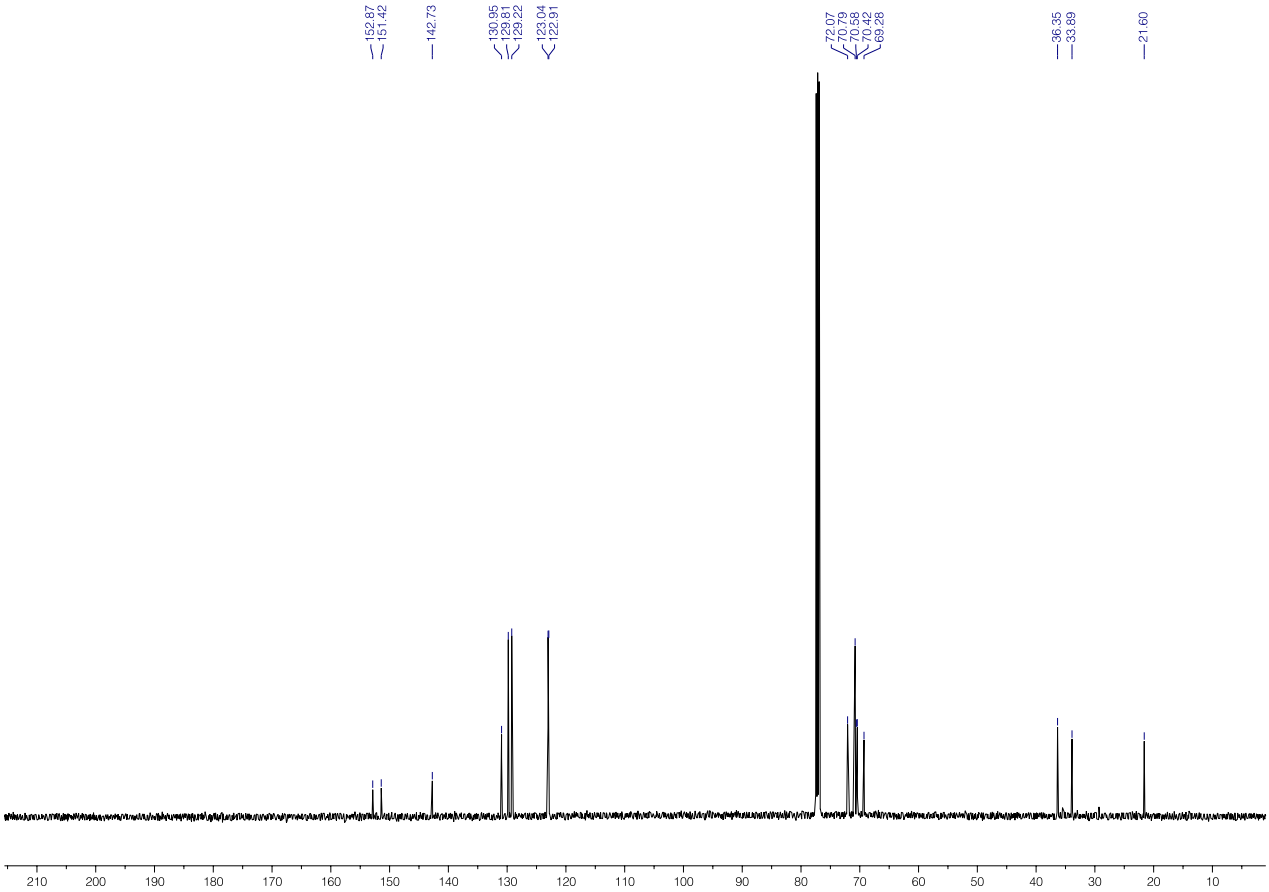

Figure S22. ^{13}C NMR spectrum of **A6** (125 MHz, $CDCl_3$).

3. Synthesis and characterization of background ligands **B1**–**B9**

3.1. Background ligand **B1**

11-mercapto-*N*,*N*,*N*-trimethylundecan-1-aminium bromide (**B1**) was synthesized based on a previously reported literature procedure.[5]

3.2. Background ligand **B2**

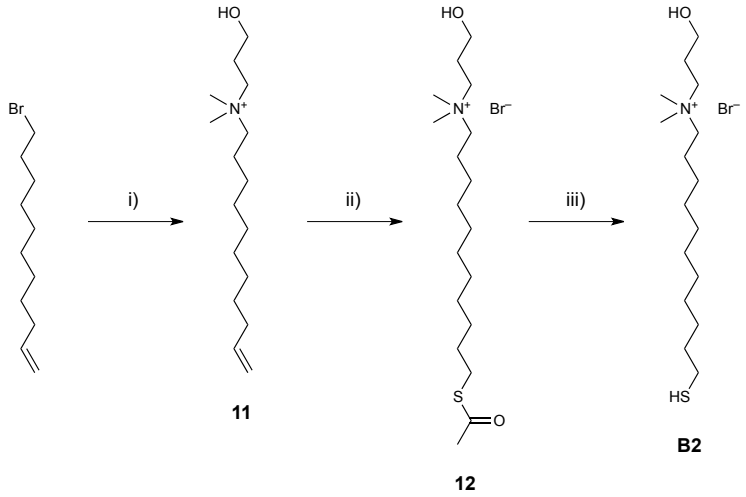

Scheme S4. Synthetic route for ligand **B2**. Reagents and conditions: i) 3-(dimethylamino)propan-1-ol, EtOAc, reflux, 8 h, 22%; ii) CH_3COSH, DCM, UVB, overnight, quantitative; iii) HCl/MeOH, reflux, 6 h, quantitative.

***N*-(3-hydroxypropyl)-*N*,*N*-dimethylundec-10-en-1-aminium bromide** (**11**): 11-bromo-1-undecene (373 mg; 1.60 mmol) and 3-dimethylamino-1-propanol (236 µL; 206 mg; 2.00 mmol) were dissolved in dry EtOAc and the solution was refluxed for 8 h. Then, the reaction mixture was cooled to room temperature, resulting in precipitation of the crude product. The precipitate was washed with diethyl ether and dried under vacuum to afford 120 mg of **11** (22%).

^{1}H NMR (400 MHz, D_2O): δ = 5.99–5.88 (m, 1H), 5.08–4.97 (m, 2H), 3.70 (t, 2H), 3.41–3.37 (m, 2H), 3.32–3.28 (m, 2H), 3.08 (s, 6H), 2.09–1.97 (m, 4H), 1.80–1.73 (m, 2H), 1.41–1.32 (m, 12H). **^{13}C NMR** (100 MHz, D_2O): δ = 140.44, 113.91, 64.22, 61.37, 58.15, 50.57, 33.08, 28.34, 28.29, 28.20, 28.08, 28.05, 25.36, 24.86, 21.73. **HRMS** calcd for $C_{16}H_{34}NO$ $[M - Br]^+$, m/z = 256.2640; found, 256.2639.

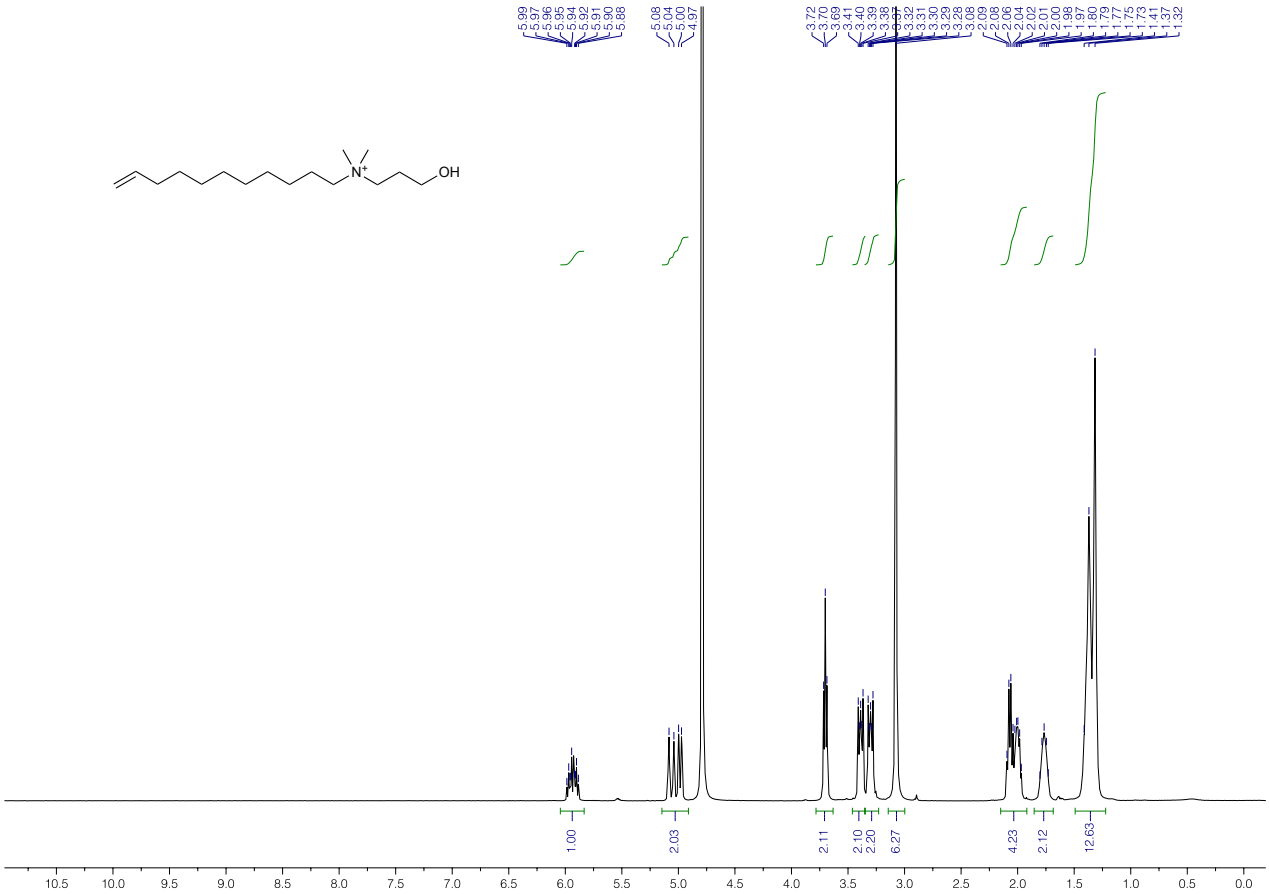

Figure S23. ^{1}H NMR spectrum of **11** (400 MHz, D_2O).

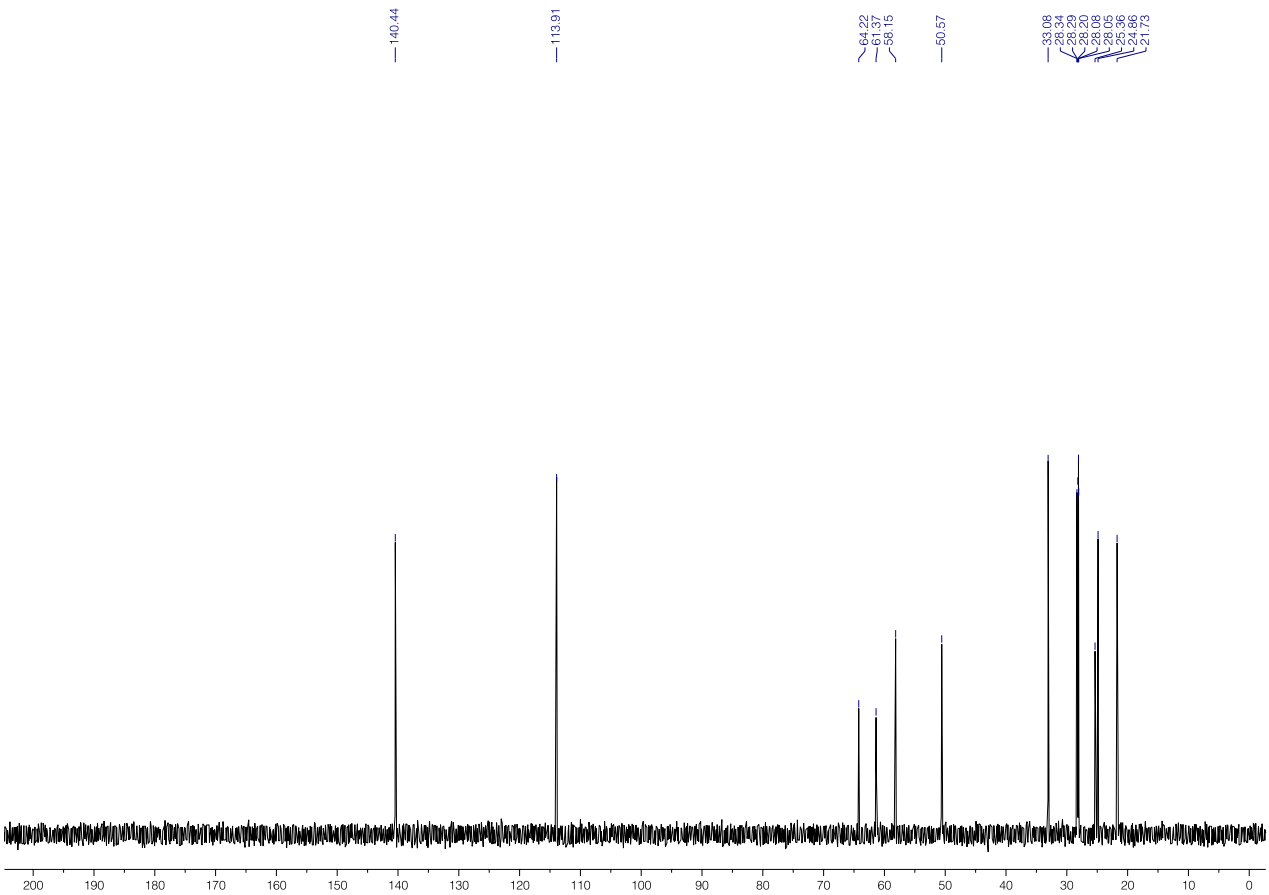

Figure S24. ^{13}C NMR spectrum of **11** (100 MHz, D_2O).

11-(acetylthio)-*N*-(3-hydroxypropyl)-*N*,*N*-dimethylundecan-1-aminium bromide (**12**): A solution of **11** (90 mg; 0.27 mmol) and thioacetic acid (72 µL; 77 mg, 1.01 mmol) in DCM (5 mL) was stirred at room temperature under UVB light overnight. Then, the reaction mixture was concentrated *in vacuo* to afford **12** in a quantitative yield.

^{1}H NMR (400 MHz, D_2O): δ = 3.70 (t, 2H), 3.41–3.37 (m, 2H), 3.33–3.28 (m, 2H), 3.08 (s, 6H), 2.90 (t, 2H), 2.38 (s, 3H), 2.04–1.97 (m, 2H), 1.79–1.75 (m, 2H), 1.61–1.55 (m, 2H), 1.37–1.30 (m, 14H). **^{13}C NMR** (100 MHz, D_2O): δ = 202.38, 64.23, 61.40, 58.16, 50.60, 30.05, 28.98, 28.54, 28.47, 28.44, 28.36, 28.13, 28.11, 27.80, 25.41, 24.88, 21.77. **HRMS** calcd for $C_{18}H_{38}NO_2S$ $[M – Br]^+$, m/z = 332.2623; found, 332.2612.

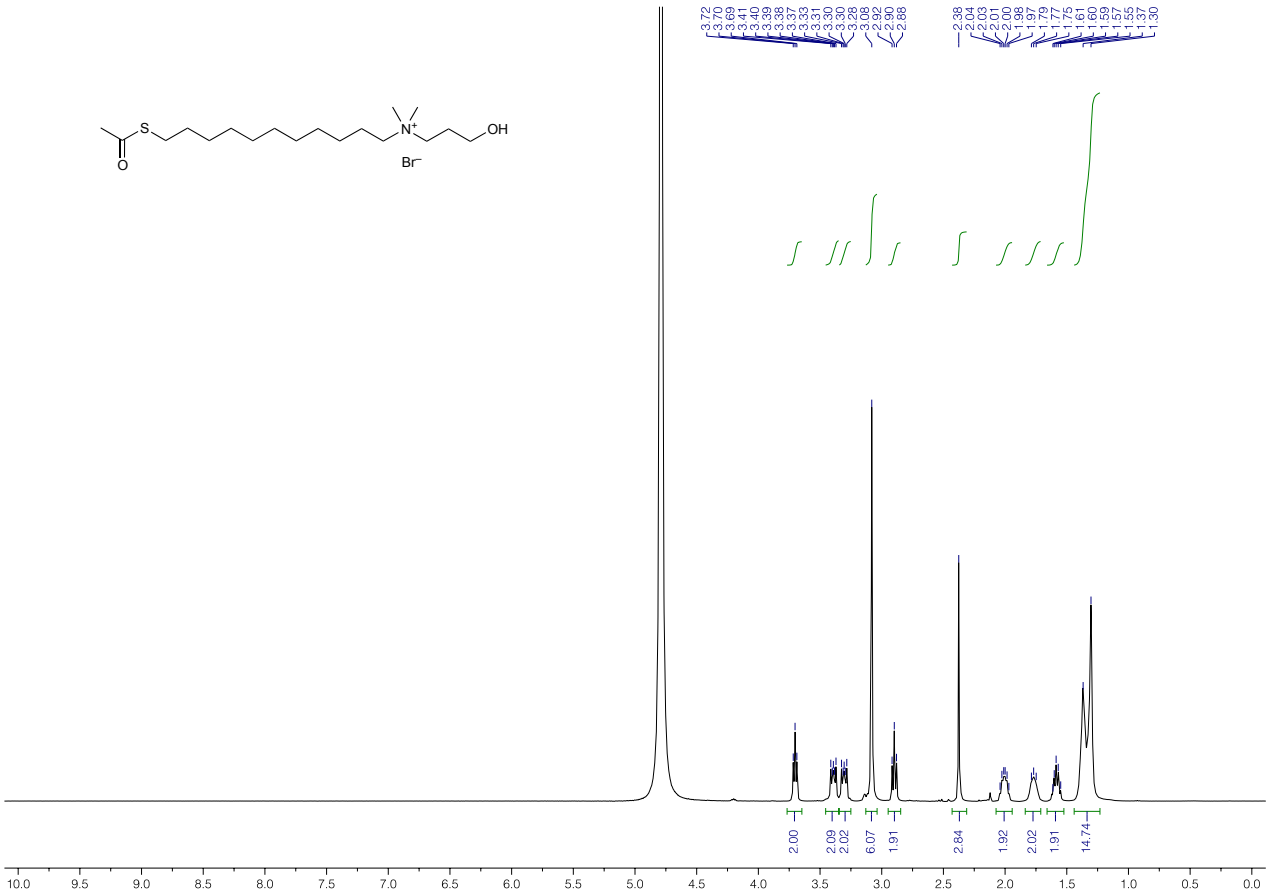

Figure S25. ^{1}H NMR spectrum of **12** (400 MHz, D_2O).

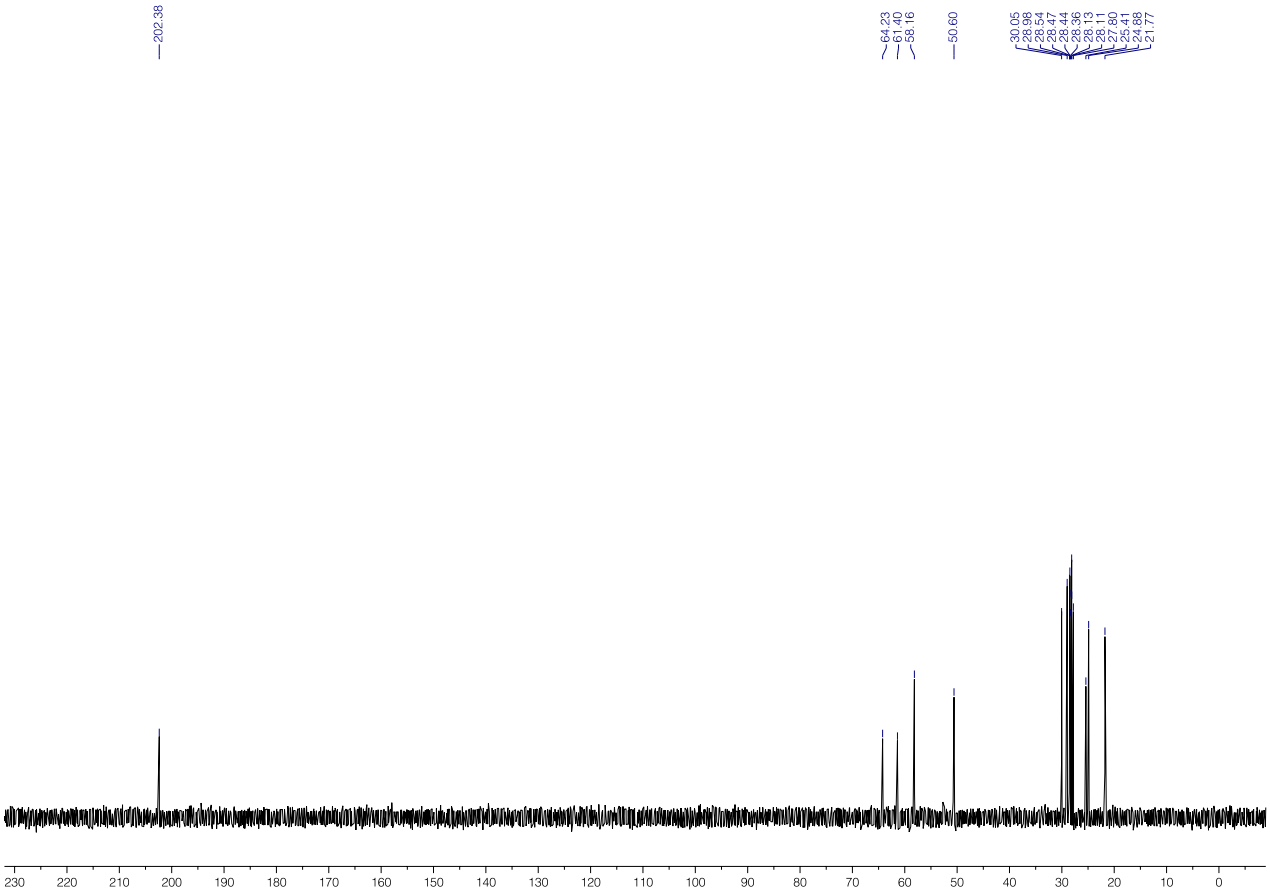

Figure S26. ^{13}C NMR spectrum of **12** (100 MHz, D_2O).

***N*-(3-hydroxypropyl)-11-mercapto-*N*,*N*-dimethylundecan-1-aminium bromide** (**B2**): A solution of **12** (70 mg; 0.17 mmol) in methanol (5 mL) was degassed by bubbling with nitrogen for 15 min. Then, 0.6 mL of 1.25 M methanolic HCl solution was added and the resulting solution was refluxed for 6 h. The reaction mixture was cooled down to room temperature and the solvent was evaporated *in vacuo* to afford **B2** in a quantitative yield.

^{1}H NMR (500 MHz, D_2O): δ = 3.63 (t, 2H), 3.34–3.31 (m, 2H), 3.26–3.22 (m, 2H), 3.01 (s, 6H), 2.49 (t, 2H), 1.96–1.90 (m, 2H), 1.73–1.67 (m, 2H), 1.57–1.51 (m, 2H), 1.34–1.24 (m, 14H). **^{13}C NMR** (125 MHz, D_2O): δ = 64.10, 61.29, 58.06, 50.54, 33.08, 28.63, 28.56, 28.45, 28.19, 28.18, 27.51, 25.41, 24.82, 23.82, 21.76. **HRMS** calcd for $C_{16}H_{36}NOS$ $[M – Br]^+$, m/z = 290.2518; found, 290.2517.

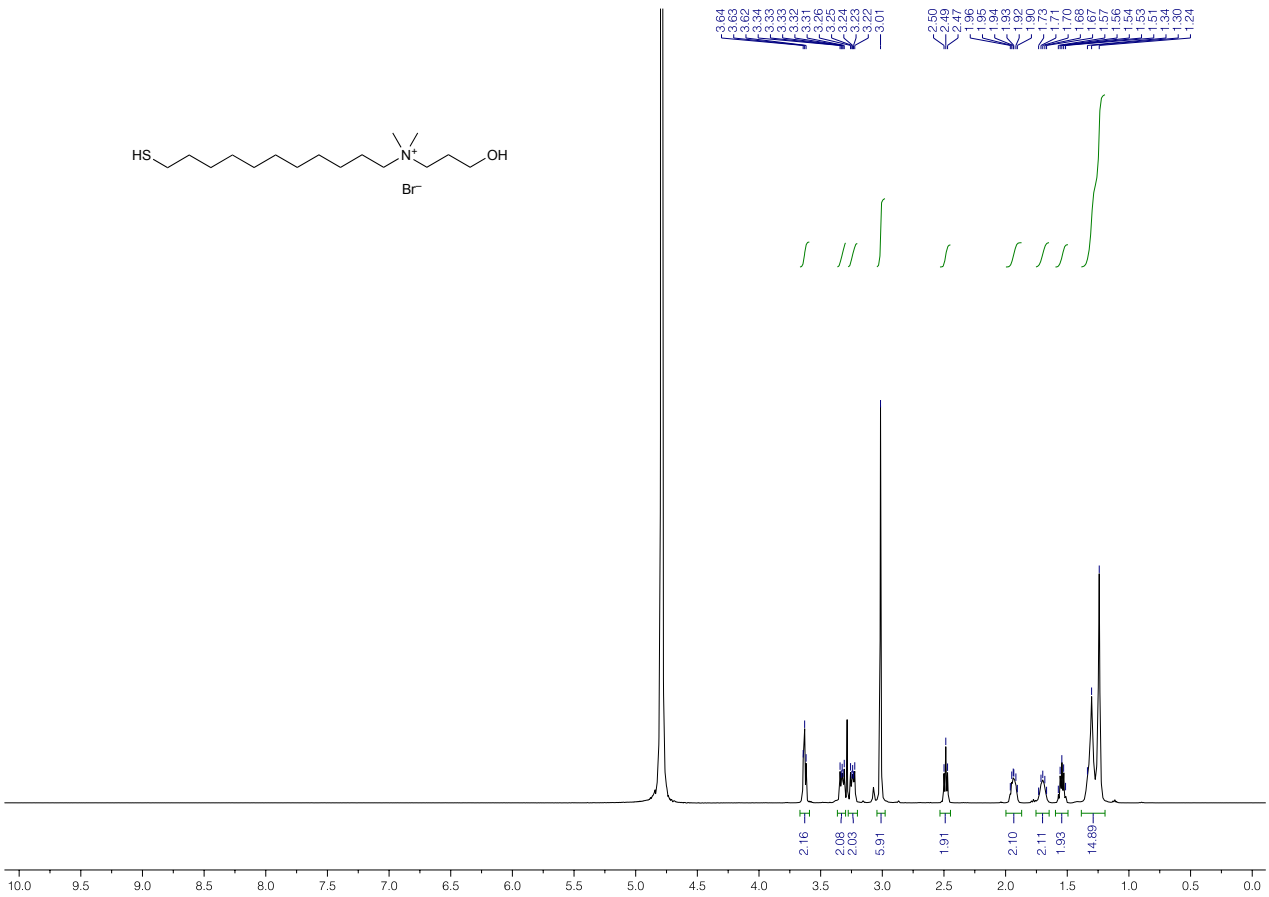

Figure S27. ^{1}H NMR spectrum of **B2** (500 MHz, D_2O).

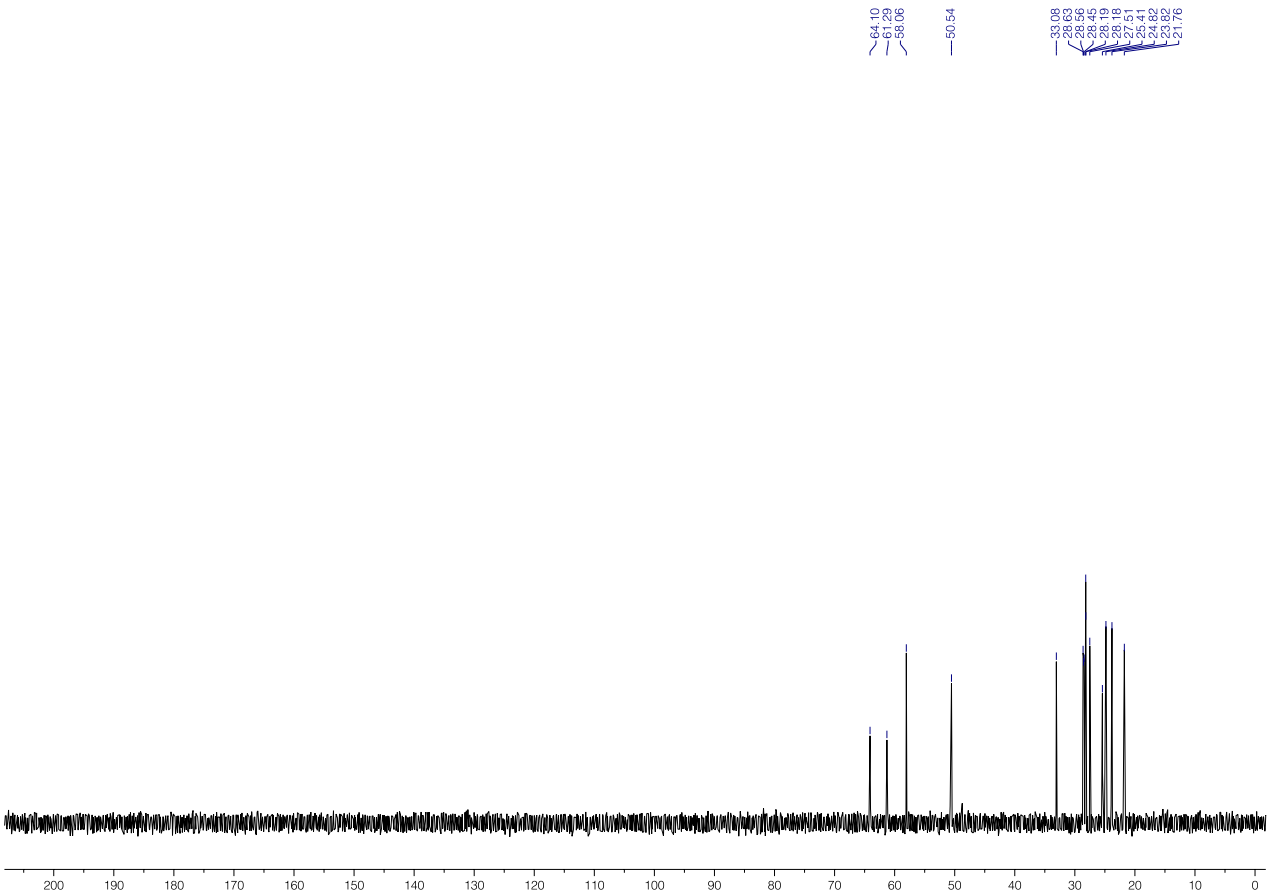

Figure S28. ^{13}C NMR spectrum of **B2** (125 MHz, D_2O).

3.3. Background ligand **B3**

Tetramethylammonium 3-mercaptopropanoate (**B3**) was obtained by neutralizing the commercially available 3-mercaptopropionic acid with tetramethylammonium hydroxide after adsorption onto nanoparticles.

3.4. Background ligand **B4**

6-mercapto-*N*,*N*,*N*-trimethylhexan-1-aminium bromide (**B4**) was synthesized based on a previously reported literature procedure.[6]

3.5. Background ligand **B5**

Tetramethylammonium 3-mercaptoundecanoate (**B5**) was obtained by neutralizing the commercially available 11-mercaptoundecanoic acid with tetramethylammonium hydroxide after adsorption onto nanoparticles.

3.6. Background ligand **B6**

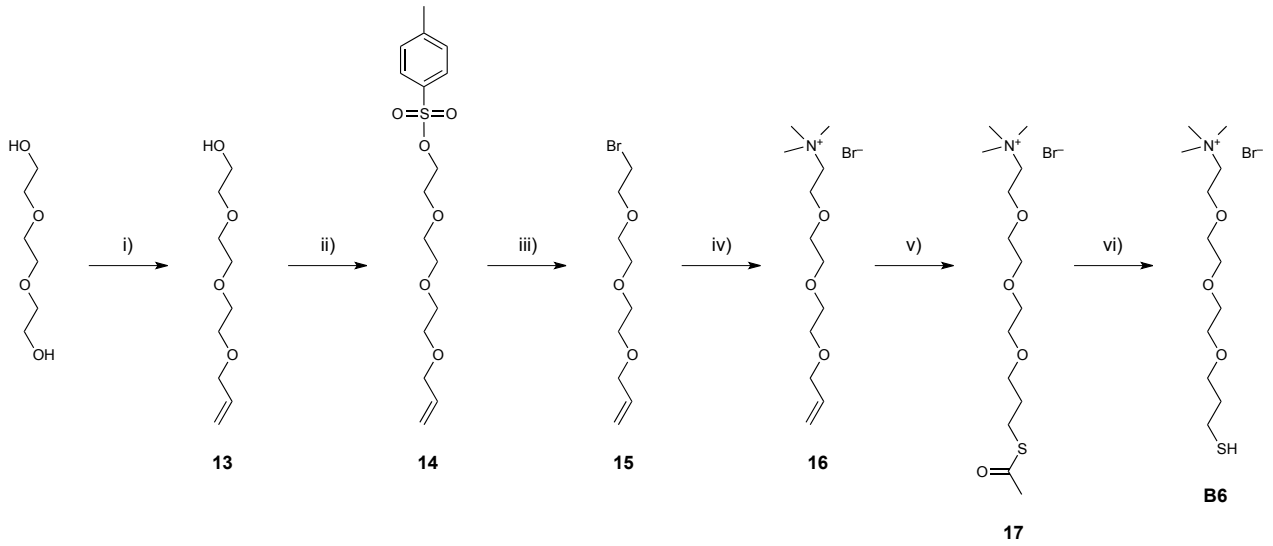

Scheme S5. Synthetic route for ligand **B6**. Reagents and conditions: i) NaOH/H_2O, allyl bromide, 100 ºC, 15 min, 88%; ii) Et_3N, TsCl, DCM, RT, overnight, 89%; iii) LiBr, acetone, reflux, overnight, 99%; iv) Me_3N/EtOH, RT, 2 d, quantitative; v) CH_3COSH, MeOH, UVB, overnight, quantitative; vi) HCl/MeOH, reflux, 6 h, quantitative.

2-(2-(2-(allyloxy)ethoxy)ethoxy)ethanol (**13**): Triethylene glycol (18.47 g; 123.0 mmol) was added to a solution of NaOH (1.32 g; 33.0 mmol) in water (1.5 mL). The resulting solution was stirred at 100 ºC for 30 min. Then, allyl bromide (3.63 g; 30.0 mmol) was added. After 15 min, the reaction mixture was cooled to room temperature and the crude product was extracted with CH_2Cl_2 (150 mL). The organic phase was washed with brine (75 mL × 2), dried over $MgSO_4$, filtered, and finally concentrated *in vacuo* to afford 5.01 g of **13** (yield = 88%).

^{1}H NMR (400 MHz, $CDCl_3$): δ = 5.96–5.87 (m, 1H), 5.29–5.17 (m, 2H), 4.03–4.01 (d, 2H), 3.73–3.59 (m, 12H). **^{13}C NMR** (100 MHz, $CDCl_3$): δ = 134.78, 117.38, 72.64, 72.41, 70.78, 70.74, 70.49, 69.51, 61.90.

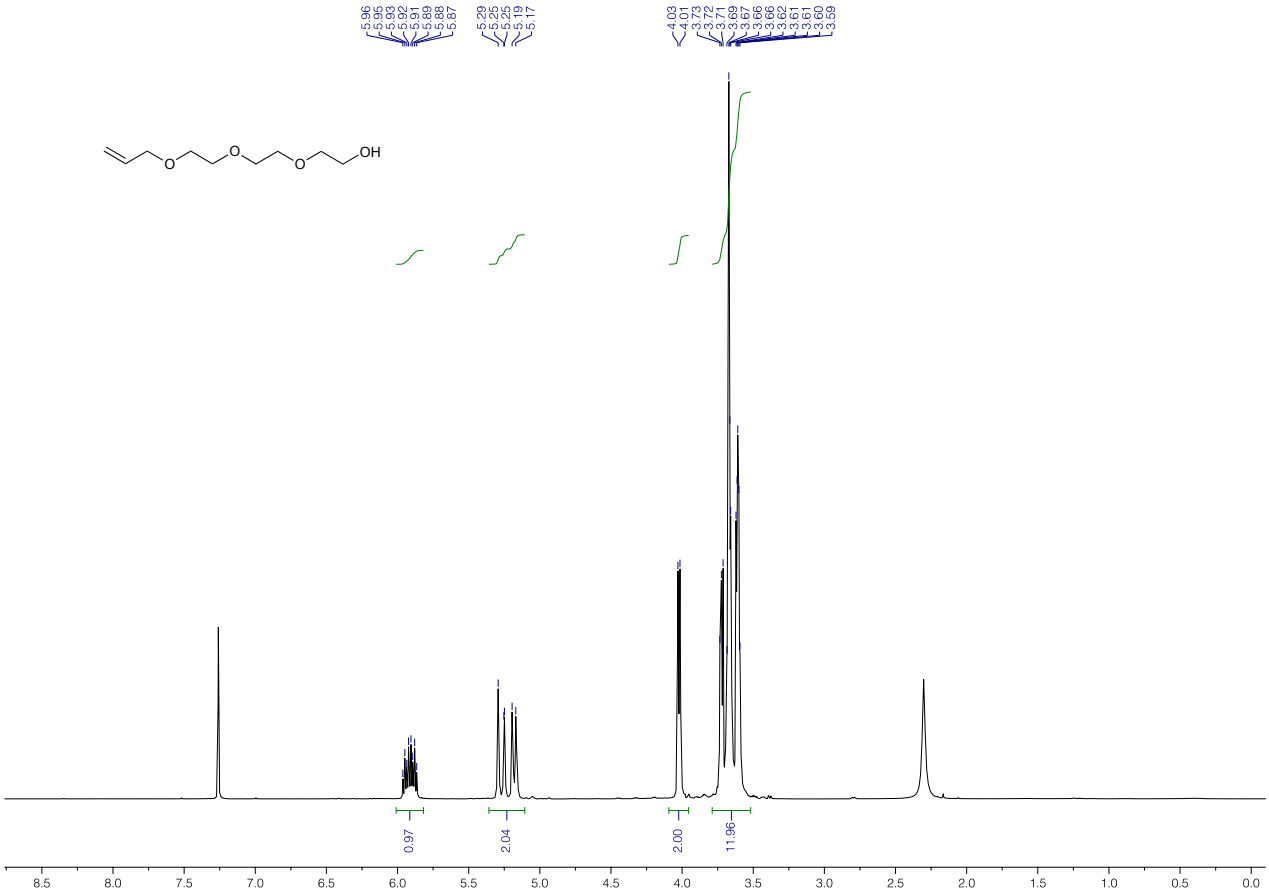

Figure S29. ^{1}H NMR spectrum of **13** (400 MHz, $CDCl_3$).

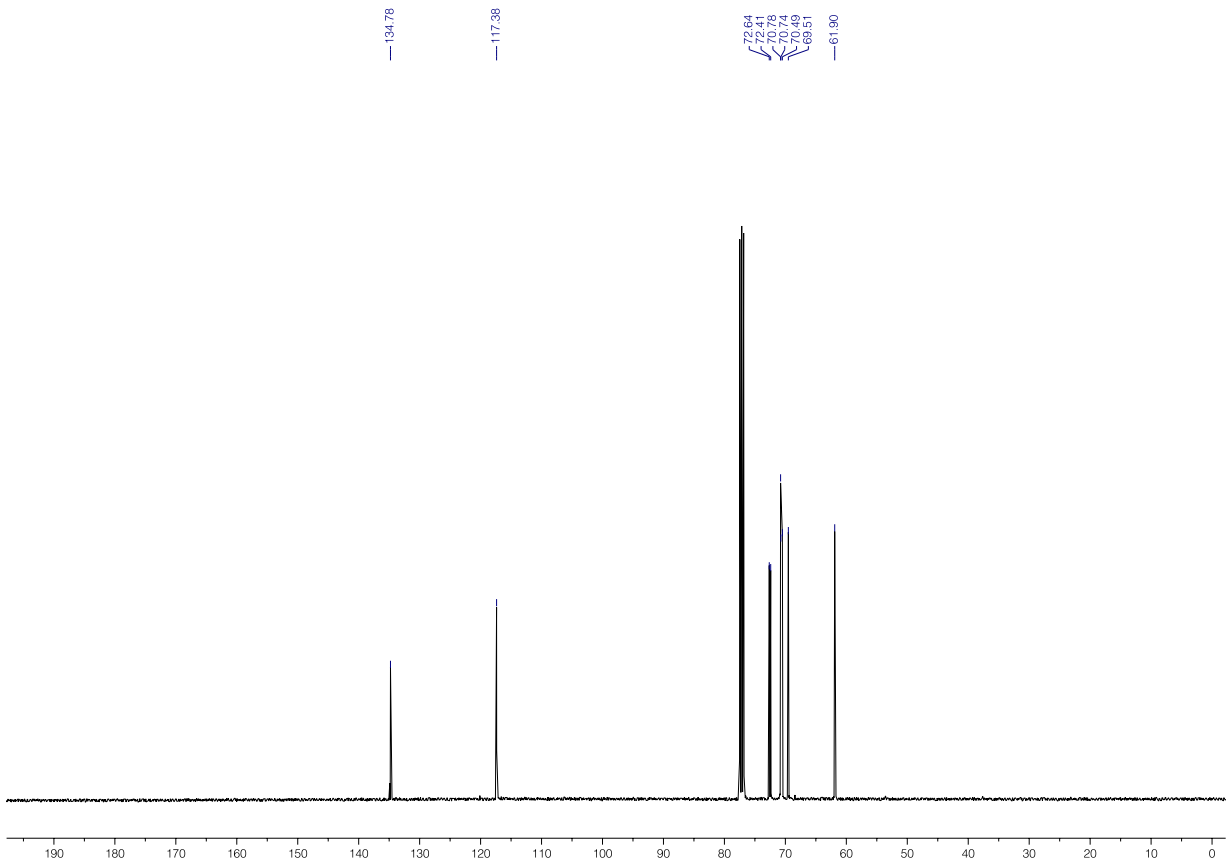

Figure S30. ^{13}C NMR spectrum of **13** (100 MHz, $CDCl_3$).

2-(2-(2-(allyloxy)ethoxy)ethoxy)ethyl 4-methylbenzenesulfonate (**14**): To a magnetically stirred solution of **13** (3.044 g, 16.00 mmol) and Et_3N (5.58 mL; 4.11 g; 40.6 mmol) in DCM (50 mL) at 0 ºC was added dropwise a solution of TsCl (9.15 g, 48.00 mmol) in DCM (30 mL). The reaction mixture was kept stirred at room temperature overnight and then washed with a saturated solution of $NaHCO_3$ in water (100 mL). The organic phase was collected and the crude product was extracted from the aqueous phase using DCM (100 mL). The combined organic layers were washed with brine (100 mL × 2), dried over $MgSO_4$, and concentrated *in vacuo*. The obtained crude product was purified by silica gel column chromatography (eluent: from hexane/EtOAc = 3/1 to hexane/EtOAc = 1/1) to afford 4.92 g of **14** (yield = 89%).

^{1}H NMR (400 MHz, $CDCl_3$): δ = 7.81–7.79 (d, 2H), 7.35–7.33 (d, 2H), 5.95–5.86 (m, 1H), 5.29–5.16 (m, 2H), 4.16 (t, 2H), 4.02–4.00 (m, 2H), 3.69 (t, 2H), 3.64–3.56 (m, 8H), 2.44 (s, 3H). **^{13}C NMR** (100 MHz, $CDCl_3$): δ = 144.91, 134.87, 133.17, 129.95, 128.13, 117.28, 72.38, 70.91, 70.82, 70.72, 69.54, 69.38, 68.83, 21.79.

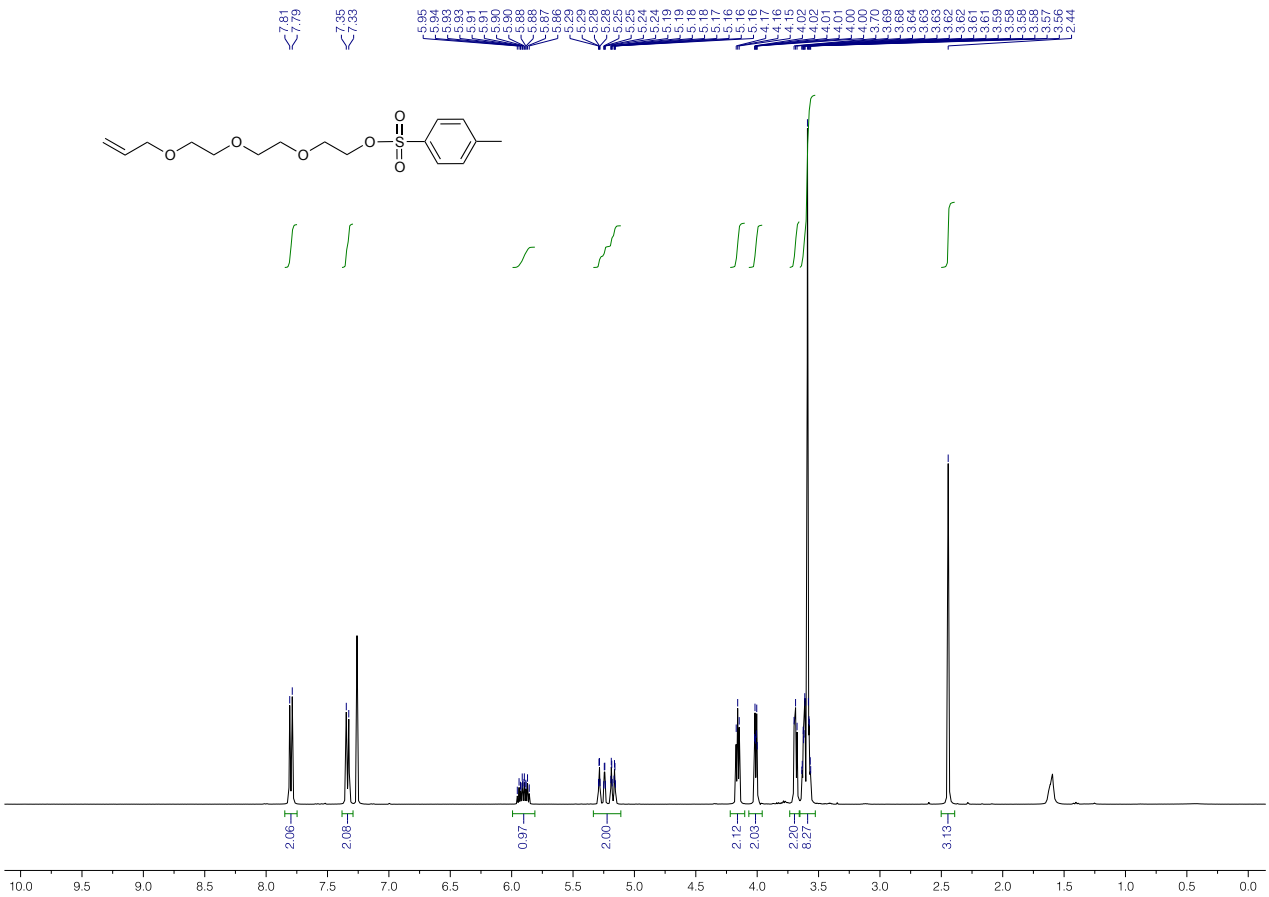

Figure S31. ^{1}H NMR spectrum of **14** (400 MHz, $CDCl_3$).

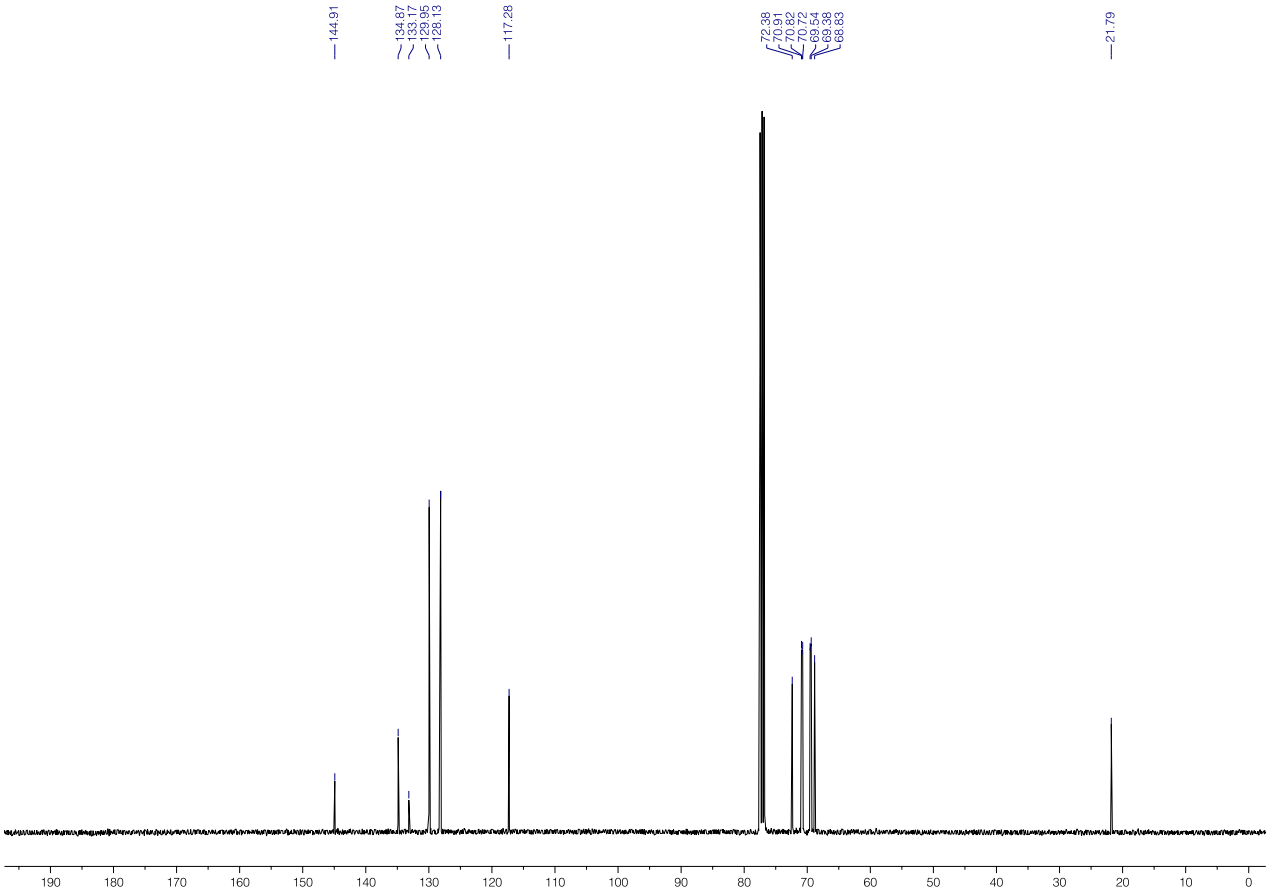

Figure S32. ^{13}C NMR spectrum of **14** (100 MHz, $CDCl_3$).

3-(2-(2-(2-bromoethoxy)ethoxy)ethoxy)prop-1-ene (**15**): To a solution of **14** (1.180 g; 34.26 mmol) in acetone (30 mL) was added lithium bromide (2.941 g; 34.26 mmol), and the mixture was refluxed under nitrogen atmosphere overnight. Then, the solvent was removed *in vacuo*. DCM (150 mL) was added to dissolve the crude product and the insoluble solids were filtered off. The filtrate was washed with brine (100 mL × 4), dried over $MgSO_4$, and concentrated *in vacuo* to afford 0.852 g of **15** (yield = 99%).

^{1}H NMR (400 MHz, $CDCl_3$): δ = 5.97–5.87 (m, 1H), 5.30–5.17 (m, 2H), 4.04–4.02 (d, 2H), 3.82 (t, 2H), 3.68–3.60 (m, 8H), 3.47 (t, 2H). **^{13}C NMR** (100 MHz, $CDCl_3$): δ = 134.89, 117.28, 72.41, 71.38, 70.88, 70.81, 70.72, 69.58, 30.45.

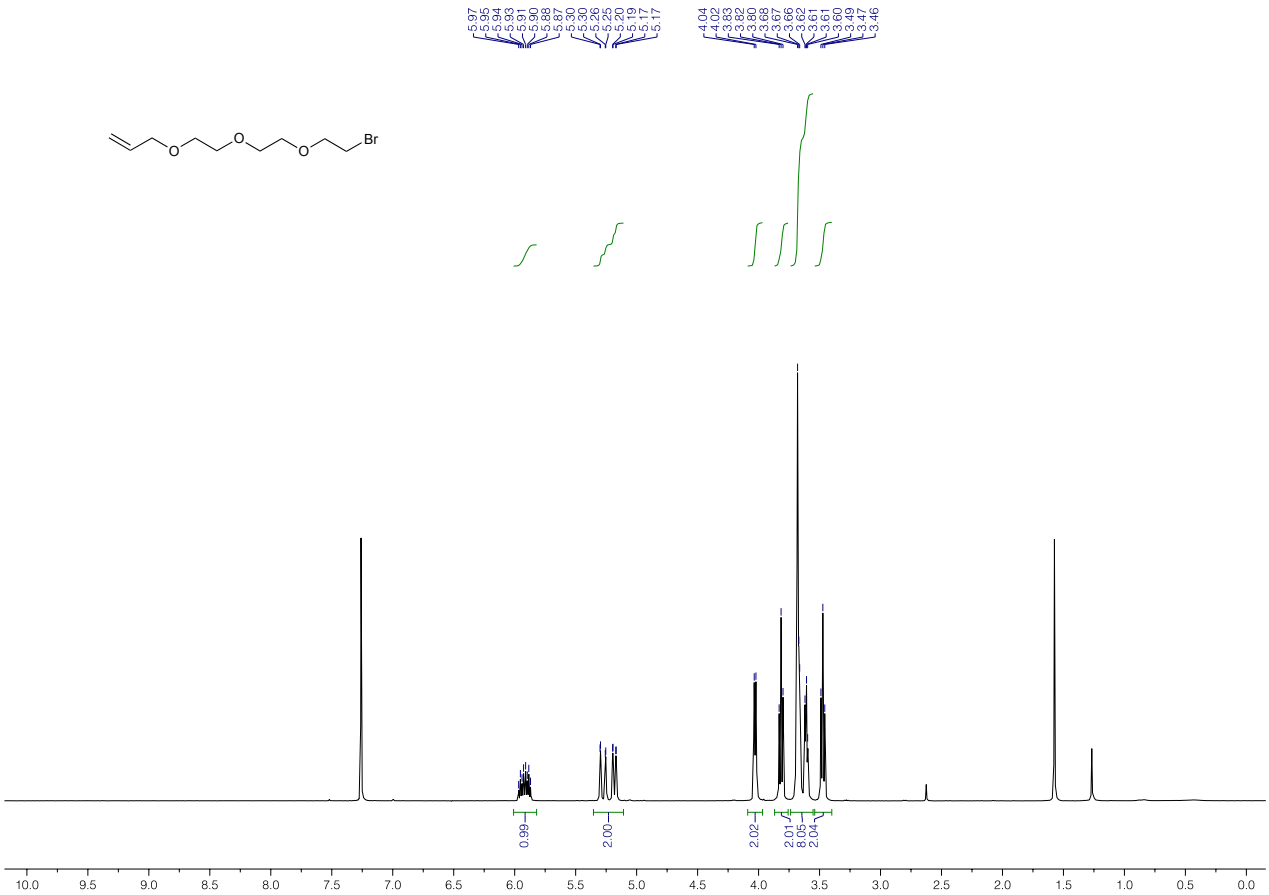

Figure S33. ^{1}H NMR spectrum of **15** (400 MHz, $CDCl_3$).

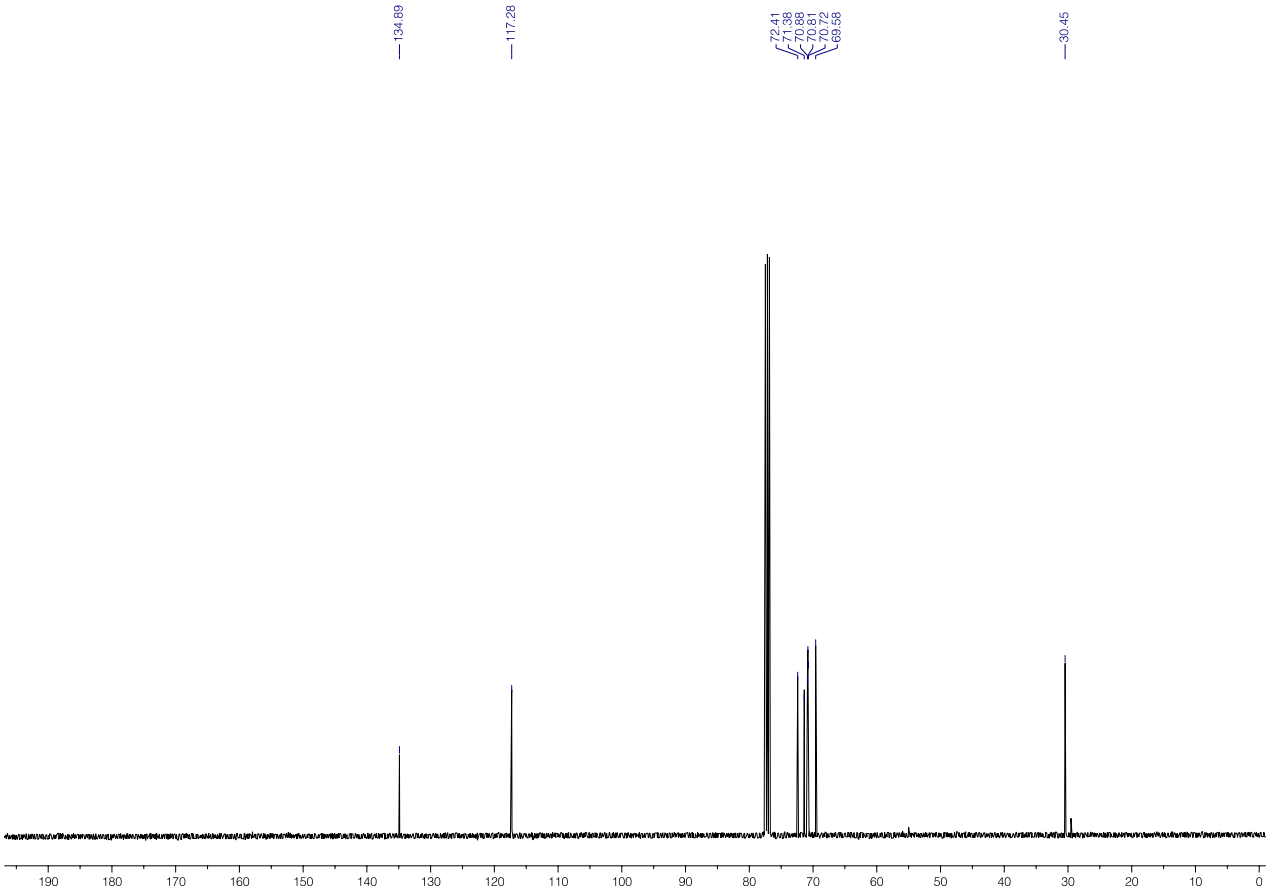

Figure S34. ^{13}C NMR spectrum of **15** (100 MHz, $CDCl_3$).

2-(2-(2-(allyloxy)ethoxy)ethoxy)-*N,N,N*-trimethylethanaminium bromide (**16**): Compound **15** (852 mg; 3.37 mmol) was stirred in 4.0 mL of 33 wt. % ethanolic solution of trimethylamine at room temperature for 2 days, after which the reaction mixture was concentrated *in vacuo* to afford **16** in a quantitative yield.

^{1}H NMR (400 MHz, $CDCl_3$): δ = 5.93–5.83 (m, 1H), 5.28–5.17 (m, 2H), 3.99–3.98 (m, 6H), 3.69–3.67 (m, 2H), 3.62–3.60 (m, 4H), 3.57–3.55 (m, 2H), 3.48 (s, 9H). **^{13}C NMR** (100 MHz, $CDCl_3$): δ = 134.71, 117.50, 72.31, 70.63, 70.52, 70.34, 69.52, 65.81, 65.37, 54.88. **HRMS** calcd for $C_{12}H_{26}NO_3$ $[M - Br]^+$, m/z = 232.1913; found, 232.1915.

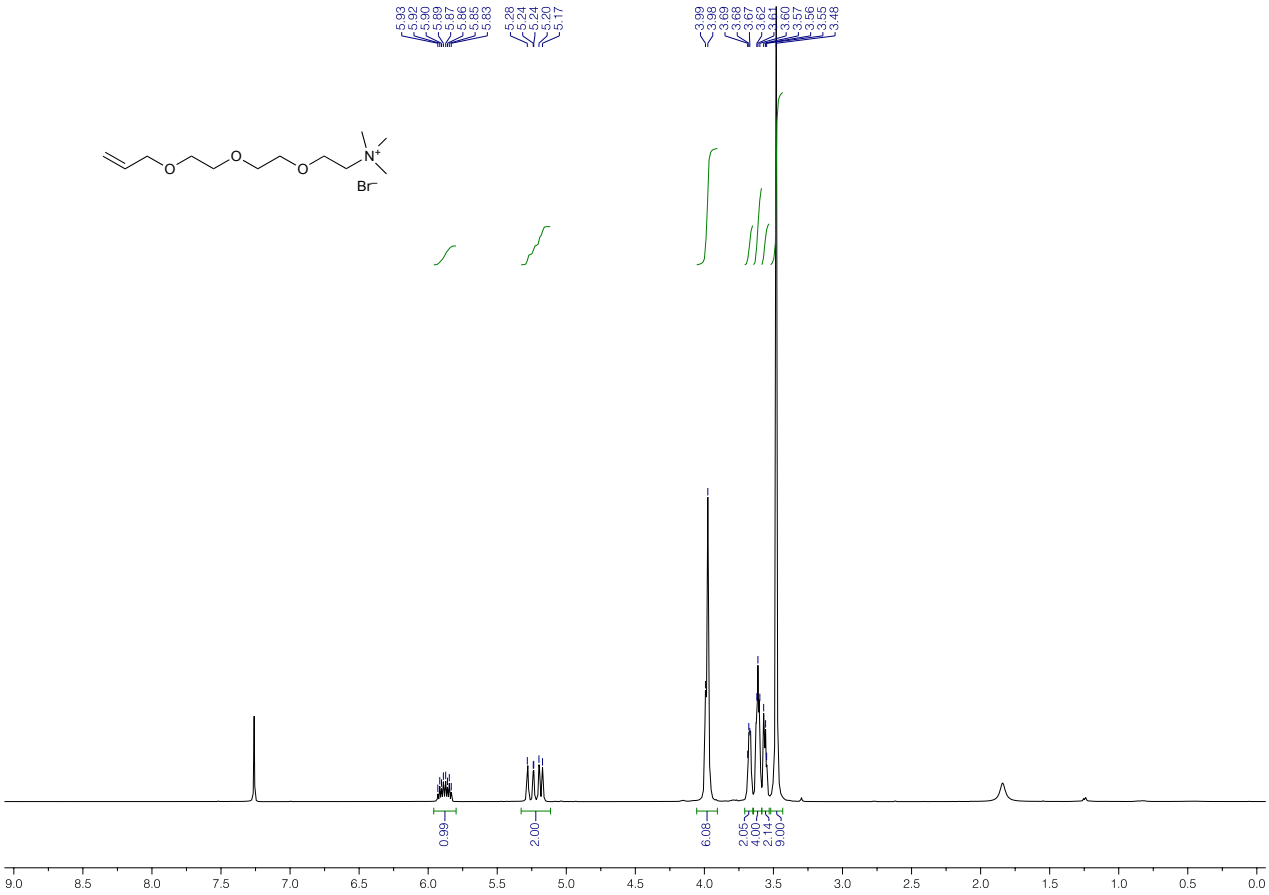

Figure S35. ^{1}H NMR spectrum of **16** (400 MHz, $CDCl_3$).

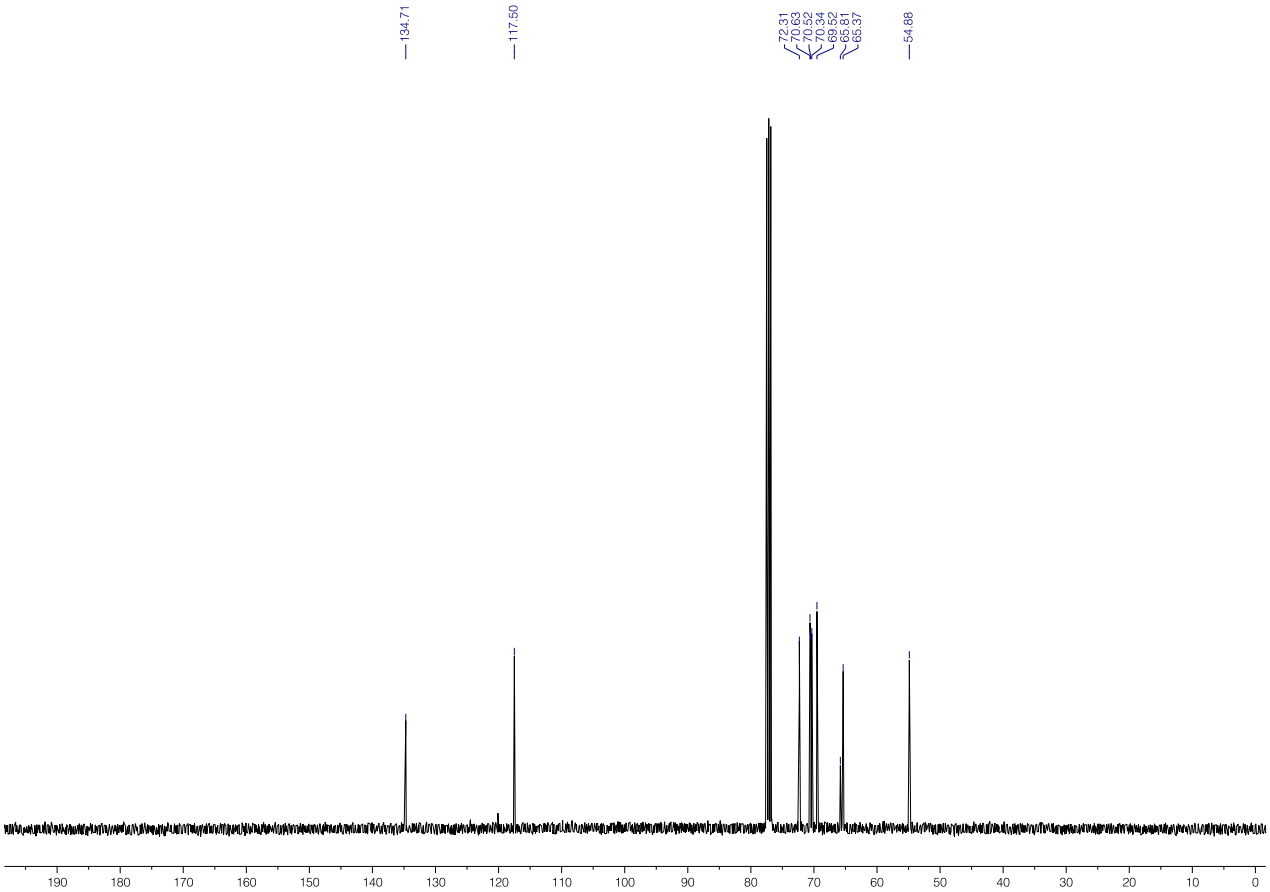

Figure S36. ^{13}C NMR spectrum of **16** (100 MHz, $CDCl_3$).

***N,N,N*-trimethyl-14-oxo-3,6,9-trioxa-13-thiapentadecan-1-aminium bromide** (**17**): A solution of **16** (1006 mg; 3.22 mmol) and thioacetic acid (680 µL; 724 mg; 9.51 mmol) in degassed methanol (6 mL) was stirred under UVB light overnight. Then, the reaction mixture was concentrated *in vacuo* at room temperature to afford **17** in a quantitative yield.

^{1}H NMR (400 MHz, $CDCl_3$): δ = 4.00 (m, 4H), 3.69–3.47 (m, 19H), 2.92 (t, 2H), 2.33 (s, 3H), 1.86–1.79 (m, 2H). **^{13}C NMR** (100 MHz, $CDCl_3$): δ = 196.27, 70.62, 70.50, 70.38, 70.35, 69.83, 65.79, 65.36, 54.86, 30.85, 29.76, 26.20. **HRMS** calcd for $C_{14}H_{30}NO_4S$ $[M – Br]^+$, m/z = 308.1896; found, 308.1898.

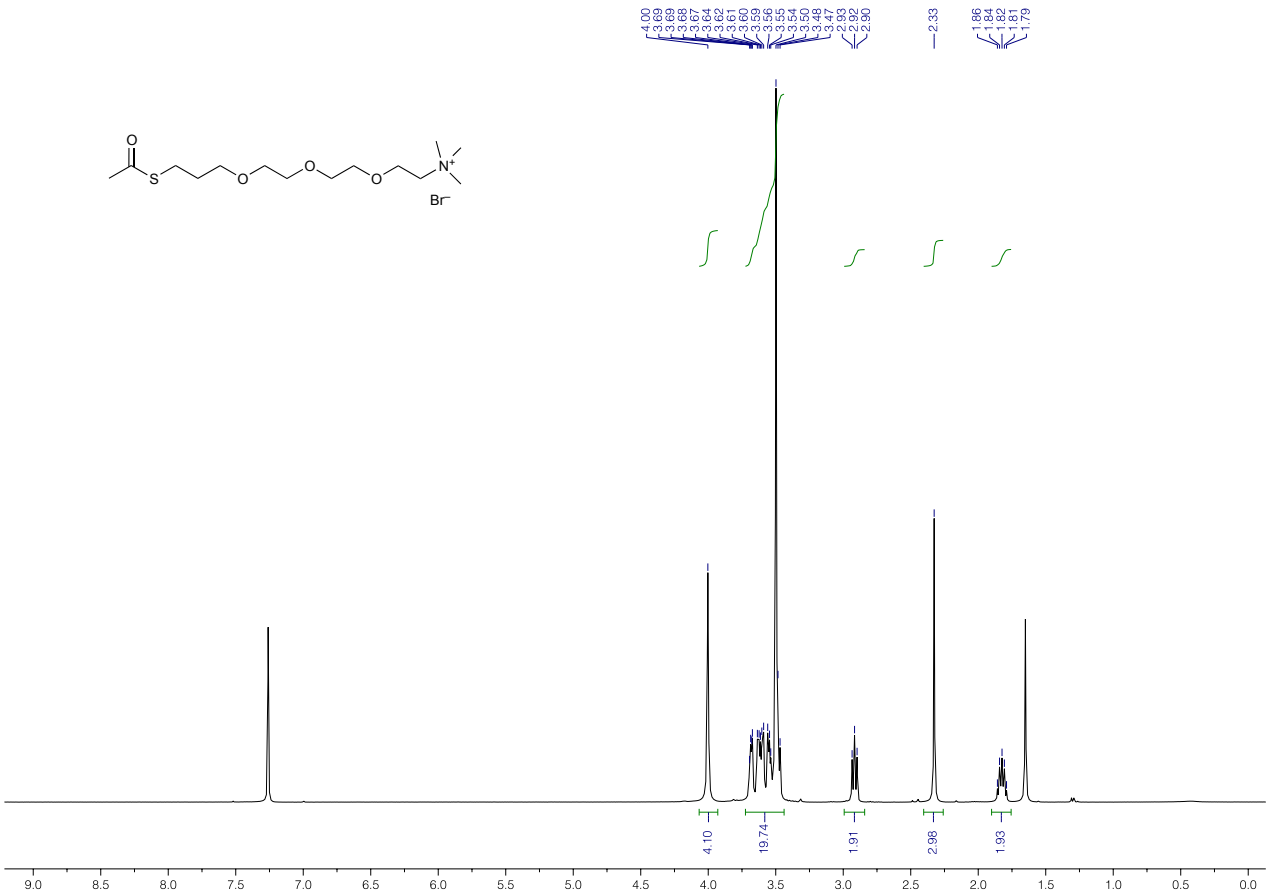

Figure S37. ^{1}H NMR spectrum of **17** (400 MHz, $CDCl_3$).

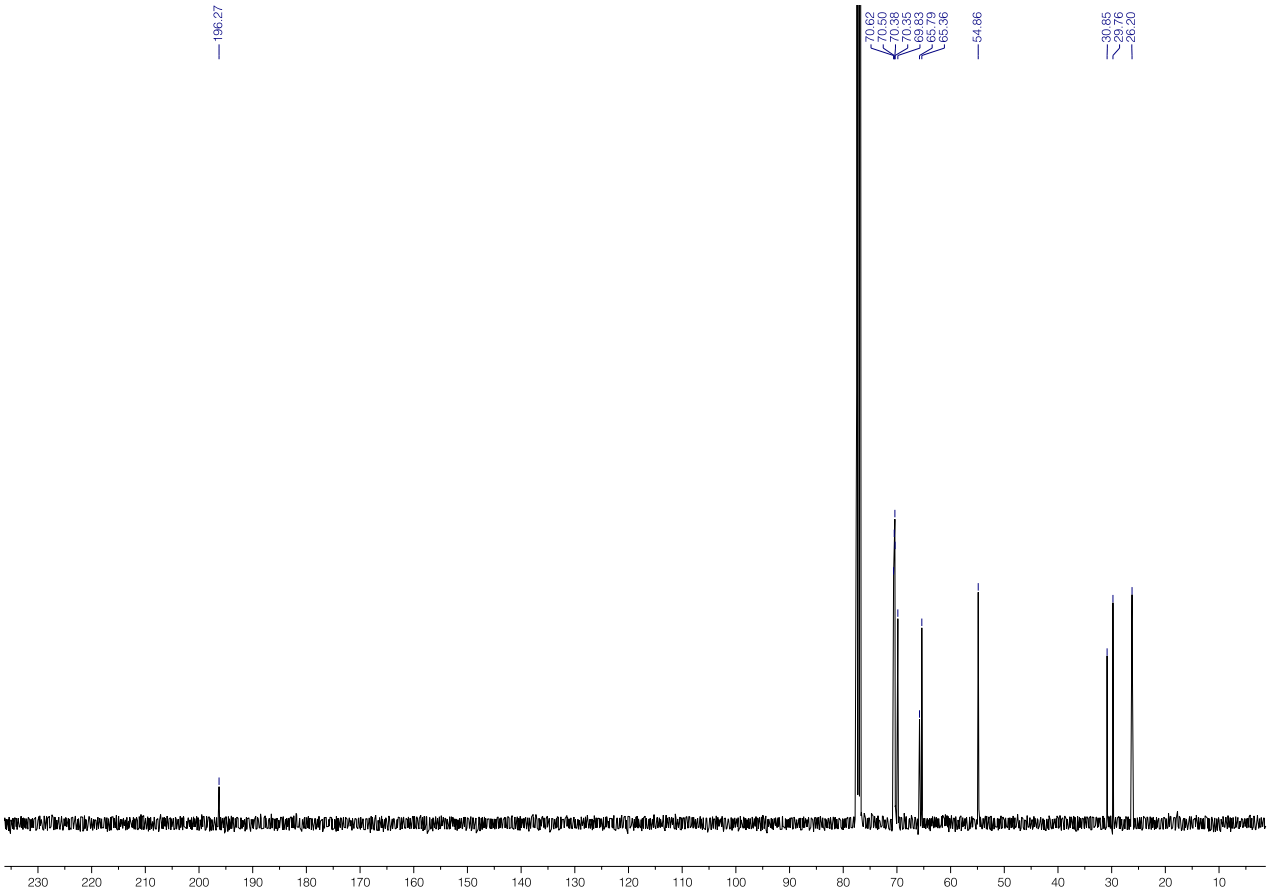

Figure S38. ^{13}C NMR spectrum of **17** (100 MHz, $CDCl_3$).

2-(2-(2-(3-mercaptopropoxy)ethoxy)ethoxy)-*N,N,N*-trimethylethanaminium bromide (**B6**): A solution of **17** (272 mg, 0.70 mmol) in methanol (10 mL) was degassed by bubbling with nitrogen for 15 min. Then, 2.2 mL of 1.25 M methanolic HCl solution was added and the reaction mixture was refluxed for 6 h. The reaction mixture was cooled down to room temperature and the solvent was removed *in vacuo* to afford **B6** in a near-quantitative fashion.

^{1}H NMR (400 MHz, $CDCl_3$): δ = 3.99–3.90 (m, 4H), 3.68–3.66 (m, 2H), 3.64–3.58 (m, 4H), 3.56–3.53 (m, 4H), 3.46 (s, 9H), 2.60 (t, 2H), 1.89–1.82 (m, 2H). **^{13}C NMR** (100 MHz, $CDCl_3$): δ = 70.61, 70.55, 70.37, 70.29, 69.23, 65.87, 65.35, 54.90, 33.71, 21.52. **HRMS** calcd for $C_{12}H_{28}NO_3S$ $[M - Br]^+$, m/z = 266.1790; found, 266.1798.

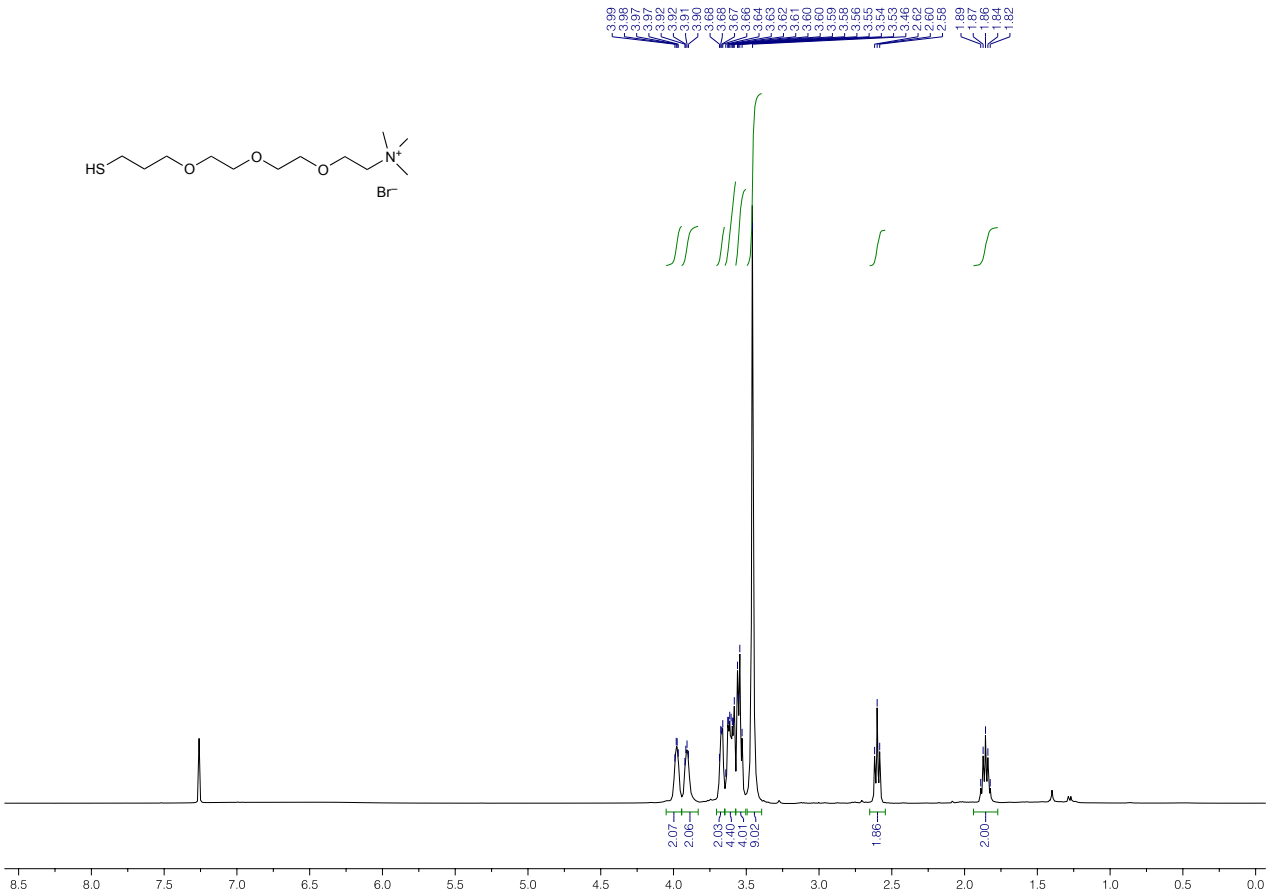

Figure S39. ^{1}H NMR spectrum of **B6** (400 MHz, $CDCl_3$).

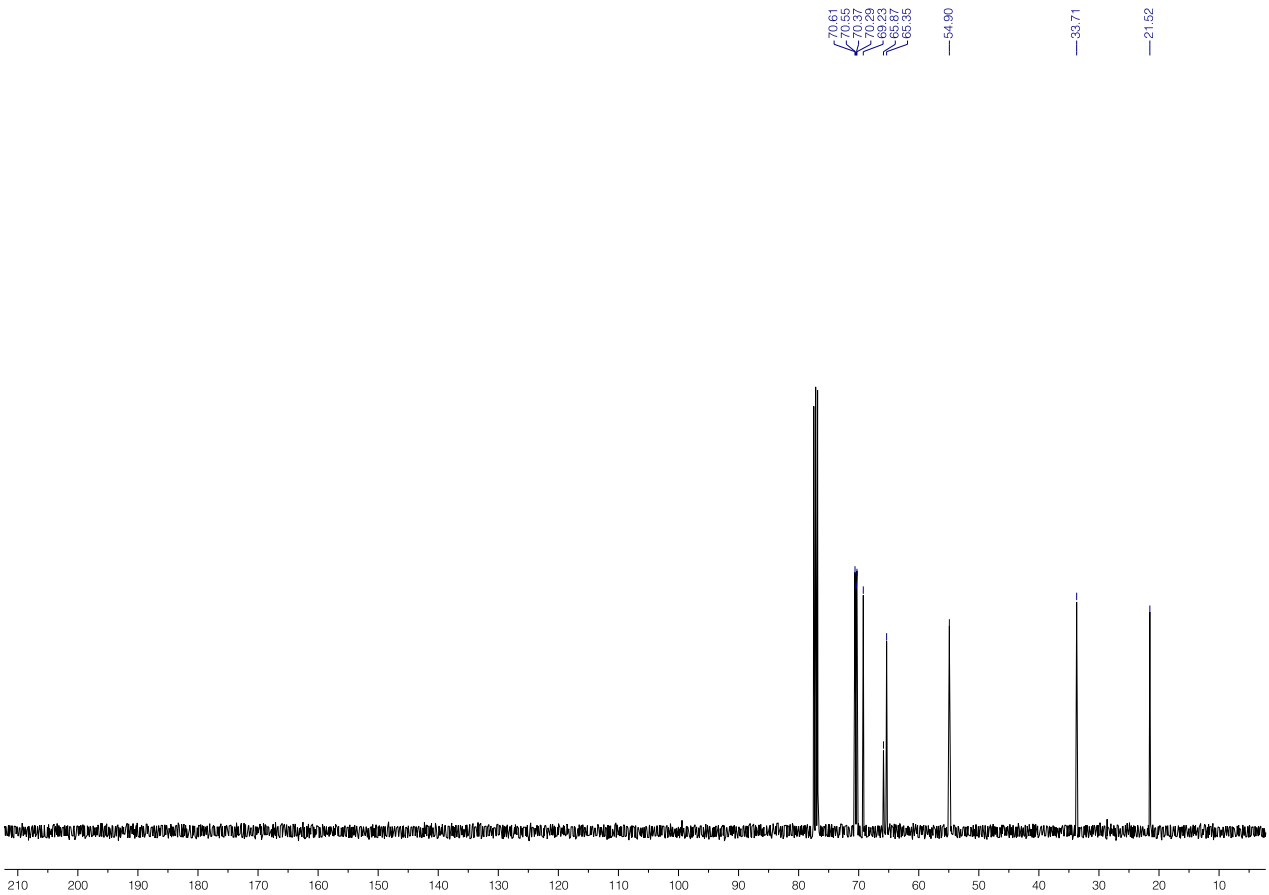

Figure S40. ^{13}C NMR spectrum of **B6** (100 MHz, $CDCl_3$).

3.7. Background ligand **B7**

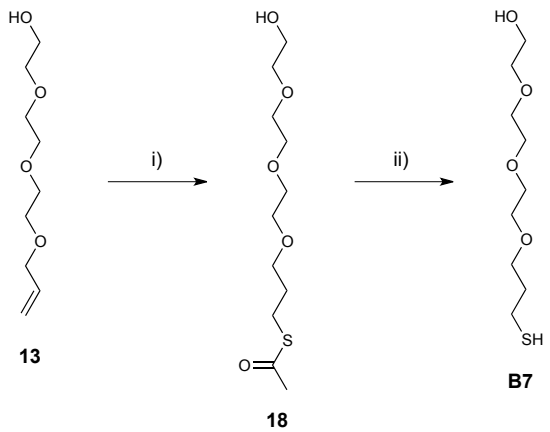

Scheme S6. Synthetic route for ligand **B7**. Reagents and conditions: i) CH_3COSH, DCM, UVB, overnight, quantitative; ii) HCl/MeOH, reflux, 6 h, quantitative.

***S*-(3-(2-(2-(2-hydroxyethoxy)ethoxy)ethoxy)propyl) ethanethioate** (**18**): A solution of **13** (obtained according to Scheme S5) (1.80 g; 9.46 mmol) and thioacetic acid (2.37 mL; 2.52 g; 33.16 mmol) in DCM (8 mL) was stirred at room temperature under UVB light overnight. Then, the reaction mixture was concentrated *in vacuo* to afford **18** in a quantitative yield.

^{1}H NMR (400 MHz, $CDCl_3$): δ = 3.73 (t, 2H), 3.69–3.58 (m, 10H), 3.51 (t, 2H), 2.95 (t, 2H), 2.32 (s, 3H), 1.89–1.82 (m, 2H). **^{13}C NMR** (100 MHz, $CDCl_3$): δ = 196.09, 72.64, 70.81, 70.70, 70.53, 70.33, 69.76, 61.93, 30.77, 29.68, 26.13.

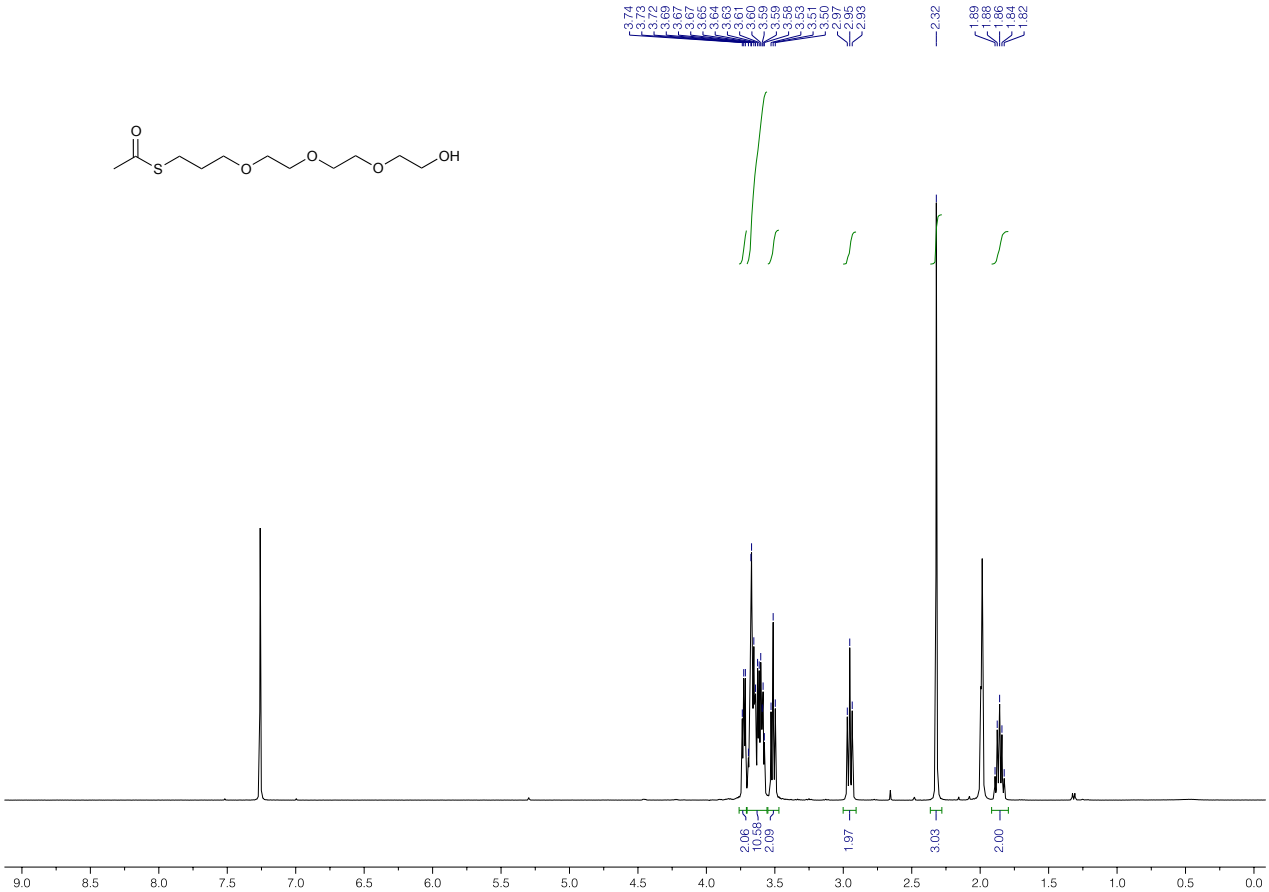

Figure S41. ^{1}H NMR spectrum of **18** (400 MHz, $CDCl_3$).

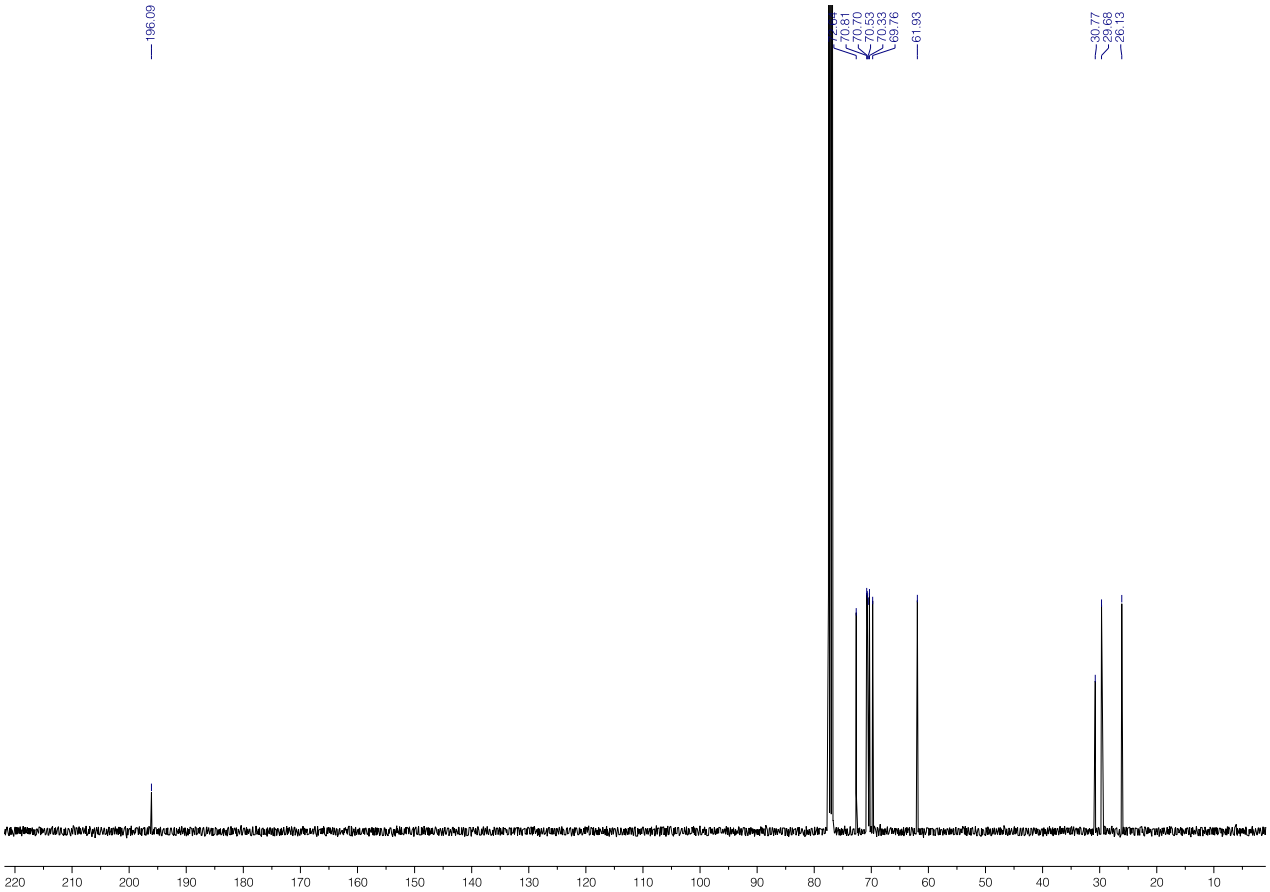

Figure S42. ^{13}C NMR spectrum of **18** (100 MHz, $CDCl_3$).

2-(2-(2-(3-mercaptopropoxy)ethoxy)ethoxy)ethanol (**B7**): A solution of **18** (266 mg; 1.00 mmol) in 10 mL of methanol was degassed by bubbling nitrogen for 15 min. Then, 5 mL of 1.25 M methanolic HCl solution was added and the reaction mixture was refluxed for 6 h. The reaction mixture was cooled down to room temperature and the solvent was evaporated *in vacuo* to afford **B7** in a quantitative yield.

^{1}H NMR (400 MHz, $CDCl_3$): δ = 3.73–3.56 (m, 14H), 2.65–2.61 (q, 2H), 1.91–1.85 (m, 2H), 1.40 (t, 1H). **^{13}C NMR** (100 MHz, $CDCl_3$): δ = 72.65, 70.79, 70.69, 70.51, 70.32, 69.26, 61.92, 33.78, 21.56. **HRMS** calcd for $C_9H_{20}NaO_4S$ $[M + Na]^+$, m/z = 247.0980; found, 247.0983.

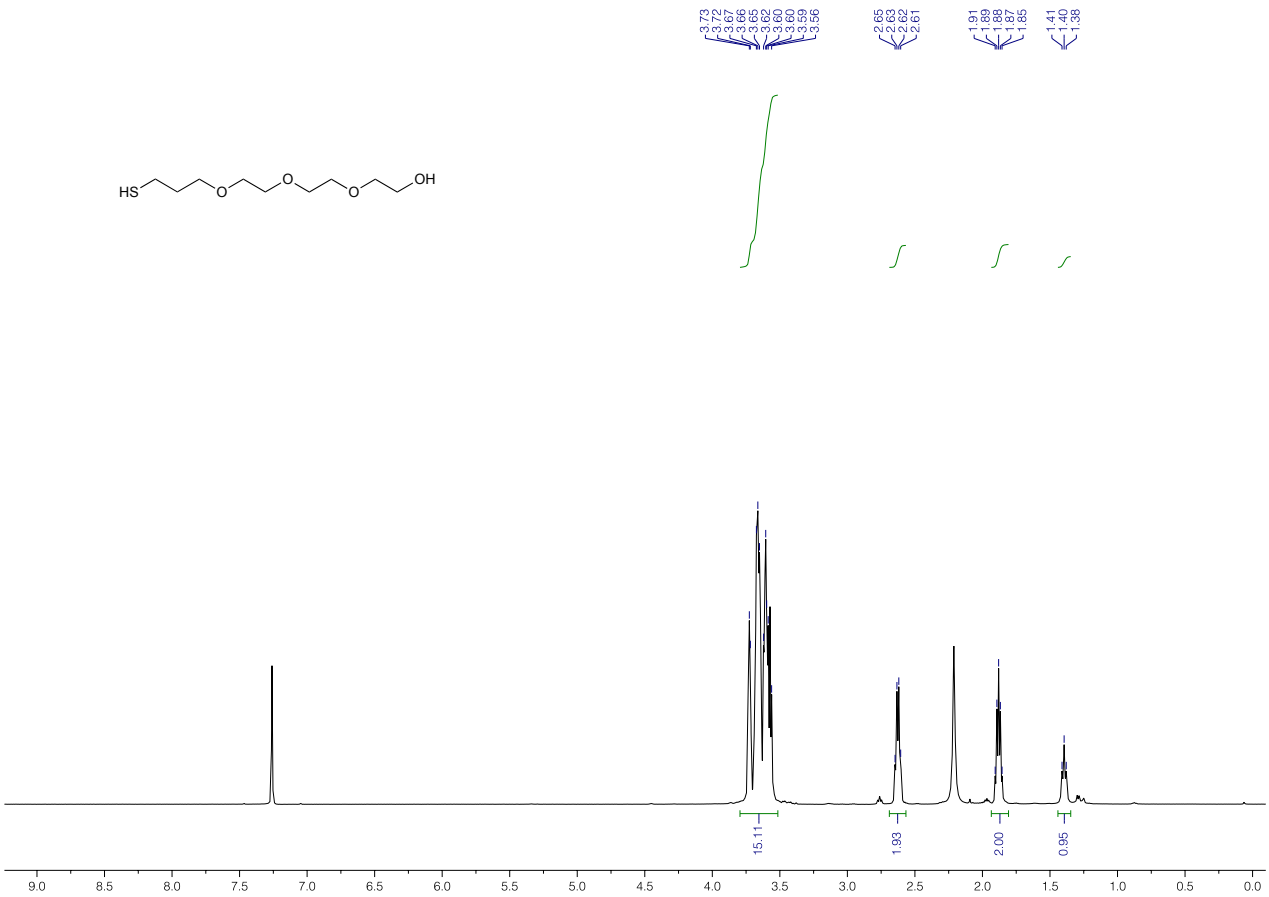

Figure S43. ^{1}H NMR spectrum of **B7** (400 MHz, $CDCl_3$).

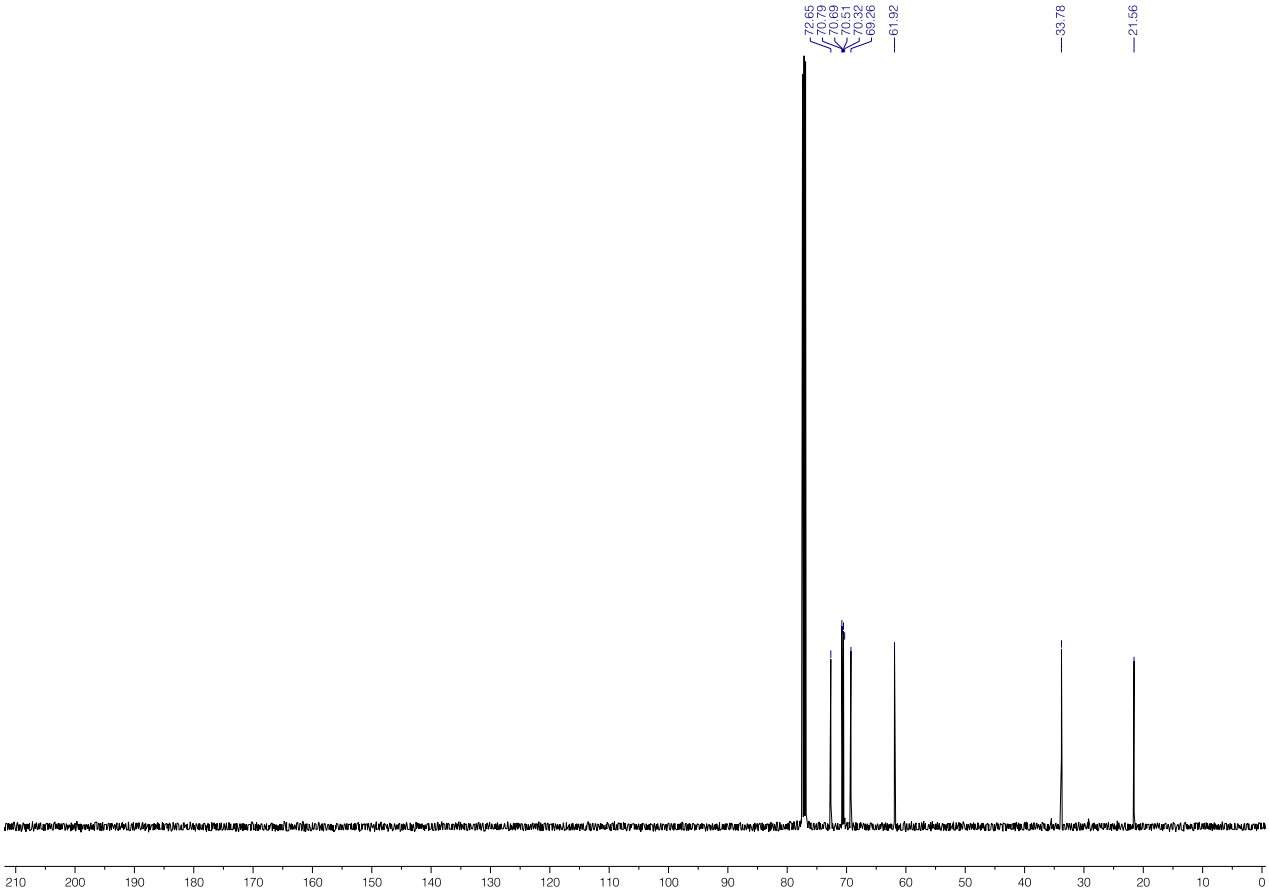

Figure S44. ^{13}C NMR spectrum of **B7** (100 MHz, $CDCl_3$).

3.8. Background ligand **B8**

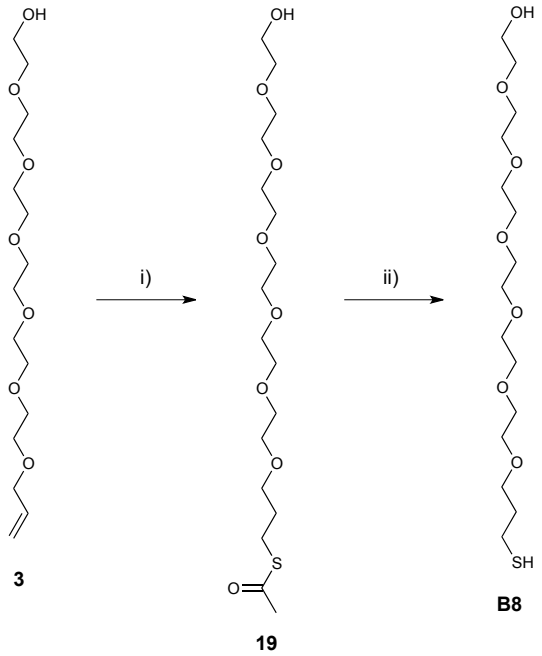

Scheme S7. Synthetic route for ligand **B8**. Reagents and conditions: i) CH_3COSH, DCM, UVB, overnight, quantitative; ii) HCl/MeOH, reflux, 6 h, quantitative.

***S*-(1-hydroxy-3,6,9,12,15,18-hexaoxahenicosan-21-yl) ethanethioate** (**19**): A solution of **3** (synthesized according to Scheme S2) (1.29 g; 4.00 mmol) and thioacetic acid (1,000 µL; 1.065 g; 13.99 mmol) in DCM (6 mL) was stirred at room temperature under UVB light overnight. Then, the reaction mixture was concentrated *in vacuo* to afford **19** in a quantitative yield.

^{1}H NMR (400 MHz, $CDCl_3$): δ = 3.73–3.70 (m, 2H), 3.66–3.56 (m, 22H), 3.50 (t, 2H), 2.94 (t, 2H), 2.53 (s, 1H), 2.32 (s, 3H), 1.88–1.82 (m, 2H). **^{13}C NMR** (100 MHz, $CDCl_3$): δ = 196.02, 72.65, 70.78, 70.77, 70.75, 70.72, 70.53, 70.37, 69.74, 61.93, 30.77, 29.72, 26.15.

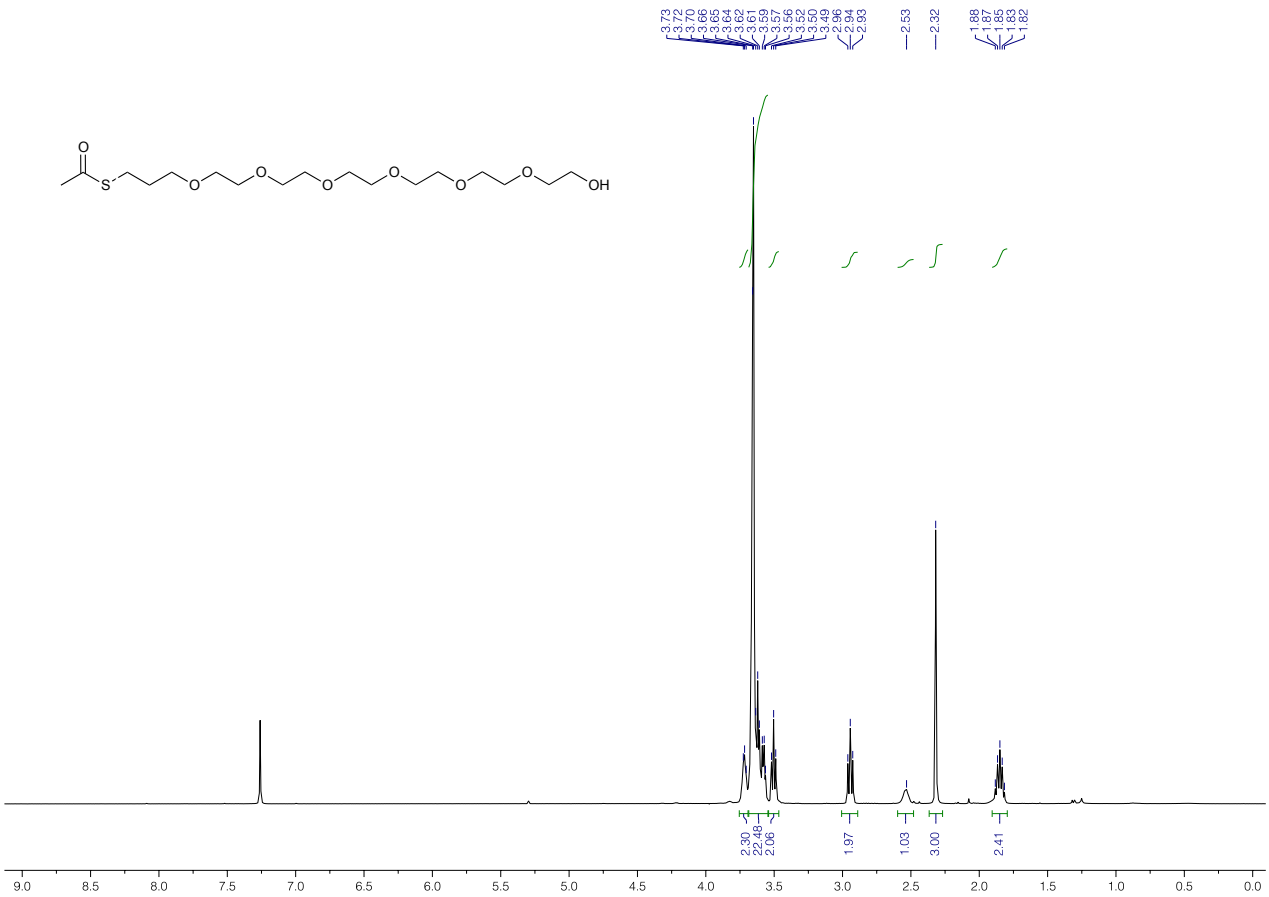

Figure S45. ^{1}H NMR spectrum of **19** (400 MHz, $CDCl_3$).

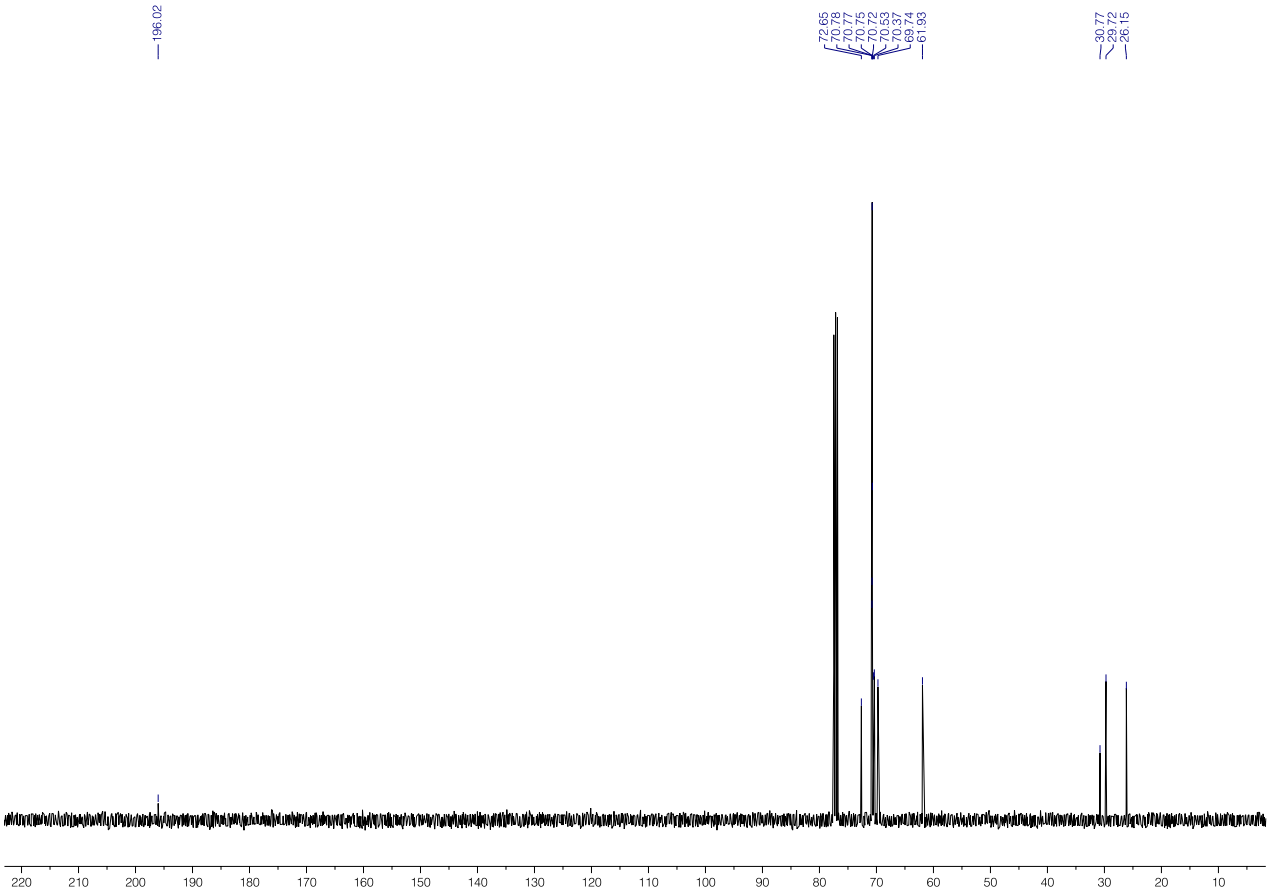

Figure S46. ^{13}C NMR spectrum of **19** (100 MHz, $CDCl_3$).

2-(2-(2-(3-mercaptopropoxy)ethoxy)ethoxy)ethanol (**B8**): A solution of **19** (199 mg; 0.50 mmol) in 10 mL of methanol was degassed by bubbling nitrogen for 15 min. Then, 3 mL of 1.25 M methanolic HCl solution was added and the reaction mixture was refluxed for 6 h. The reaction mixture was cooled down to room temperature and the solvent was evaporated *in vacuo* to afford **B8** in a quantitative yield.

^{1}H NMR (400 MHz, $CDCl_3$): δ = 3.74–3.71 (m, 2H), 3.66–3.55 (m, 24H), 2.65–2.59 (q, 2H), 1.91–1.84 (m, 2H), 1.38 (t, 1H). **^{13}C NMR** (100 MHz, $CDCl_3$): δ = 77.16, 72.66, 70.77, 70.76, 70.74, 70.70, 70.50, 70.37, 69.25, 61.91, 33.88, 21.58. **HRMS** calcd for $C_{15}H_{32}NaO_7S$ $[M + Na]^+$, m/z = 379.1766; found, 379.1764.

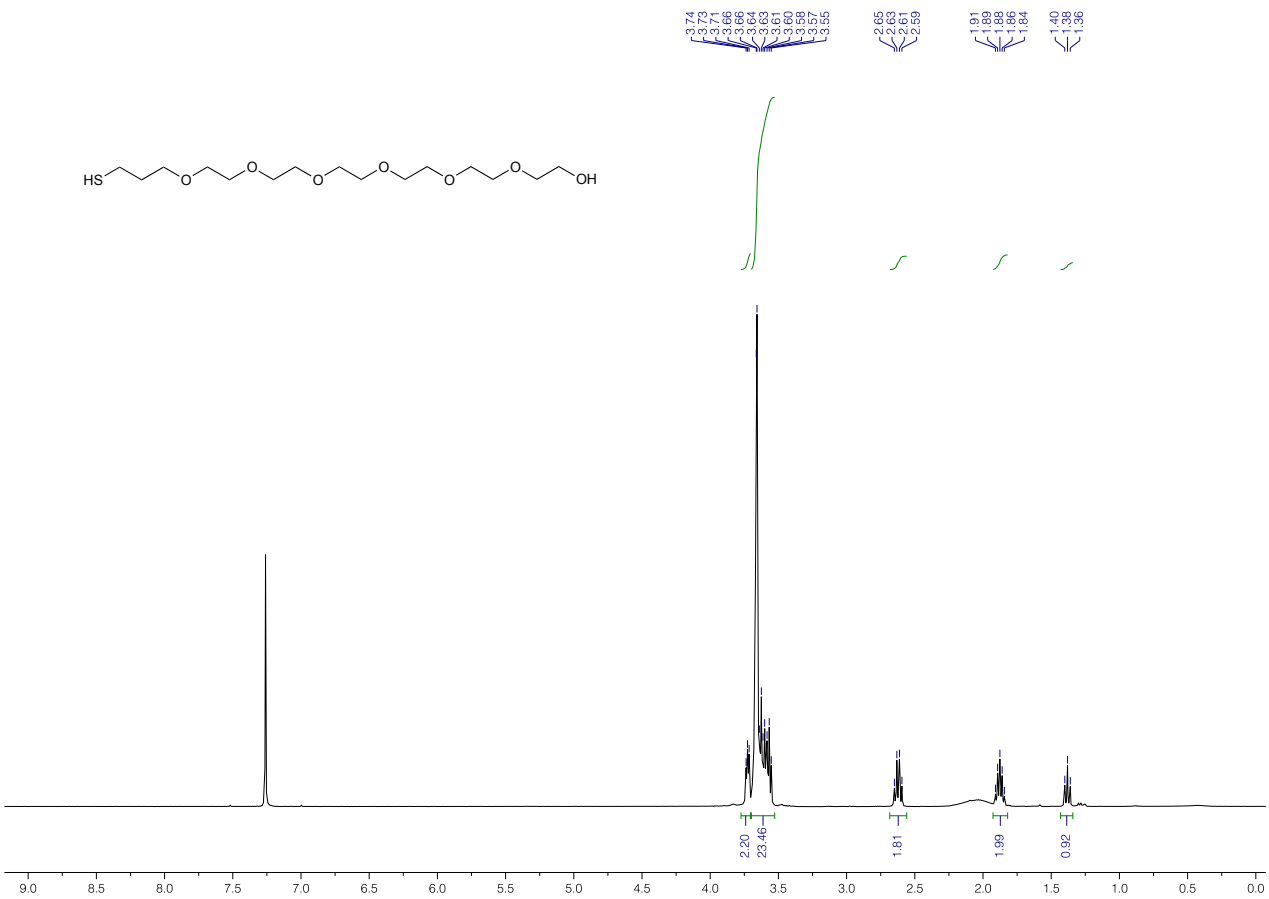

Figure S47. ^{1}H NMR spectrum of **B8** (400 MHz, $CDCl_3$).

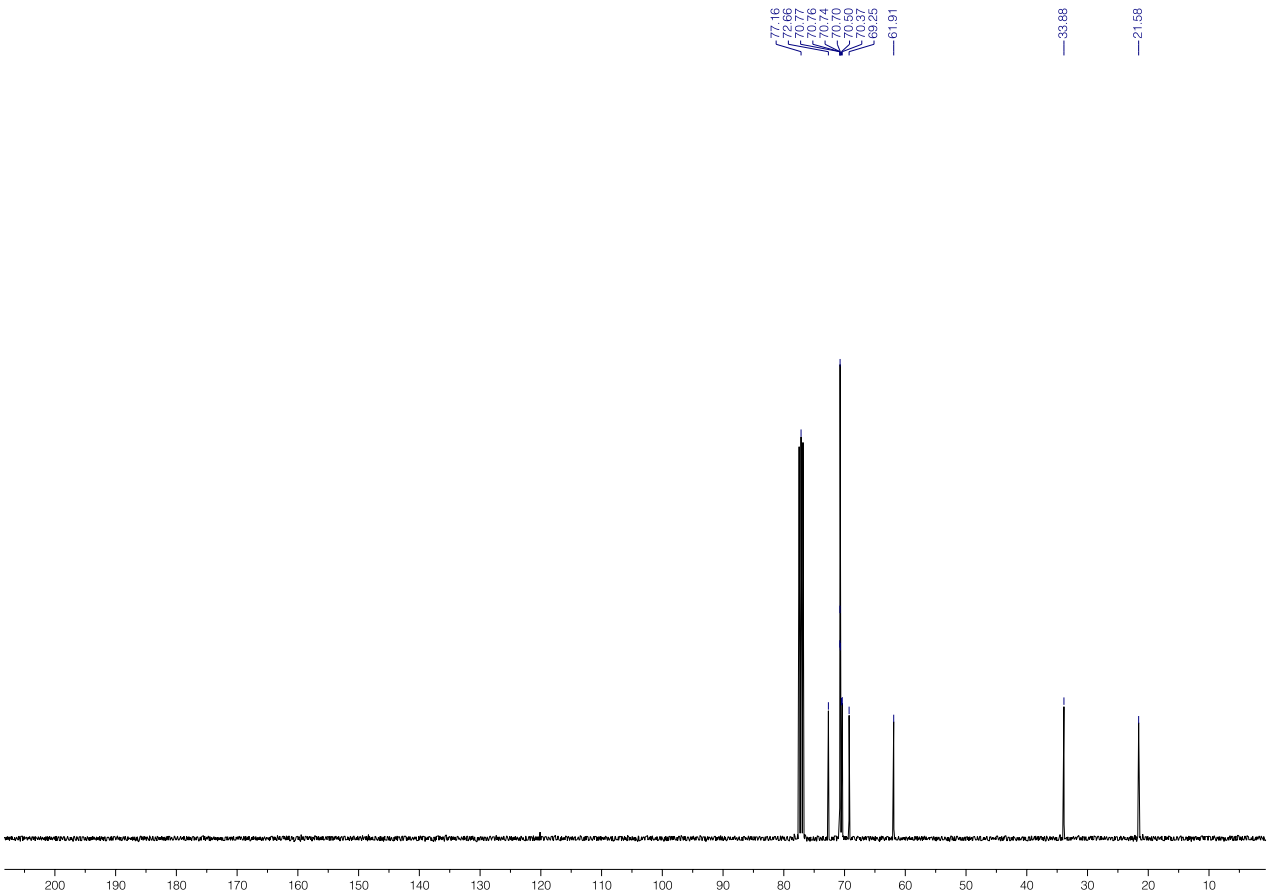

Figure S48. ^{13}C NMR spectrum of **B8** (100 MHz, $CDCl_3$).

3.9. Background ligand **B9**

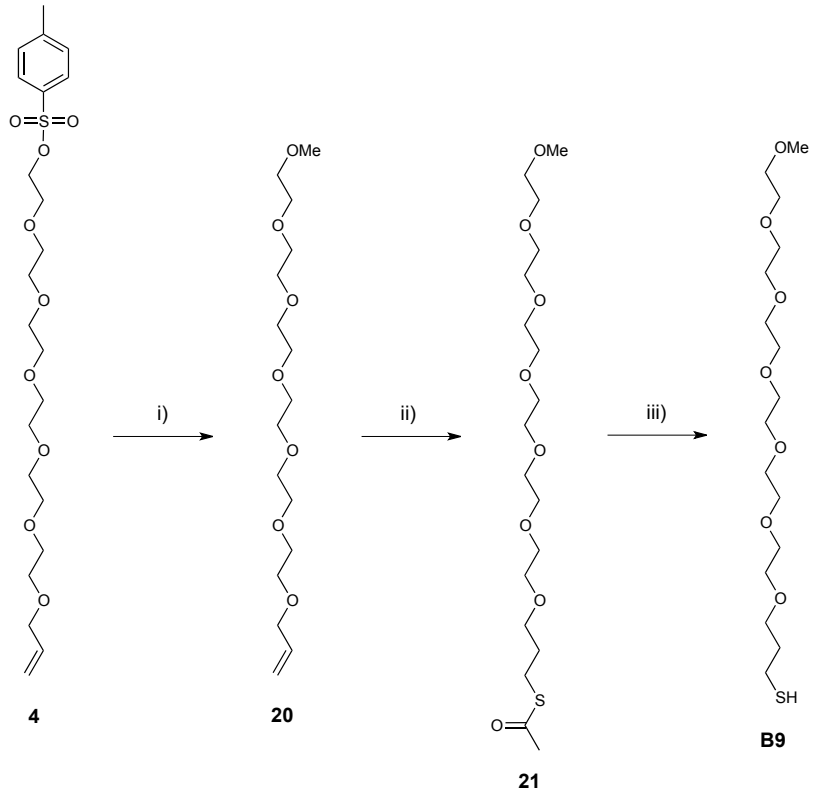

Scheme S8. Synthetic route for ligand **B9**. Reagents and conditions: i) NaH/MeOH/THF, 50 ºC, overnight, 80%; ii) CH_3COSH, DCM, UVB, overnight, quantitative; iii) HCl/MeOH, reflux, 6 h, quantitative.

2,5,8,11,14,17,20-heptaoxatricos-22-ene (**20**): A round-bottom flask containing a mixture of dry methanol (5 mL) and dry THF (5 mL) at 0 ºC was charged with 60% NaH (80 mg; 2 mmol) in oil. After ca. 10 min, a solution compound **4** (obtained according to Scheme S2) (190.6 mg, 0.40 mmol) in dry THF (5 mL) was added dropwise. The reaction mixture was heated to 50 °C and stirred at this temperature overnight. Then, the solvent was removed *in vacuo*; the residue was dissolved in $CHCl_3$ (50 mL), the resulting solution was washed with brine (100 mL × 2), dried over Na_2SO_4, and finally concentrated *in vacuo*. The crude product was purified by silica gel column chromatography (eluent: from Hexane to $CHCl_3$) to afford 108 mg of **20** (yield = 80%).

^{1}H NMR (400 MHz, $CDCl_3$): δ = 5.96–5.87 (m, 1H), 5.29–5.16 (m, 2H), 4.03–4.02 (d, 2H), 3.66–3.59 (m, 22H), 3.56–3.54 (m, 2H), 3.38 (s, 3H). **^{13}C NMR** (100 MHz, $CDCl_3$): δ = 134.92, 117.24, 72.40, 72.10, 70.79, 70.77, 70.75, 70.68, 69.58, 59.19.

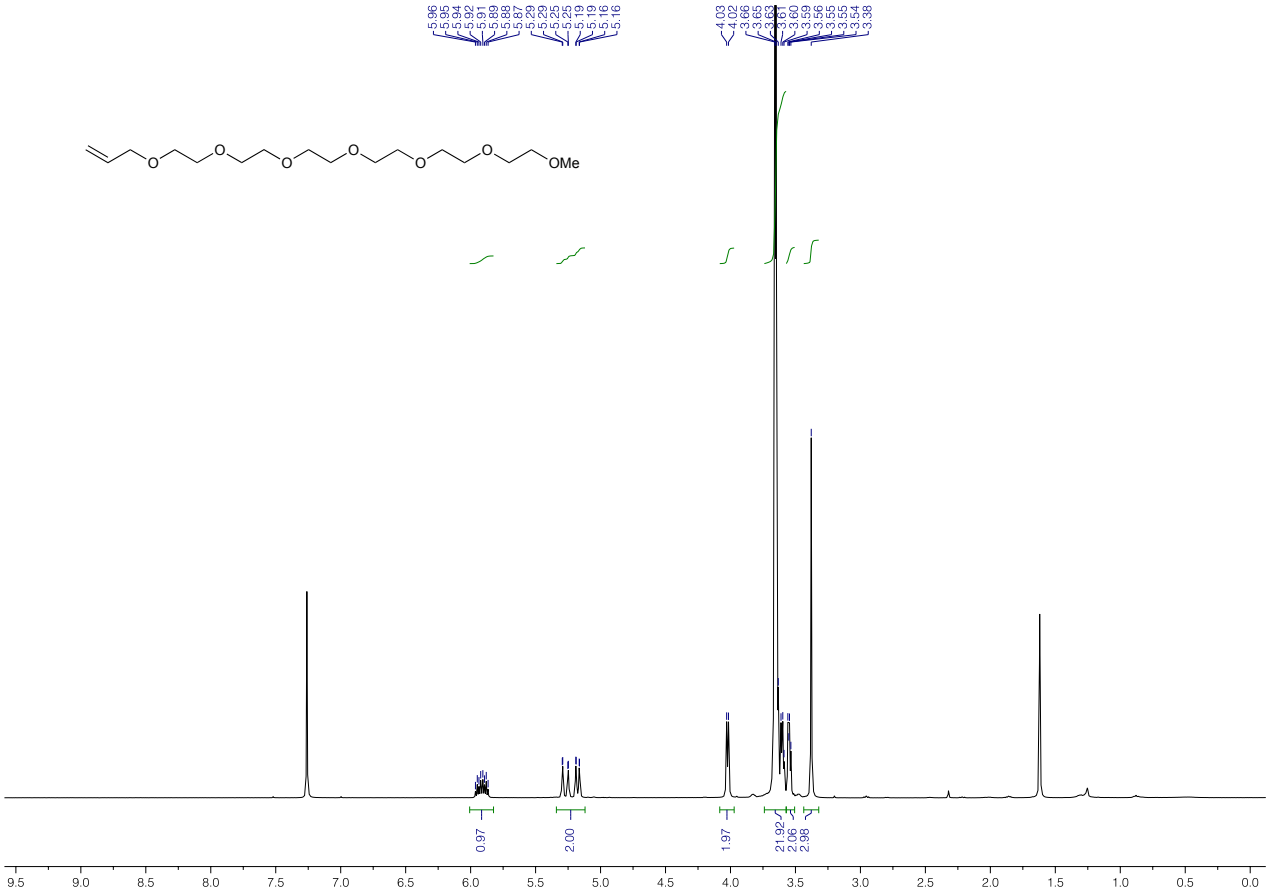

Figure S49. ^{1}H NMR spectrum of **20** (400 MHz, $CDCl_3$).

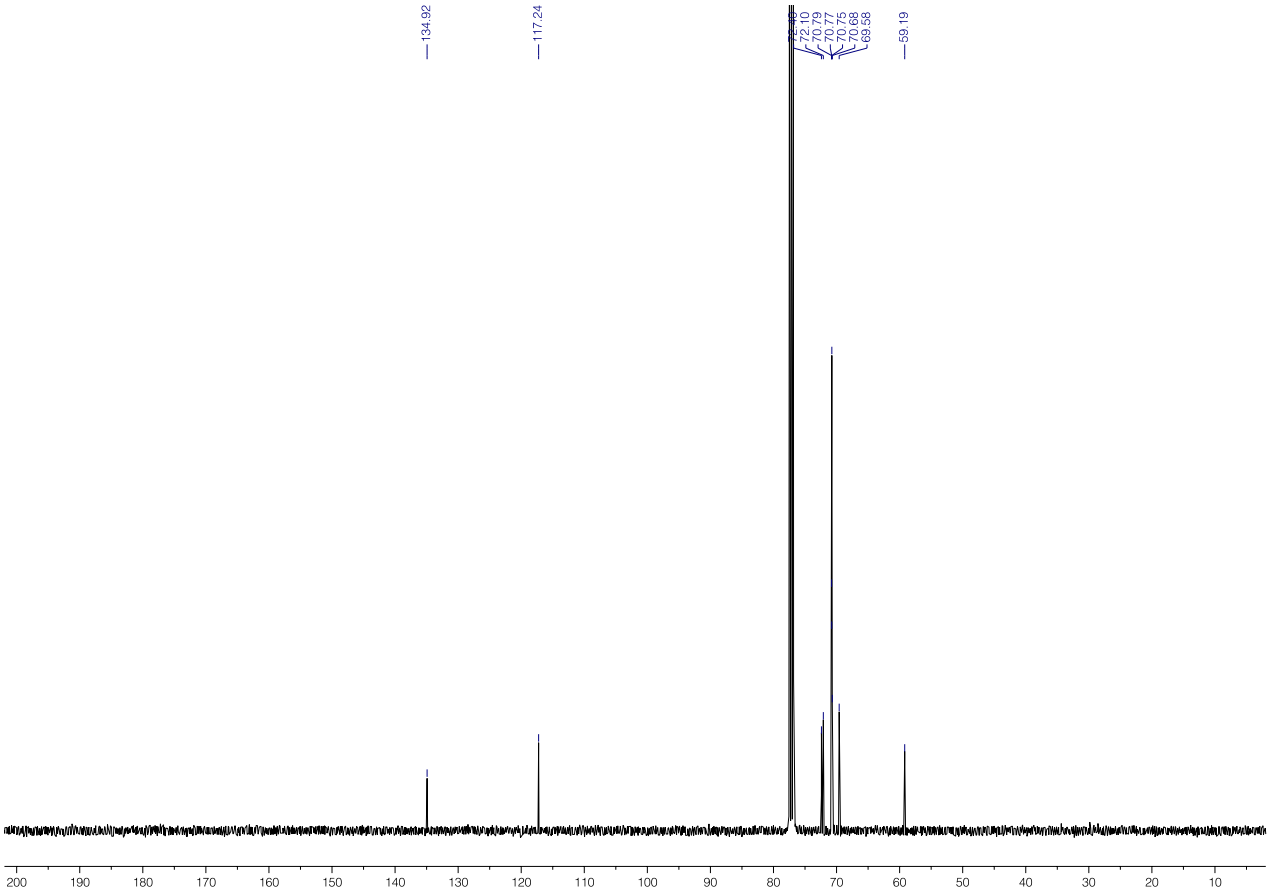

Figure S50. ^{13}C NMR spectrum of **20** (100 MHz, $CDCl_3$).

***S*-2,5,8,11,14,17,20-heptaoxatricosan-23-yl ethanethioate** (**21**): A solution of **20** (100 mg; 0.30 mmol) and thioacetic acid (214 µL; 228 mg; 3.0 mmol) in DCM (6 mL) was stirred at room temperature under UVB light overnight. Then, the reaction mixture was concentrated *in vacuo* to afford **21** in a quantitative yield.

^{1}H NMR (400 MHz, $CDCl_3$): δ = 3.66–3.49 (m, 26H), 3.38 (s, 3H), 2.95 (t, 2H), 2.32 (s, 3H), 1.89–1.82 (m, 2H). **^{13}C NMR** (100 MHz, $CDCl_3$): δ = 196.02, 72.10, 70.77, 70.74, 70.68, 69.74, 59.19, 30.78, 29.73, 26.15. **HRMS** calcd for $C_{18}H_{36}NaO_8S$ $[M + Na]^+$, m/z = 435.2029; found, 435.2030.

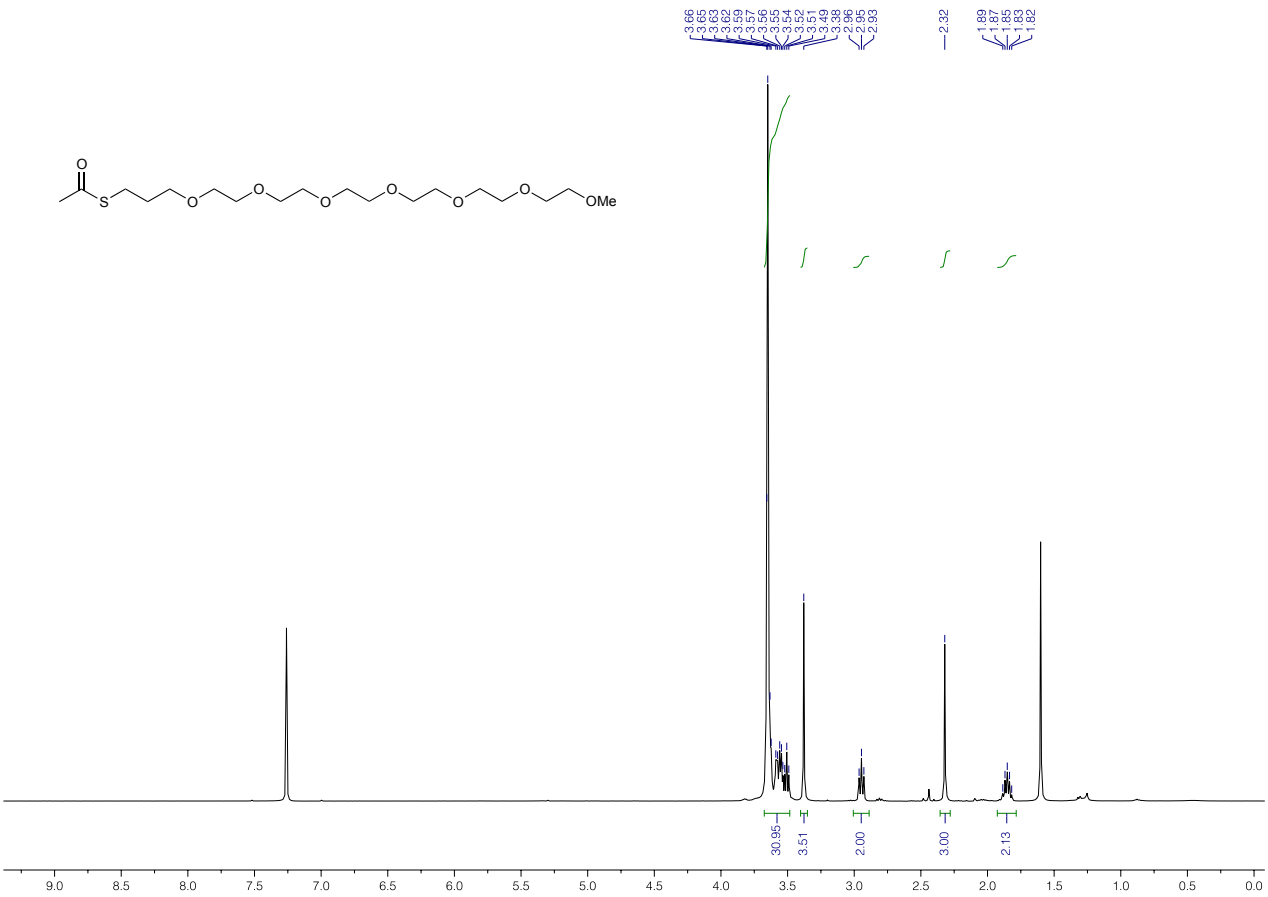

Figure S51. ^{1}H NMR spectrum of **21** (400 MHz, $CDCl_3$).

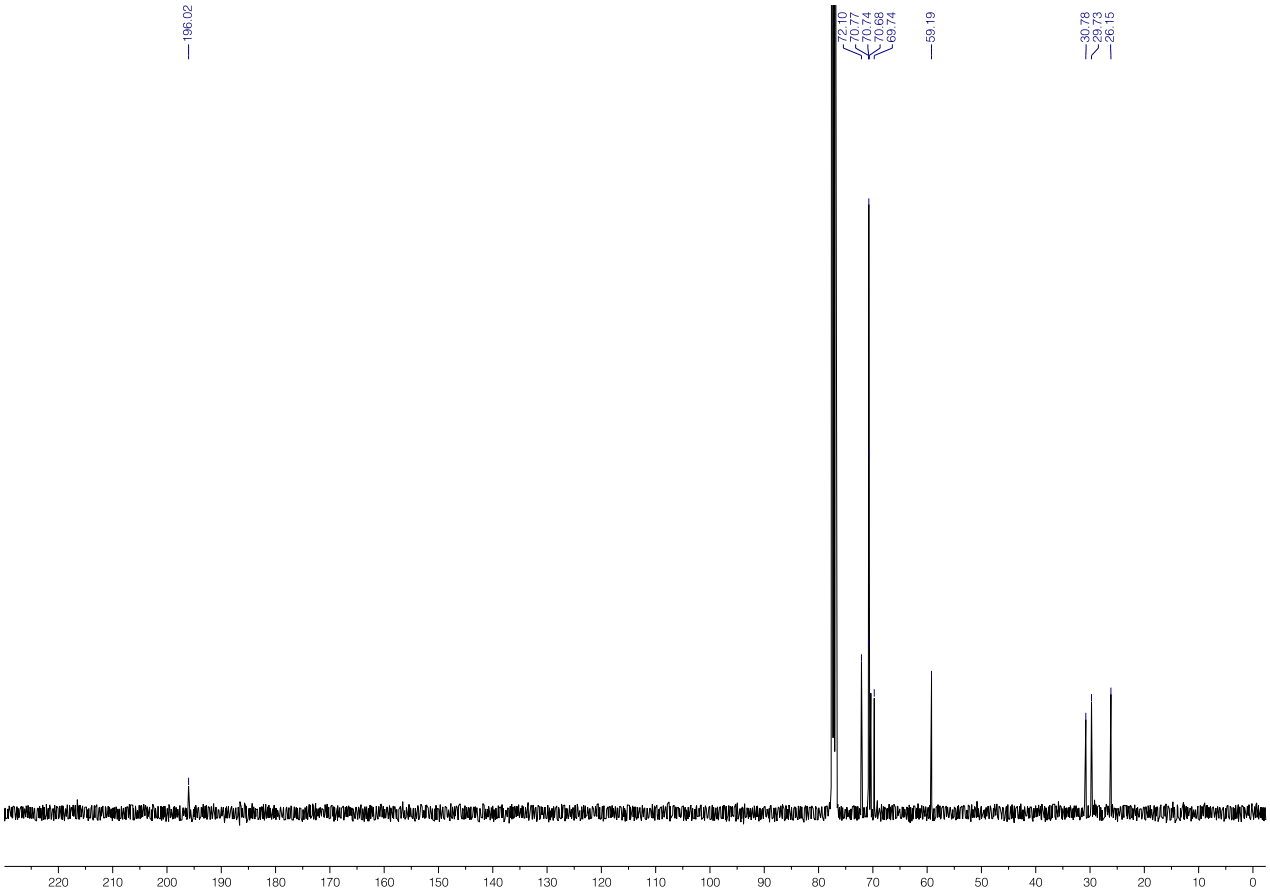

Figure S52. ^{13}C NMR spectrum of **21** (100 MHz, $CDCl_3$).

2,5,8,11,14,17,20-heptaoxatricosane-23-thiol (B9): A solution of **21** (82.5 mg; 0.20 mmol) in 10 mL of methanol was degassed by bubbling nitrogen for 15 min. Then, 1.2 mL of 1.25 M methanolic HCl solution was added and the reaction mixture was refluxed for 6 h. Finally, the reaction mixture was cooled down to room temperature and the solvent was evaporated *in vacuo* to afford **B9** in a quantitative yield.

^{1}H NMR (400 MHz, $CDCl_3$): δ = 3.65–3.38 (m, 26H), 3.38 (s, 3H), 2.65–2.59 (q, 2H), 1.91–1.84 (m, 2H), 1.38 (t, 1H). **^{13}C NMR** (100 MHz, $CDCl_3$): δ = 72.10, 70.74, 70.68, 70.39, 69.26, 59.19, 33.89, 21.59. **HRMS** calcd for $C_{16}H_{34}NaO_7S$ $[M + Na]^+$, m/z = 393.1923; found, 393.1920.

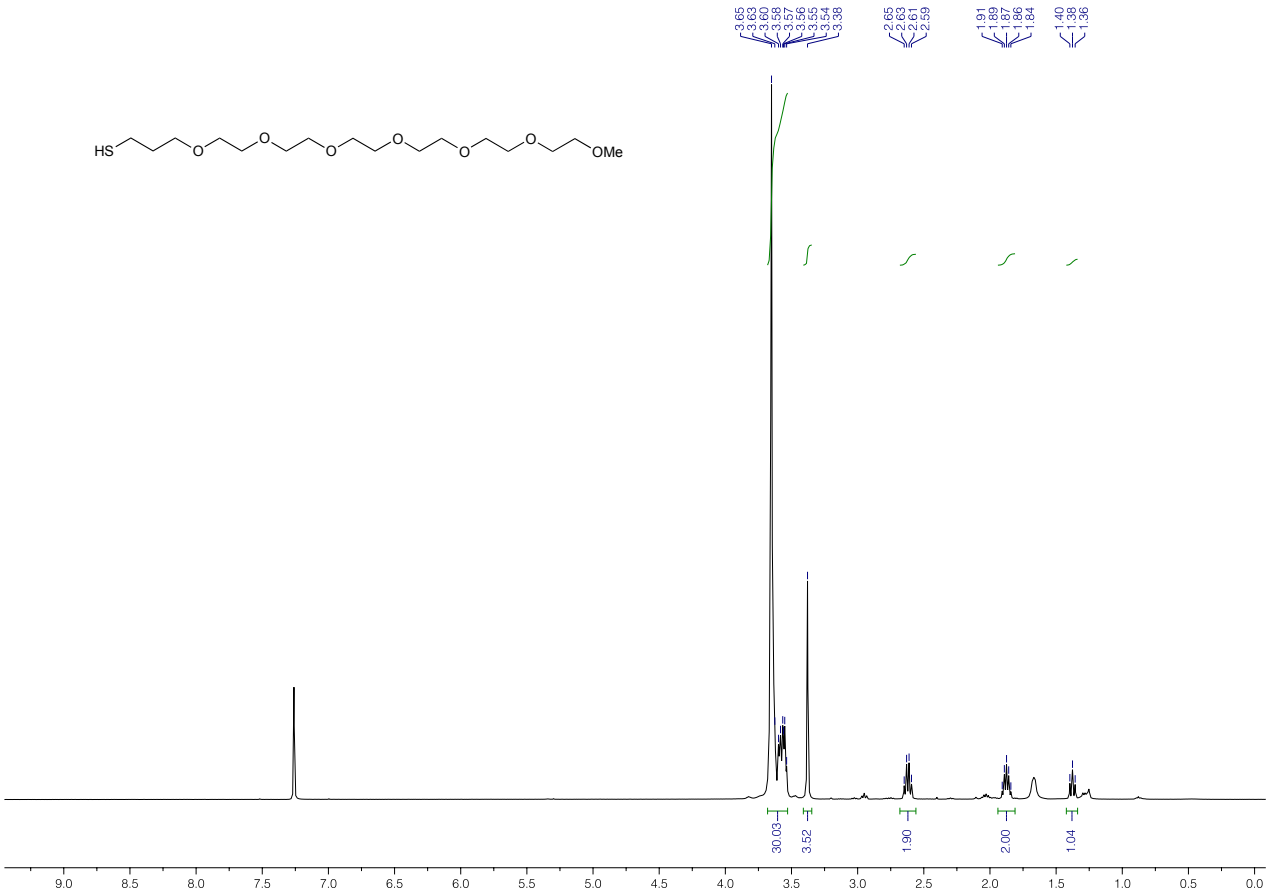

Figure S53. ^{1}H NMR spectrum of **B9** (400 MHz, $CDCl_3$).

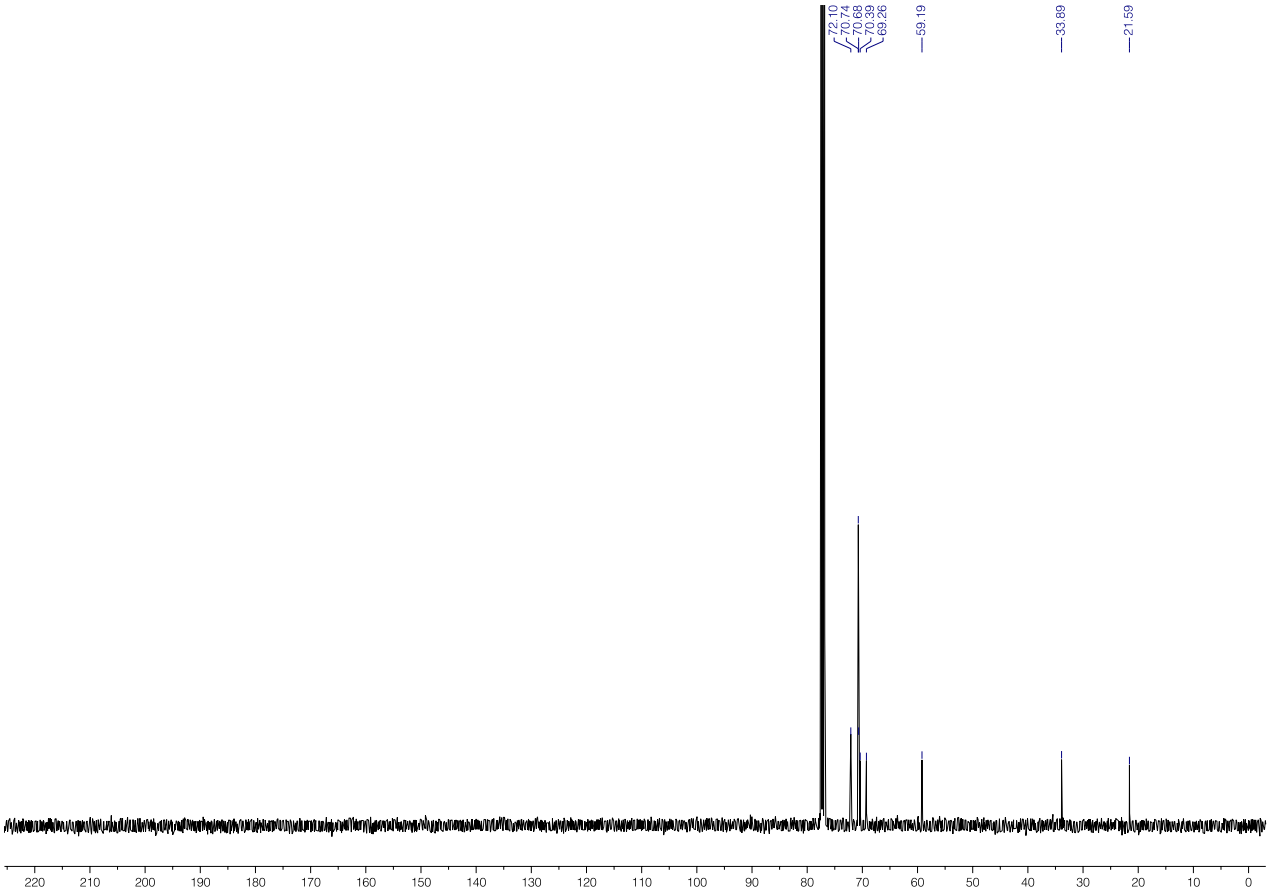

Figure S54. ^{13}C NMR spectrum of **B9** (100 MHz, $CDCl_3$).

4. Synthesis and functionalization of gold nanoparticles

4.1. Synthesis of 2.5 nm gold nanoparticles

Gold nanoparticles with an average diameter of 2.5 nm were prepared by reducing $HAuCl_4$ with tetrabutylammonium borohydride (TBAB) in toluene in the presence of dodecylamine (DDA) and didodecyldimethylammonium bromide (DDAB) as the surfactants, according to a previously reported procedure.[2,7] Specifically, DDAB stock solution was first prepared by dissolving DDAB (925 mg; 2.00 mmol) in toluene (20 mL) with ultrasonication. DDA (450 mg; 2.43 mmol) and $HAuCl_4 \cdot 3H_2O$ (50 mg; 127 μmol) were then added to 12.5 mL of the stock solution and sonicated until completely dissolved. Gold(III) was then reduced by rapidly injecting a solution of tetrabutylammonium borohydride (TBAB) (125 mg; 486 μmol) in 5 mL of the DDAB stock solution under vigorous stirring. Gentle stirring was continued for an additional 2–3 h.

4.1.1. Functionalization of 2.5 nm gold nanoparticles by the simultaneous addition of two thiols

A mixture of desired thiolated azobenzene **A*m*** (***m*** = **1–5**) and background ligand **B*n*** (***n*** = **1–9**) (dissolved in DMSO, DMF, or MeOH) was added to a solution of 2.5 nm gold NPs under gentle stirring. The total amount of thiols corresponded to a 10-fold excess with respect to the number of the binding sites on Au (calculated assuming that a single thiolate moiety occupies an area of 0.214 nm^2 on the surface of gold[8]). The mixture was shaken on an orbital shaker for 4 h, resulting in the precipitation of NPs (in rare cases, the NPs remained colloidally stable; they were then precipitated with the help of a non-solvent). Then, the supernatant was discarded and the NPs were washed repeatedly with DCM. Finally, gold NPs were dried under ambient pressure and dissolved in deionized water.

4.1.2. Functionalization of 2.5 nm gold nanoparticles by the consecutive addition of two thiols

Thiolated azobenzene **A*m*** (***m*** = **1–5**) (θ equivalents; $\theta < 1$; equiv with respect to the number of binding sites on Au) dissolved in either DMF or DMSO was added dropwise to a fresh toluene solution of 2.5 nm Au NPs under vigorous stirring. After having been shaken on an orbital shaker for 1 h, background ligand **B*n*** (***n*** = **1–9**) (y equiv, where $y = 1 - \theta$) dissolved in either DMSO or MeOH was introduced. After having been shaken on an orbital shaker for an additional 2 h, a solution mixture of θ equiv of **A*m*** and y equiv of **B*n*** was added and the system was allowed to equilibrate for another ~1 h. Surface functionalization of NPs resulted in precipitation from the solution; if no precipitation occurred spontaneously, it was induced with a non-solvent. Then the supernatant was discarded and the NPs were washed repeatedly with DCM. Finally, the functionalized gold NPs were dried under ambient pressure and finally dissolved in deionized water.

4.2. Synthesis of 5.5 nm gold nanoparticles

Gold nanoparticles with an average diameter of 5.5 nm were synthesized based on a previously reported procedure.[2,7] First, 2.5 nm NPs ("seeds") were prepared as described above (Section 4.1) and left on an orbital shaker for 24 h. Growth solution was prepared by adding to 50 mL of toluene in the following order: DDAB (1.00 g), DDA (1.85 g), $HAuCl_4 \cdot 3H_2O$ (200 mg), and the seed solution (7.0 mL). Finally, 131 μL of hydrazine dissolved (with ultrasonication) in 20 mL of the DDAB stock solution was added dropwise (~1 drop/sec) to the growth solution under vigorous stirring and the resulting solution was stirred overnight.

4.2.1. Functionalization of 5.5 nm gold nanoparticles

Prior to functionalization, gold NPs were purified from an excess of surfactants. A toluene solution of gold NPs was mixed with the same volume of methanol and the resulting black precipitate was collected (ca. 1 h after adding methanol) by decantation. The precipitate was washed with methanol once and dissolved in pure toluene. Ligand exchange was carried out as described for 2.5 nm NPs (Sections 4.1.1 and 4.1.2).

5. Determining the values of χ on **A*m***-functionalized gold nanoparticles

The values of χ for all combinations of thiolated azobenzene **A*m*** and backgrond thiol **B*n*** were determined as described here for the **A1**/**B1** system.

First, we determined the molar absorptivity of **A1** by recording a series of UV/Vis absorption spectra of solutions of **A1** in an organic solvent (toluene or DMSO, depending on azobenzene; here, toluene) at different concentrations (Figure S55a; $\varepsilon = 2.02 \cdot 10^4$ M^{-1}cm^{-1}). Next, we subtracted the spectrum of **B1**-functionalized 2.5 nm NPs from the spectra of **A1B1**-functionalized NPs of the same size (see Figure 2c in the main text) – the resulting spectra are shown in Figure S55b. The values of χ were determined based on the assumption that a single thiol ligand (either **A1** or **B1**) occupies a surface area of 0.214 nm^2 on the surface of gold.[8]

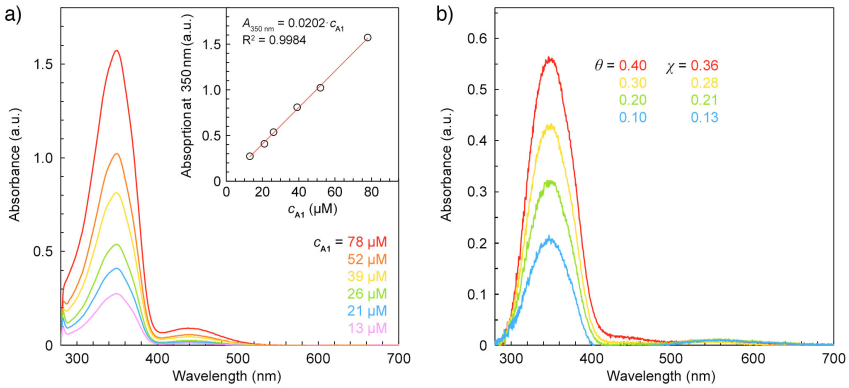

Figure S55. (a) UV/Vis absorption spectra of toluene solutions of **A1** at different concentrations of **A1**. (b) UV/Vis absorption spectra of four batches of **A1**/**B1**-functionalized 2.5 nm Au NPs obtained with increasing molar fractions of **A1**, θ, after subtracting the spectrum of **B1**-functionalized NPs of the same size. The concentration of NPs in all samples amounted to 0.40 mM (concentration in terms of gold atoms). Light path length = 10 mm.

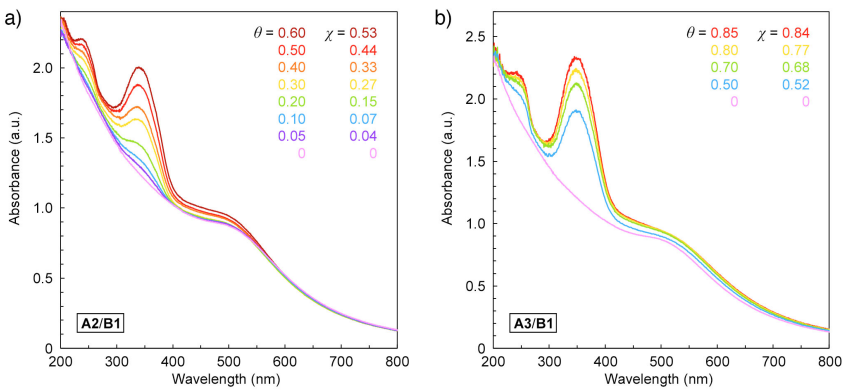

Figure S56. UV/Vis absorption spectra of (a) **A2**/**B1**- and (b) **A3**/**B1**-functionalized 2.5 nm gold NPs obtained using various molar fractions of azobenzenes **A2** and **A3** (θ). The resulting molar fractions of **A2** and **A3** on the NPs are denoted as χ. The highest χ values for NPs colloidally stable in pure water corresponded to 0.53 for **A2**/**B1**-functionalized NPs and 0.84 for **A3**/**B1**-functionalized NPs.

6. Determining the photoisomerization yield of azobenzene on gold nanoparticles

We used a combination of UV/Vis absorption spectroscopy and NMR spectroscopy to accurately determine the composition of *trans*/*cis* mixtures on NP surfaces. The procedure is described here for **A1**/**B1**-functionalized 2.5 nm gold NPs as an example. UV irradiation of these NPs leads to decreased absorbance at 350 nm due to the π→π* transition in *trans*-**A1**. However, the extent of this decrease is not directly proportional to the isomerization yield because *cis*-**A1** also absorbs at this wavelength. Having determined the molar absorptivity of *trans*-**A1** at 350 nm as $\varepsilon_{trans} = 2.02 \cdot 10^4$ $M^{-1}cm^{-1}$ (see Supporting Information, Section 5), we therefore proceeded to estimate the absorptivity of *cis*-**A1**. First, we generated a *cis*-rich solution of **A1** in DMSO-d_6 by exposure to UV light until the system reached a photostationary state (PSS). Integrating the signals due to *trans*- and *cis*-**A1** allowed us to estimate the composition of PSS as 2.1% *trans* and 97.9% *cis* (Figure S57).

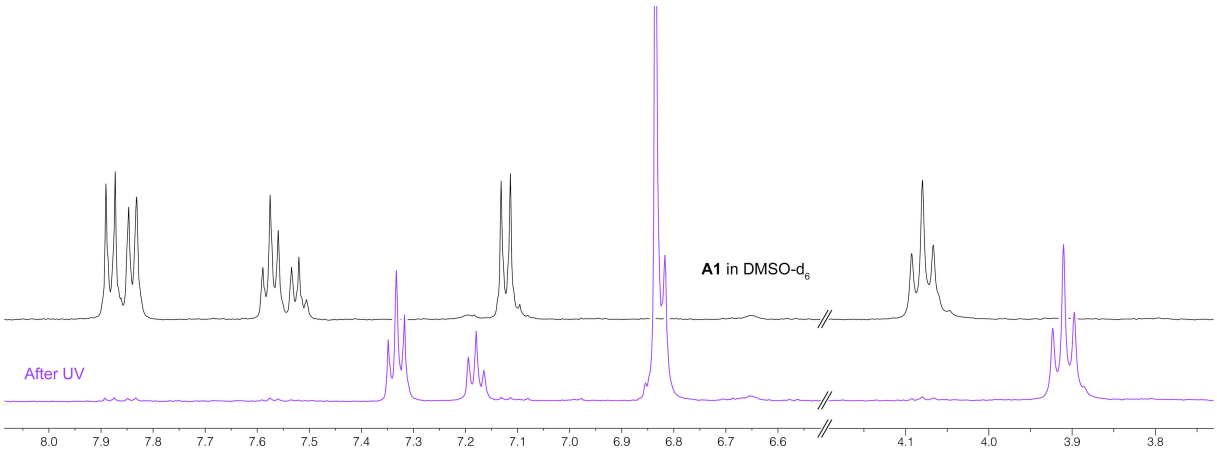

Figure S57. Partial ^{1}H NMR spectrum of **A1** in DMSO-d_6 (c = 2.4 mM) before (black) and after (purple) exposure to UV light for 20 min (500 MHz).

To determine the molar absorptivity of PSS at 350 nm, we rapidly diluted the UV-irradiated solution with DMSO and recorded a series of UV/Vis spectra (see Figure S58) (we verified that the rate of thermal back-isomerization in DMSO was such that the composition of PSS changed by only ~1% within 20 min after exposure to UV light). We found that $\varepsilon_{PSS} = 0.18 \cdot 10^4$ $M^{-1}cm^{-1}$, which, provided that the composition of PSS is known, allowed us to estimate ε_{cis} as $0.14 \cdot 10^4$ $M^{-1}cm^{-1}$.

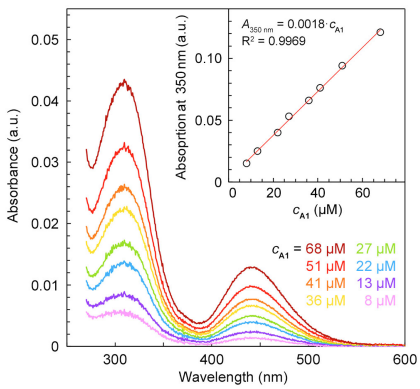

Figure S58. UV/Vis absorption spectra of DMSO solutions of **A1** pre-exposed to UV at different concentrations of **A1**. Light path length = 10 mm.

Therefore, the molar fraction of the *trans* isomer in the PSS can be calculated as,

$$\text{Molar \% } trans = \frac{A - A_{\mathbf{B1}} - l \cdot c_{\text{total}} \cdot \varepsilon_{cis}}{l \cdot c_{\text{total}} \cdot (\varepsilon_{trans} - \varepsilon_{cis})} \cdot 100\% ,$$

where A = absorbance of **A1**/**B1**-functionalized 2.5 nm Au NPs at 350 nm after exposure to light, $A_{\mathbf{B1}}$ = absorbance at 350 nm of a solution of **B1**-functionalized 2.5 nm Au NPs at the same NP concentration, l = light path length, and c_{total} = total concentration of azobenzene **A1**.

The same procedure was adopted for azobenzenes **A2**–**A5**, for which molar absorptivities were independently determined (none of background ligands **B1**–**B9** absorbs at 350 nm). These considerations assume that the molar absorptivity of azobenzene is solvent independent.

7. Azobenzene photoisomerization and thermal relaxation on water-soluble gold nanoparticles

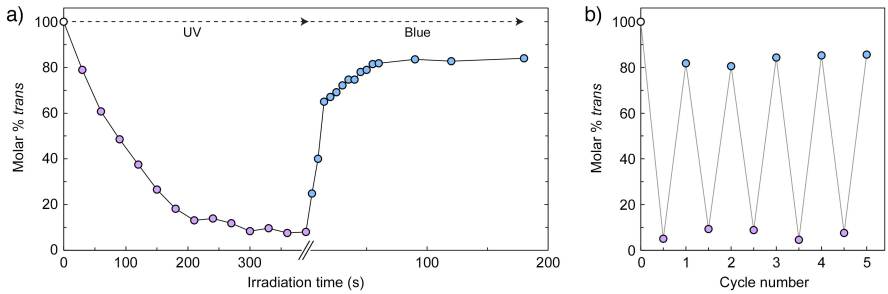

Figure S59. Photoswitching of azobenzene **A1** on **A1**/**B1**-functionalized 2.5 nm gold NPs at χ = 0.17. (a) Fraction of the *trans* isomer as a function of irradiation time with UV and blue light. (b) Reversible switching for five cycles (10 min of UV and 1 min of blue light irradiation were applied). The photostationary state (PSS) under UV light comprises 7±2 % of the *trans* isomer. The PSS under blue light comprises 84±2 % of the *trans* isomer.

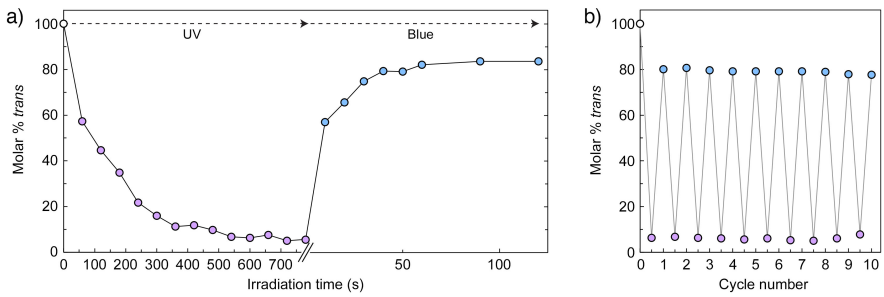

Figure S60. Photoswitching of azobenzene **A1** on **A1**/**B1**-functionalized 2.5 nm gold NPs at χ = 0.28. (a) Fraction of the *trans* isomer as a function of irradiation time with UV and blue light. (b) Reversible switching for five cycles (10 min of UV and 1 min of blue light irradiation were applied). The PSS under UV light comprises 6±1 % of the *trans* isomer. The PSS under blue light comprises 79±1 % of the *trans* isomer.

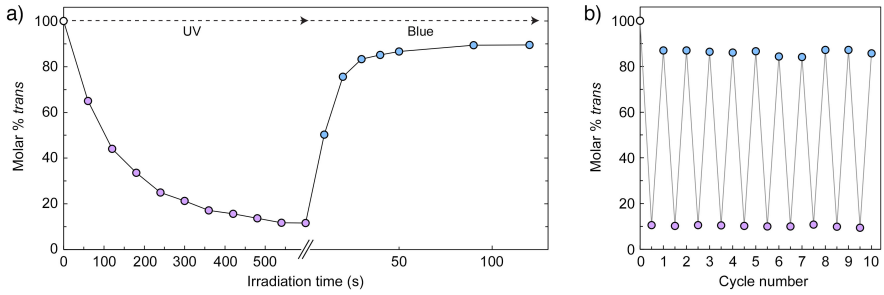

Figure S61. Photoswitching of azobenzene **A1** on **A1**/**B1**-functionalized 2.5 nm gold NPs at χ = 0.36. (a) Fraction of the *trans* isomer as a function of irradiation time with UV and blue light. (b) Reversible switching for five cycles (10 min of UV and 1 min of blue light irradiation were applied) (replotted from Figure 3e in the main text). The PSS under UV light comprises 10±1 % of the *trans* isomer. The PSS under blue light comprises 86±1 % of the *trans* isomer.

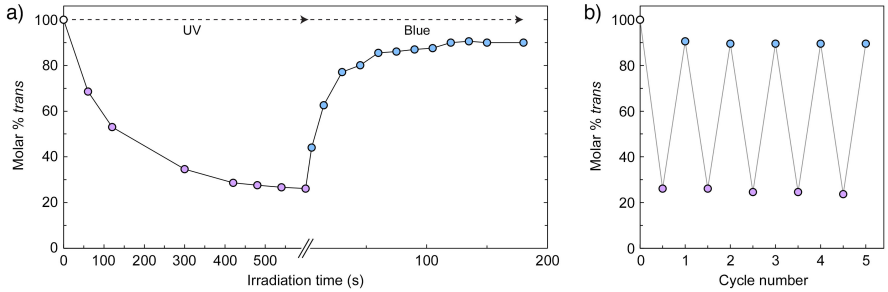

Figure S62. Photoswitching of azobenzene **A2** on **A2**/**B1**-functionalized 2.5 nm gold NPs at χ = 0.15. (a) Fraction of the *trans* isomer as a function of irradiation time with UV and blue light. (b) Reversible switching for five cycles (10 min of UV and 2 min of blue light irradiation were applied). The PSS under UV light comprises 25±1 % of the *trans* isomer. The PSS under blue light comprises 90±1 % of the *trans* isomer.

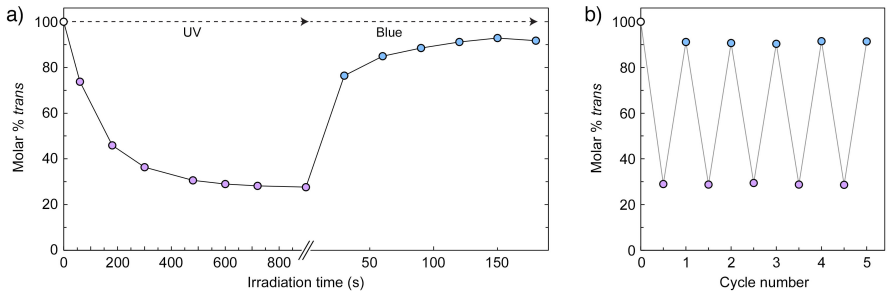

Figure S63. Photoswitching of azobenzene **A2** on **A2**/**B1**-functionalized 2.5 nm gold NPs at χ = 0.44. (a) Fraction of the *trans* isomer as a function of irradiation time with UV and blue light. (b) Reversible switching for five cycles (10 min of UV and 2 min of blue light irradiation were applied). The PSS under UV light comprises 30±1 % of the *trans* isomer. The PSS under blue light comprises 91±1 % of the *trans* isomer.

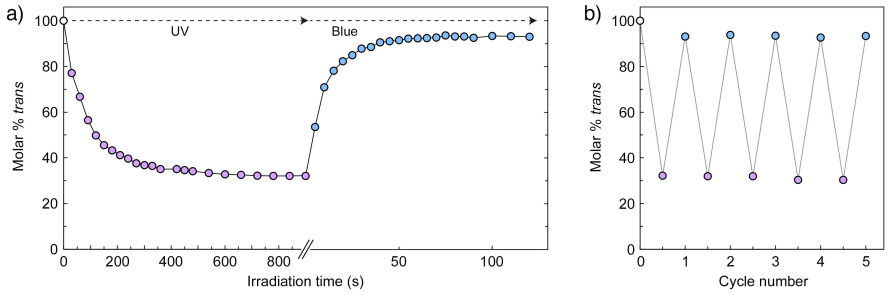

Figure S64. Photoswitching of azobenzene **A2** on **A2**/**B1**-functionalized 2.5 nm gold NPs at χ = 0.53. (a) Fraction of the *trans* isomer as a function of irradiation time with UV and blue light. (b) Reversible switching for five cycles (10 min of UV and 2 min of blue light irradiation were applied). The PSS under UV light comprises 31±1 % of the *trans* isomer. The PSS under blue light comprises 93±1 % of the *trans* isomer.

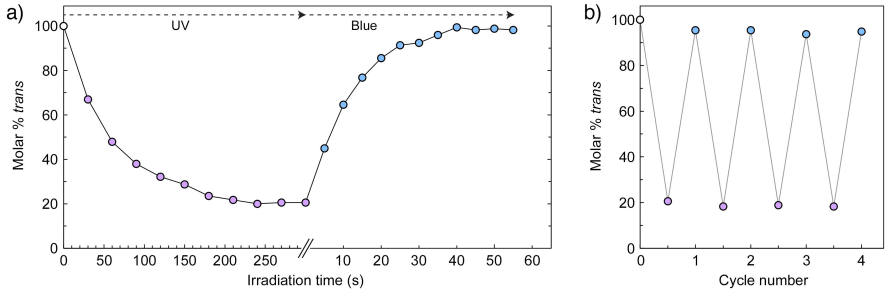

Figure S65. Photoswitching of azobenzene **A3** on **A3**/**B1**-functionalized 2.5 nm gold NPs at χ = 0.16. (a) Fraction of the *trans* isomer as a function of irradiation time with UV and blue light. (b) Reversible switching for five cycles (5 min of UV and 1 min of blue light irradiation were applied). The PSS under UV light comprises 19±1 % of the *trans* isomer. The PSS under blue light comprises 95±1 % of the *trans* isomer.

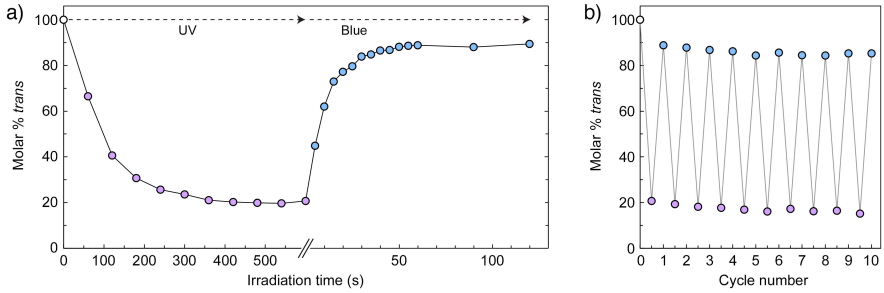

Figure S66. Photoswitching of azobenzene **A3** on **A3**/**B1**-functionalized 2.5 nm gold NPs at χ = 0.52. (a) Fraction of the *trans* isomer as a function of irradiation time with UV and blue light. (b) Reversible switching for ten cycles (10 min of UV and 1 min of blue light irradiation were applied). The PSS under UV light comprises 17±2 % of the *trans* isomer. The PSS under blue light comprises 86±2 % of the *trans* isomer.

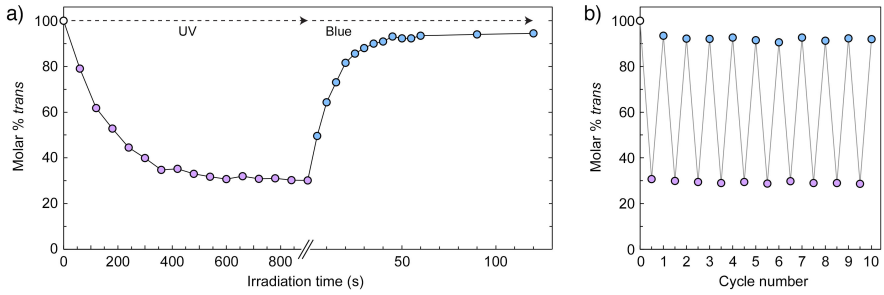

Figure S67. Photoswitching of azobenzene **A3** on **A3**/**B1**-functionalized 2.5 nm gold NPs at χ = 0.84. (a) Fraction of the *trans* isomer as a function of irradiation time with UV and blue light. (b) Reversible switching for ten cycles (10 min of UV and 1 min of blue light irradiation were applied). The PSS under UV light comprises 29±1 % of the *trans* isomer. The PSS under blue light comprises 92±1 % of the *trans* isomer.

In all cases, thermal relaxation of *cis*-azobenzene followed first-order kinetics, which can be described as[9,10]:

$$\ln\frac{A_\infty - A_t}{A_\infty - A_0} = -kt,$$

where A_∞ is the absorbance at λ_{max} (typically ~350 nm) before irradiation (i.e., pure *trans*), A_0 – absorbance immediately after extended exposure to UV light, A_t – absorbance after thermal (dark) relaxation for time t, and k is the rate constant.

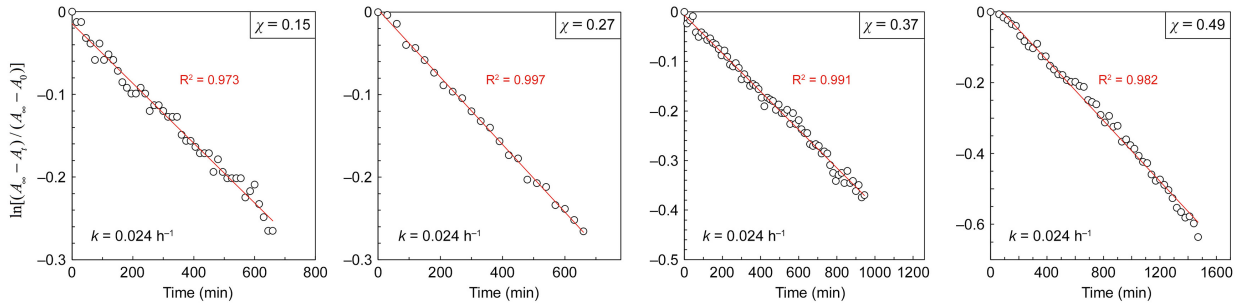

Figure S68. Kinetics of the thermal back-isomerization of **A2** on **A2**/**B1**-functionalized 2.5 nm gold NPs as a function of χ.

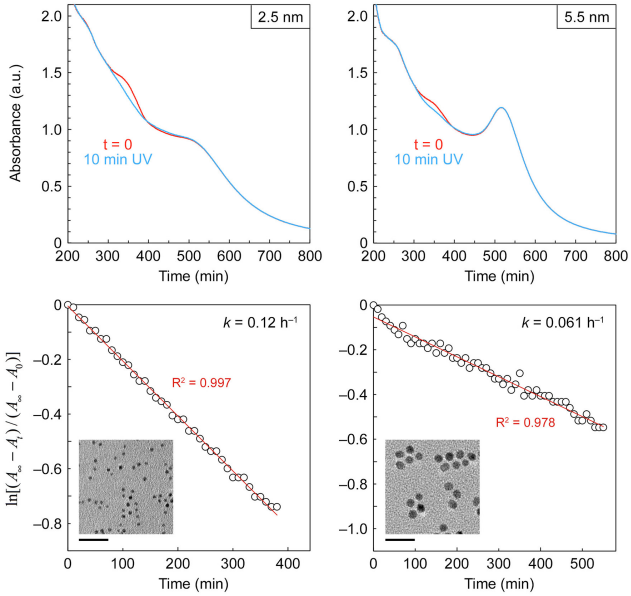

Figure S69. *Top*: UV/Vis spectra of **A2**/**B2**-functionalized 2.5 nm gold NPs (left; χ = 0.13) and 5.5 nm gold NPs (right; χ = 0.15) before (red) and after (blue) exposure to UV light. *Bottom*: Kinetics of the thermal back-isomerization of **A2** on **A2**/**B2**-functionalized 2.5 nm gold NPs (left) and 5.5 nm gold NPs (right). The insets show representative TEM images of **A2**/**B2**-coated 2.5 nm and 5.5 nm NPs (scale bars correspond to 20 nm). Solvent = 9:1 *v*/*v* water–methanol.

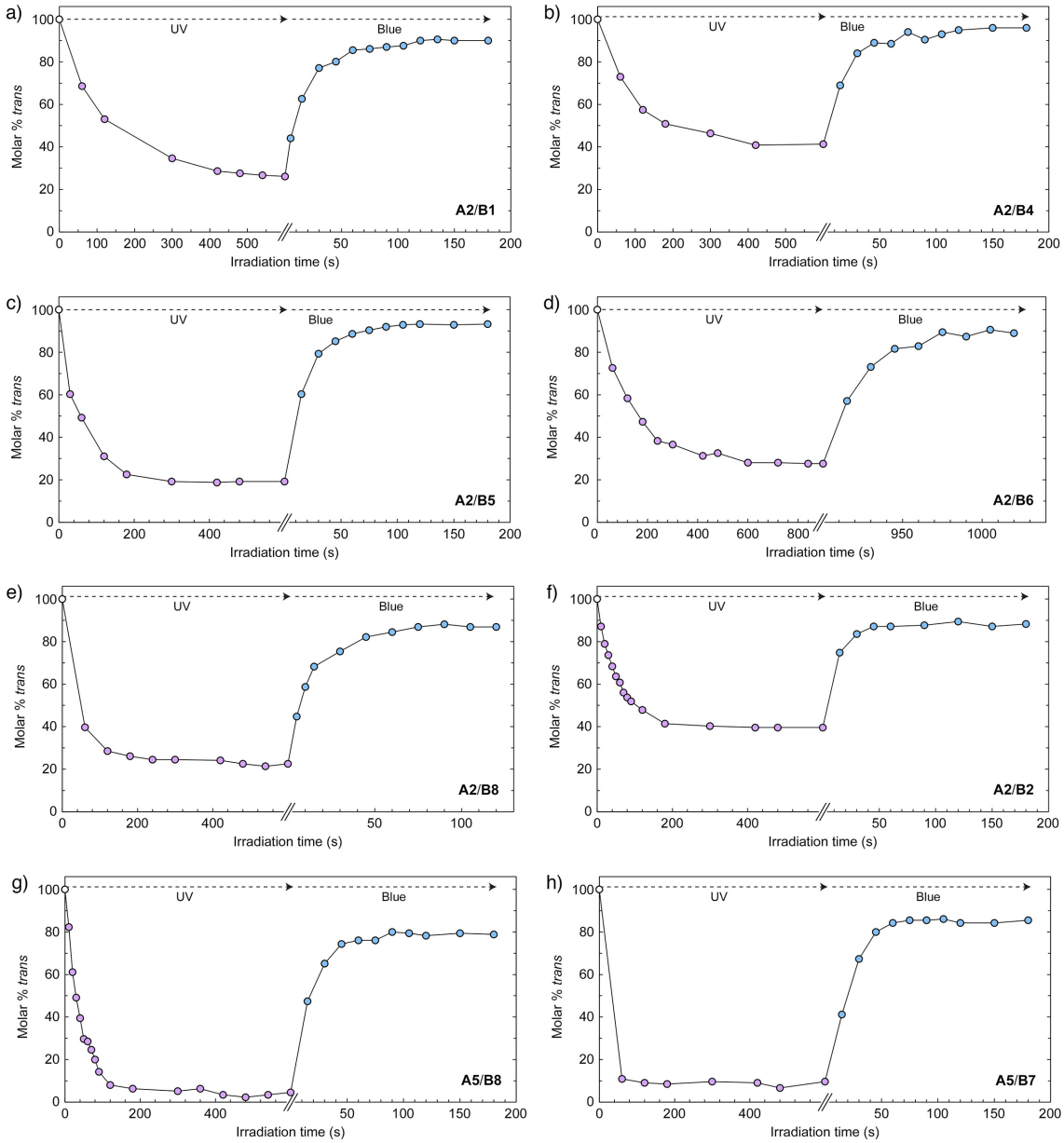

Figure S70. Reversible photoswitching of azobenzenes **A2** and **A5** co-adsorbed on 2.5 nm Au NPs with different background ligands (all at $\chi \approx 0.15$)

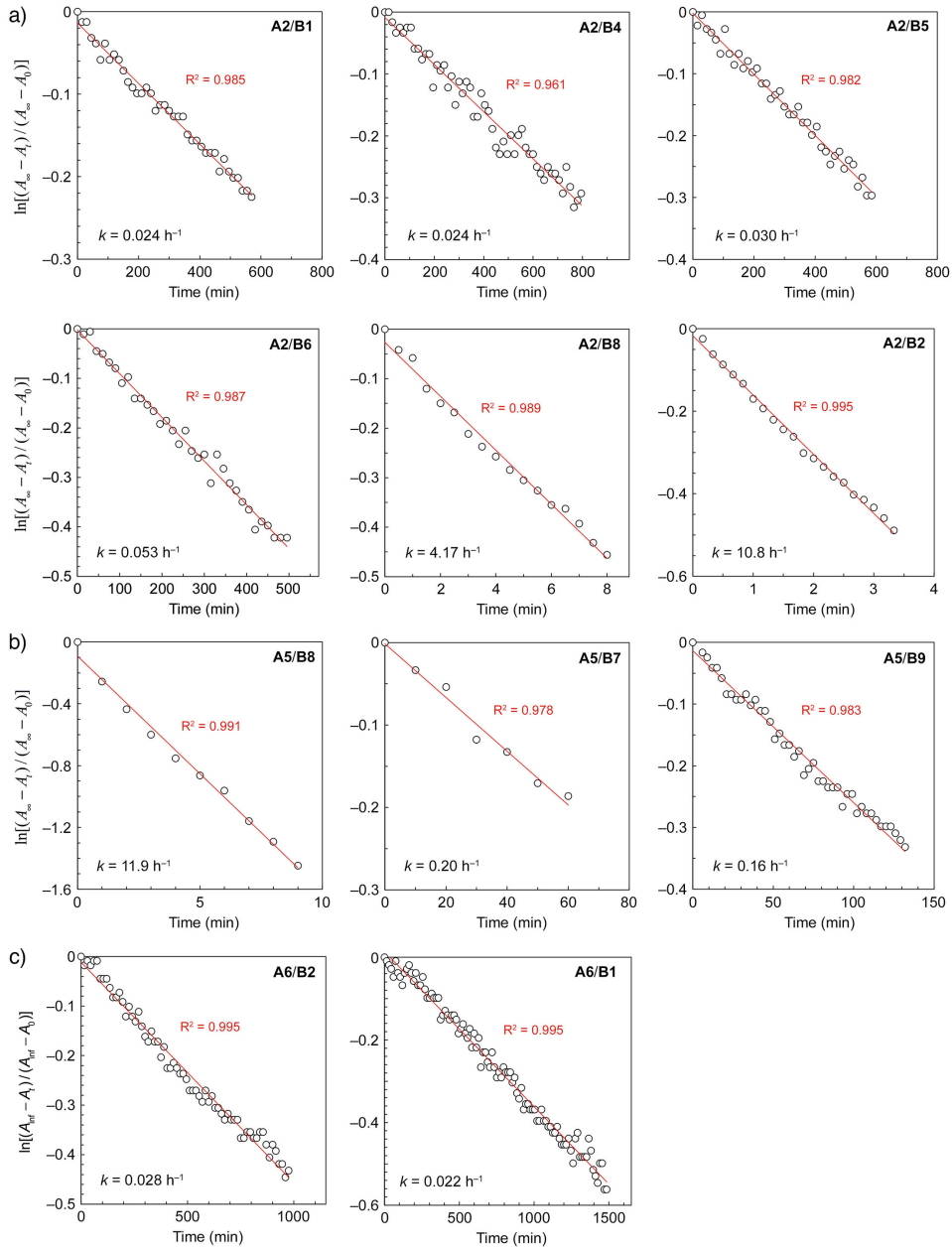

Figure S71. (a) Kinetics of the thermal back-isomerization of **A2** on **A2**/**B*n***-functionalized 2.5 nm gold NPs (all at $\chi \approx 0.15$) in water. (b) Kinetics of the thermal back-isomerization of **A5** on **A5**/**B*n***-functionalized 2.5 nm gold NPs (all at $\chi \approx 0.15$) in water. (c) Kinetics of the thermal back-isomerization of **A6** on **A6**/**B*n***-coated 2.5 nm gold NPs (both at $\chi \approx 0.15$) in water.

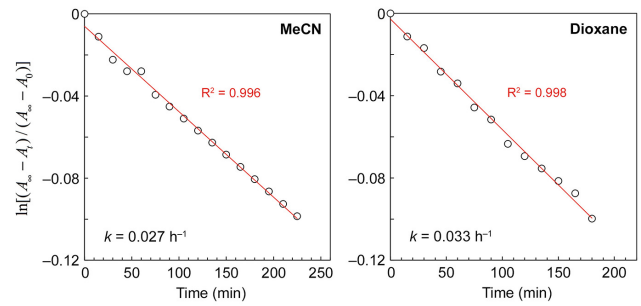

Figure S72. Kinetics of the thermal back-isomerization of free **A5** in acetonitrile (left) and dioxane (right).

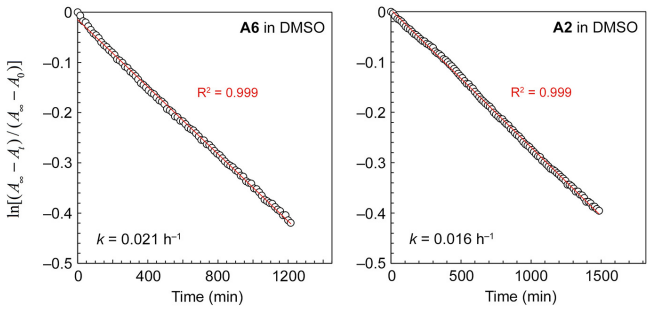

Figure S73. Kinetics of the thermal back-isomerization of free **A6** (left) and **A2** (right) in DMSO.

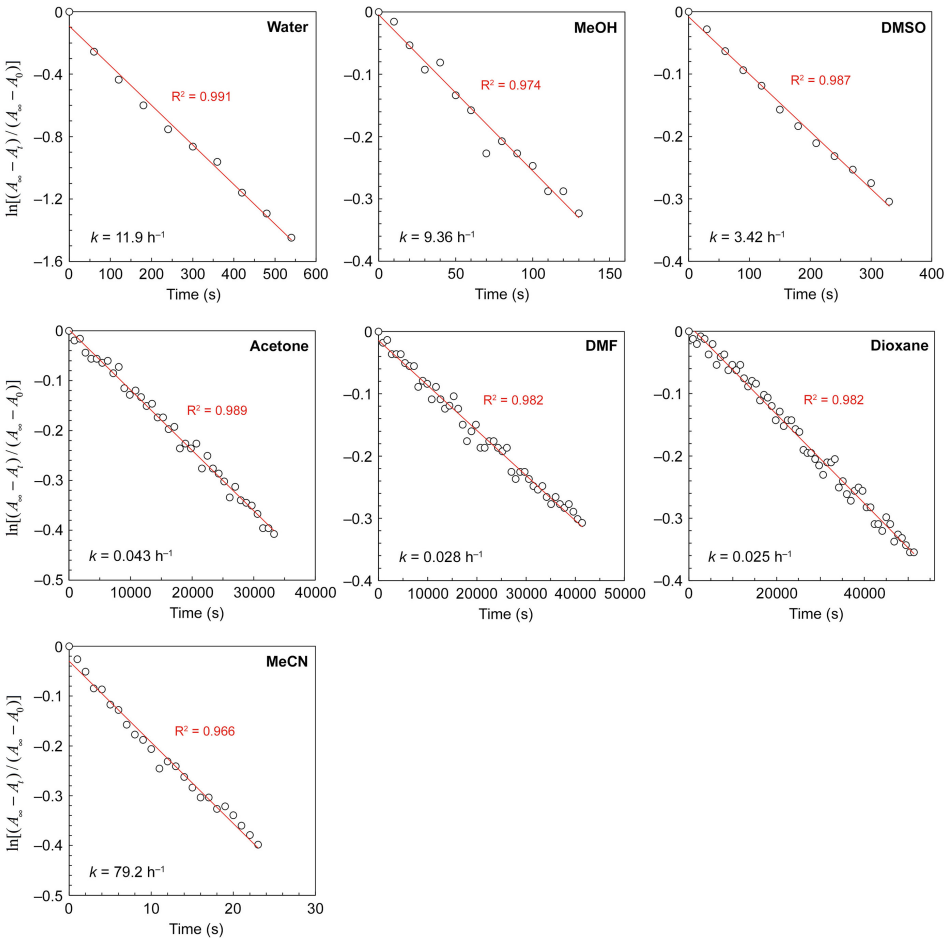

Figure S74. Kinetics of the thermal back-isomerization of **A5** on **A5**/**B8**-functionalized 2.5 nm gold NPs ($\chi \approx 0.15$) in different 1:24 water-solvent mixtures, where the solvent is indicated in the plots.

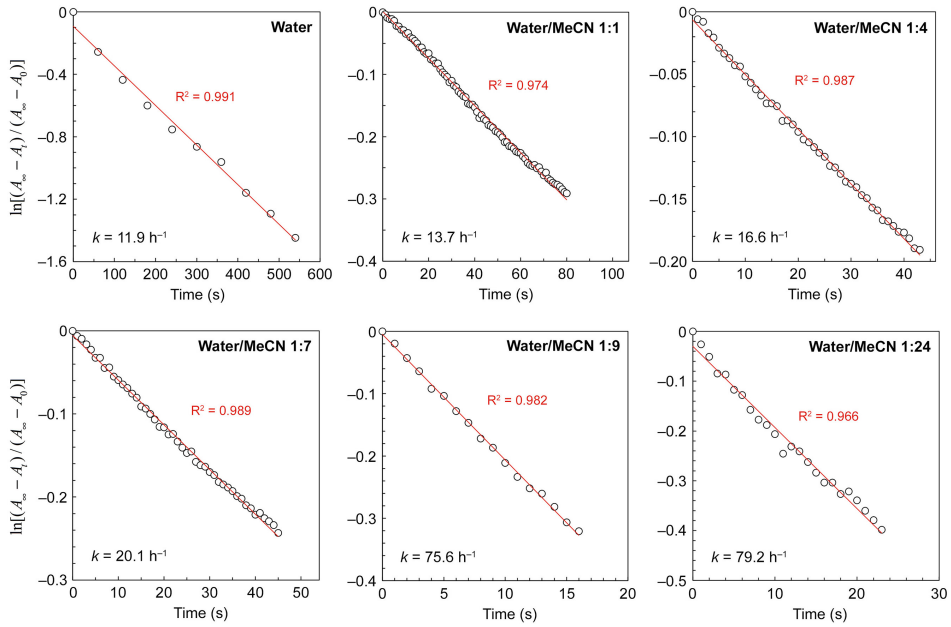

Figure S75. Kinetics of the thermal back-isomerization of **A5** on **A5**/**B8**-functionalized 2.5 nm gold NPs ($\chi \approx$ 0.15) in different water-acetonitrile mixtures.

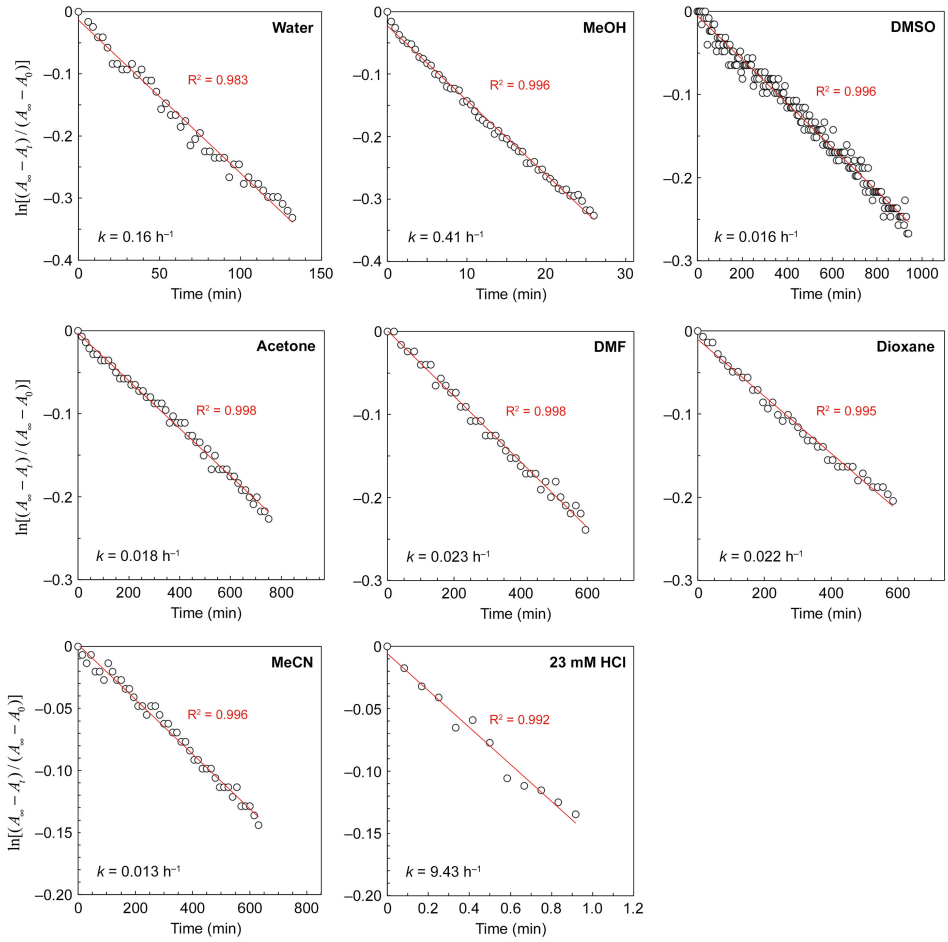

Figure S76. Kinetics of the thermal back-isomerization of **A5** on **A5**/**B9**-functionalized 2.5 nm gold NPs ($\chi \approx$ 0.15) in different 1:24 water–organic solvent mixtures, where the solvent is indicated in the plots. Bottom center: aqueous solution containing 23 mM HCl.

8. Synthesis and functionalization of 3.5 nm palladium nanoparticles

Synthesis: Palladium nanoparticles were prepared by reducing $PdCl_2$ with *tert*-butylamine–borane complex, based on the method described by Sun and coworkers.[11] Briefly, 50 mg of $PdCl_2$ was dissolved in 4 mL of a mixed solvent composed of toluene and oleylamine (1:1 *v*/*v*) under nitrogen atmosphere. The mixture was heated at 80 °C until a clear (slightly yellow) solution was obtained. To this mixture, a solution of 100 mg of the *tert*-butylamine–borane complex in a 1:1 (*v*/*v*) mixture of toluene and oleylamine was rapidly injected under vigorous stirring. The color turned black within 5 seconds and stirring was continued for an additional 30 minutes. Then, the solution was cooled to room temperature and 10 mL of ethanol was added to induce NP flocculation. The NPs were collected by centrifugation, redispersed in 2 mL of toluene, precipitated with ethanol (10 mL), once again redispersed in 2 mL of toluene and precipitated with ethanol (10 mL), and finally redispersed in 20 mL of toluene.

Functionalization: A solution of **A2** (c = 16.5 mM) and **B2** (c = 14.9 mM) in toluene (100 μL) was added to a stirred solution of Pd NPs in toluene (1 mL) obtained as described above. The mixture was stirred on an orbital shaker for 12 h, resulting in precipitation of functionalized NPs. The precipitate was collected, washed repeatedly with DCM, dried under ambient pressure, and redispersed in deionized water (1 mL). The fractional coverage of azobenzene on the resulting NPs was estimated as $\chi \approx 0.10$, assuming that a single thiol ligand occupies the same surface area on Pd than on Au (i.e., 0.214 nm^2). However, it is most likely that the actual χ is higher due to the previously reported[12] oxidation of Pd NP surface to PdO, which decreases the overall density of thiolate ligands on Pd NPs.

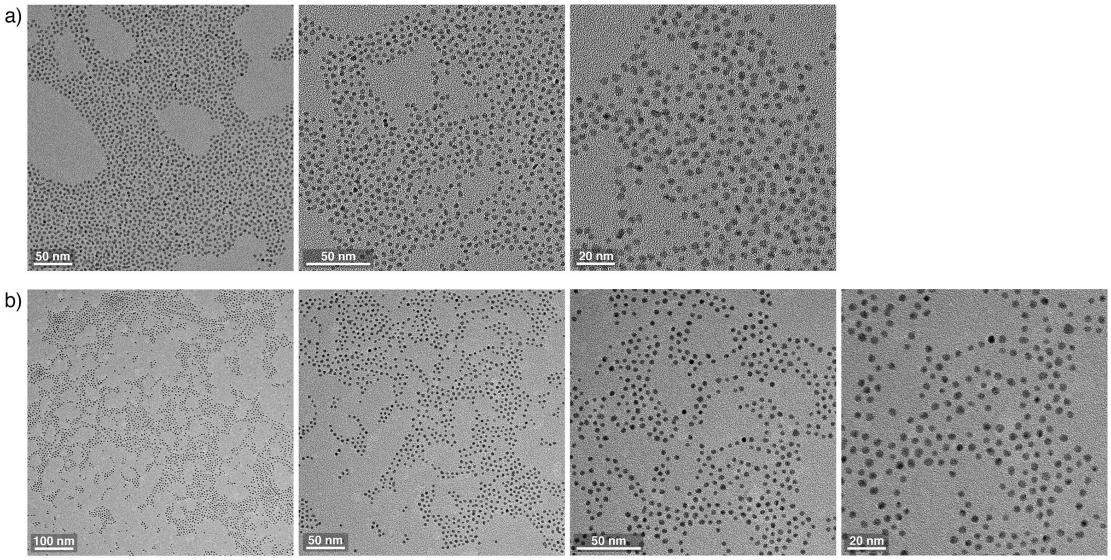

Figure S77. Representative TEM images of (a) toluene-soluble, 3.5 nm Pd NPs capped with oleylamine and (b) water-soluble, 3.5 nm Pd NPs co-functionalized with a mixture of **A2** and **B2** ($\chi \approx 0.10$).

9. Synthesis and functionalization of 4.0 nm magnetite nanoparticles

9.1. Synthesis of 4.0 nm magnetite nanoparticles

Magnetite nanoparticles (4.0 ±0.3 nm) were synthesized according to the procedure reported in Ref. 13.

9.2. Synthesis of azobenzene-terminated catechol **A7**

Compound **A7** was synthesized according to the procedure reported in Ref. 14.

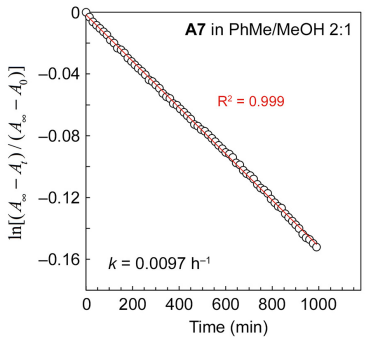

Figure S78. Kinetics of the thermal back-isomerization of free **A7** in 2:1 *v*/*v* PhMe–MeOH.

9.3. Synthesis of background ligand **B10**

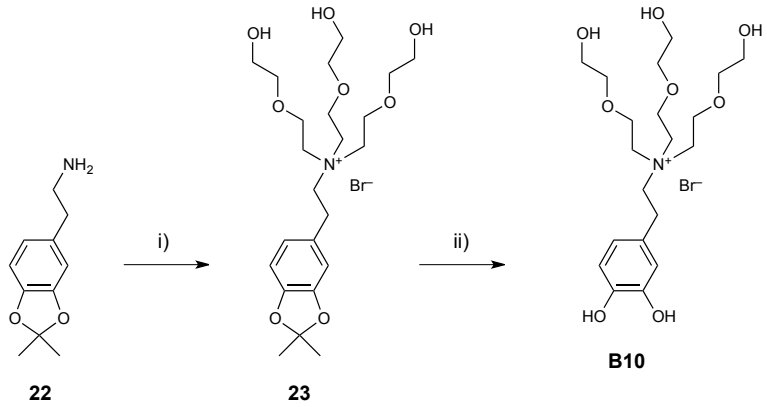

Scheme S9. Synthetic route for ligand **B10**. Reagents and conditions: i) 2-(2-bromoethoxy)ethanol, K_2CO_3, MeCN, reflux, 2d, 20%; ii) TFA, MeCN/$CHCl_3$, RT, 89%.

2-(2,2-dimethylbenzo[d][1,3]dioxol-5-yl)-*N*,*N*,*N*-tris(2-(2-hydroxyethoxy)ethyl)ethanaminium bromide (**23**): 2-(2,2-dimethylbenzo[d][1,3]dioxol-5-yl)ethanamine **22** (220 mg; 1.14 mmol; synthesized according to the procedure reported Ref. 15 and purified by silica gel column chromatography using 2→6% MeOH in DCM with 1% triethylamine) and 2-(2-bromoethoxy)ethanol (693 mg; 4.10 mmol; synthesized according to the procedure reported Ref. 16) were dissolved in 10 mL of acetonitrile in the presence of K_2CO_3 (315 mg; 2.28 mmol) and the mixture was refluxed for two days under nitrogen atmosphere. Then, the mixture was cooled to 4 °C, insoluble solids were removed by centrifugation and the supernatant was concentrated *in vacuo* (final volume ≈ 1 mL). Crude product was precipitated by the addition of 30 mL of 9:1 *v*/*v* Et_2O–EtOAc; it was washed with Et_2O (10 mL × 2) and dried to afford 120 mg of **23** (yield = 20%).

^{1}H NMR (500 MHz, D_2O): δ = 6.84–6.79 (m, 3H), 3.99 (bs, 6H), 3.85–3.83 (m, 6H), 3.74–3.70 (m, 8H), 3.65–3.64 (m, 6H), 3.11–3.07 (m, 2H), 1.70 (s, 6H). **^{13}C NMR** (125 MHz, D_2O): δ = 146.96, 145.76, 129.29, 121.79, 119.04, 109.25, 108.79, 71.93, 63.96, 61.76, 60.36, 59.44, 27.62, 24.61. **HRMS** calcd for $C_{23}H_{40}NO_8$ $[M-Br]^+$, m/z = 458.2754; found, 458.2737.

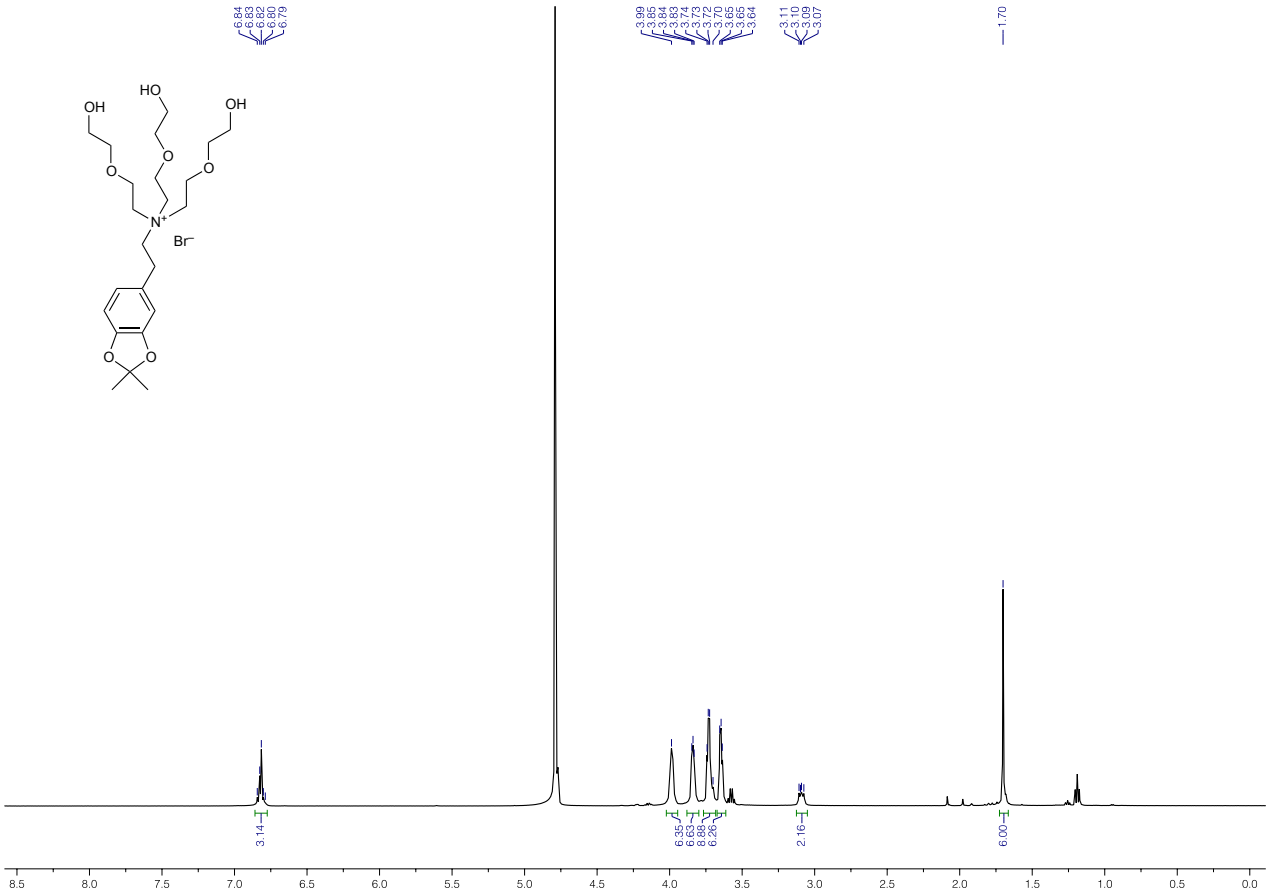

Figure S79. ^{1}H NMR spectrum of **23** (500 MHz, D_2O).

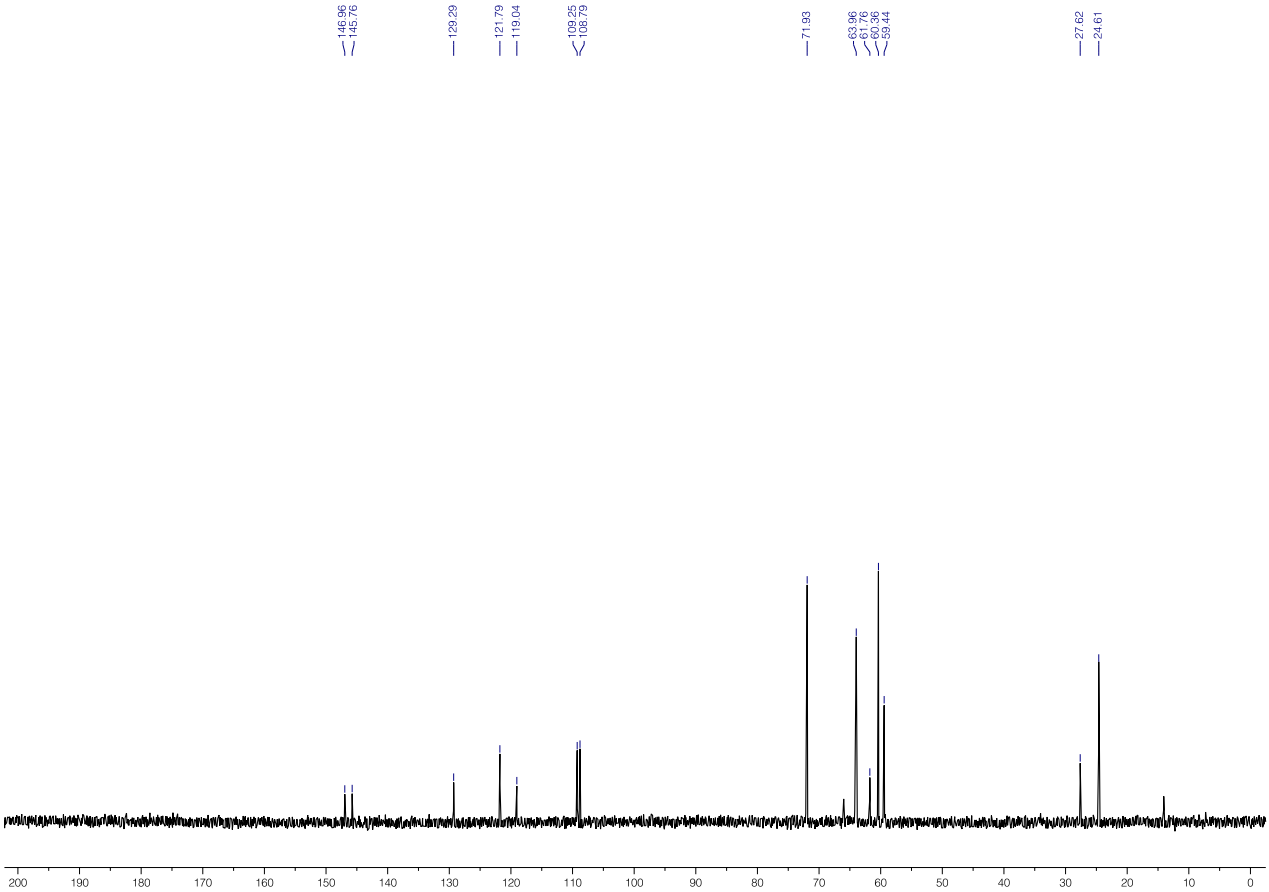

Figure S80. ^{13}C NMR spectrum of **23** (125 MHz, D_2O).

***N*-(3,4-dihydroxyphenethyl)-2-(2-hydroxyethoxy)-*N*,*N*-bis(2-(2-hydroxyethoxy)ethyl)ethanaminium bromide** (**B10**): A solution of **23** (53.8 mg; 1.00 mmol) in 1:5 *v*/*v* MeCN–$CHCl_3$ (6 mL) was degassed. Degassed trifluoroacetic acid (1.5 mL) was added and the reaction mixture was stirred for six hours at room temperature under nitrogen atmosphere. Then, the solvent was removed *in vacuo*, the crude product was dissolved in water (10 mL), and washed with 9:1 *v*/*v* Et_2O–EtOAc (5 mL × 2). Finally, the aqueous phase was freeze-dried to afford 43.8 mg of **B10** (yield = 89%).

^{1}H NMR (400 MHz, D_2O): δ = 6.91–6.71 (m, 3H), 3.98–3.96 (m, 6H), 3.83–3.81 (m, 6H), 3.73–3.68 (m, 8H), 3.64–3.62 (m, 6H), 3.05–3.00 (m, 2H). **^{13}C NMR** (100 MHz, D_2O): δ = 144.16, 143.04, 128.49, 121.12, 116.57, 116.45, 71.91, 63.93, 61.67, 60.37, 59.42, 27.17. **HRMS** calcd for $C_{20}H_{36}NO_8$ $[M-Br]^+$, m/z = 418.2441; found, 418.2414.

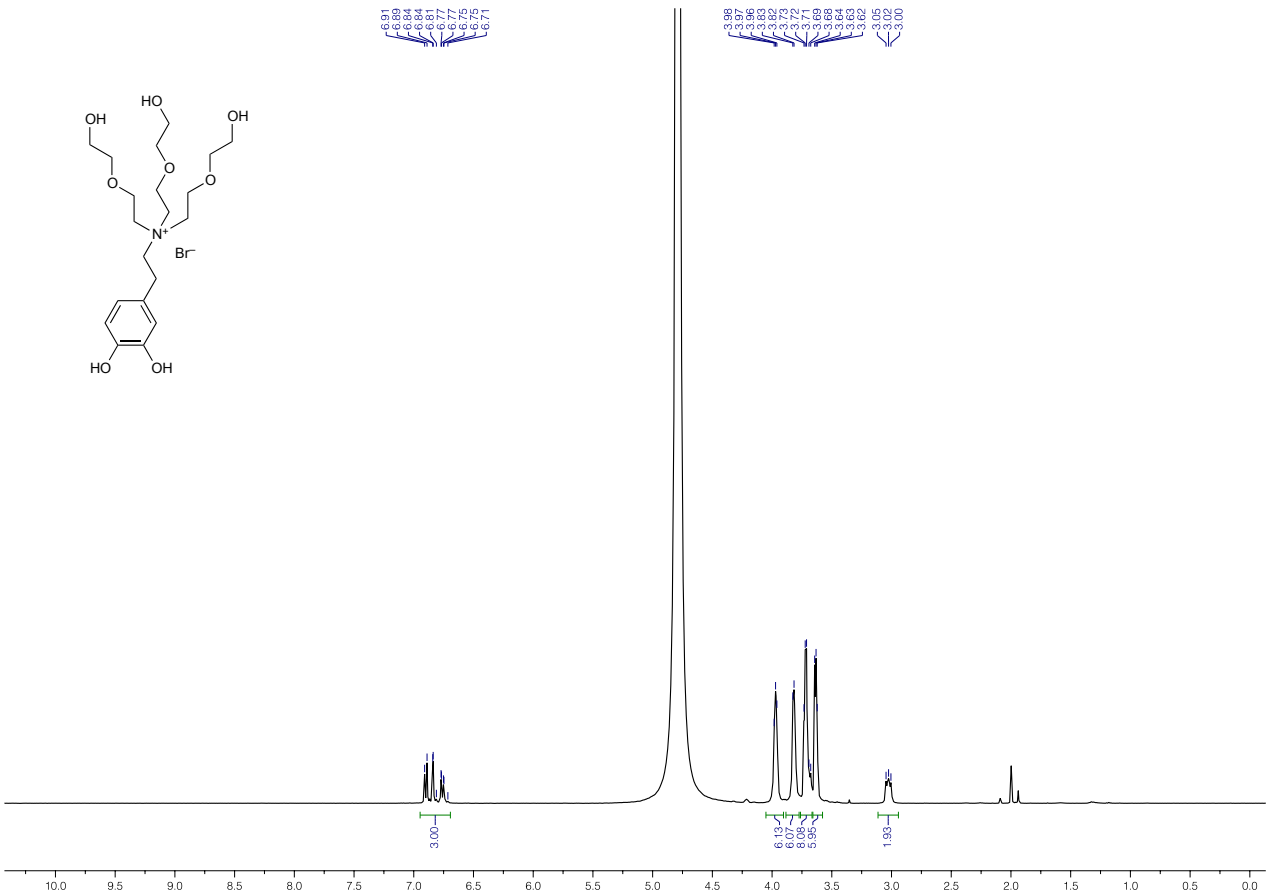

Figure S81. ^{1}H NMR spectrum of **B10** (400 MHz, D_2O).

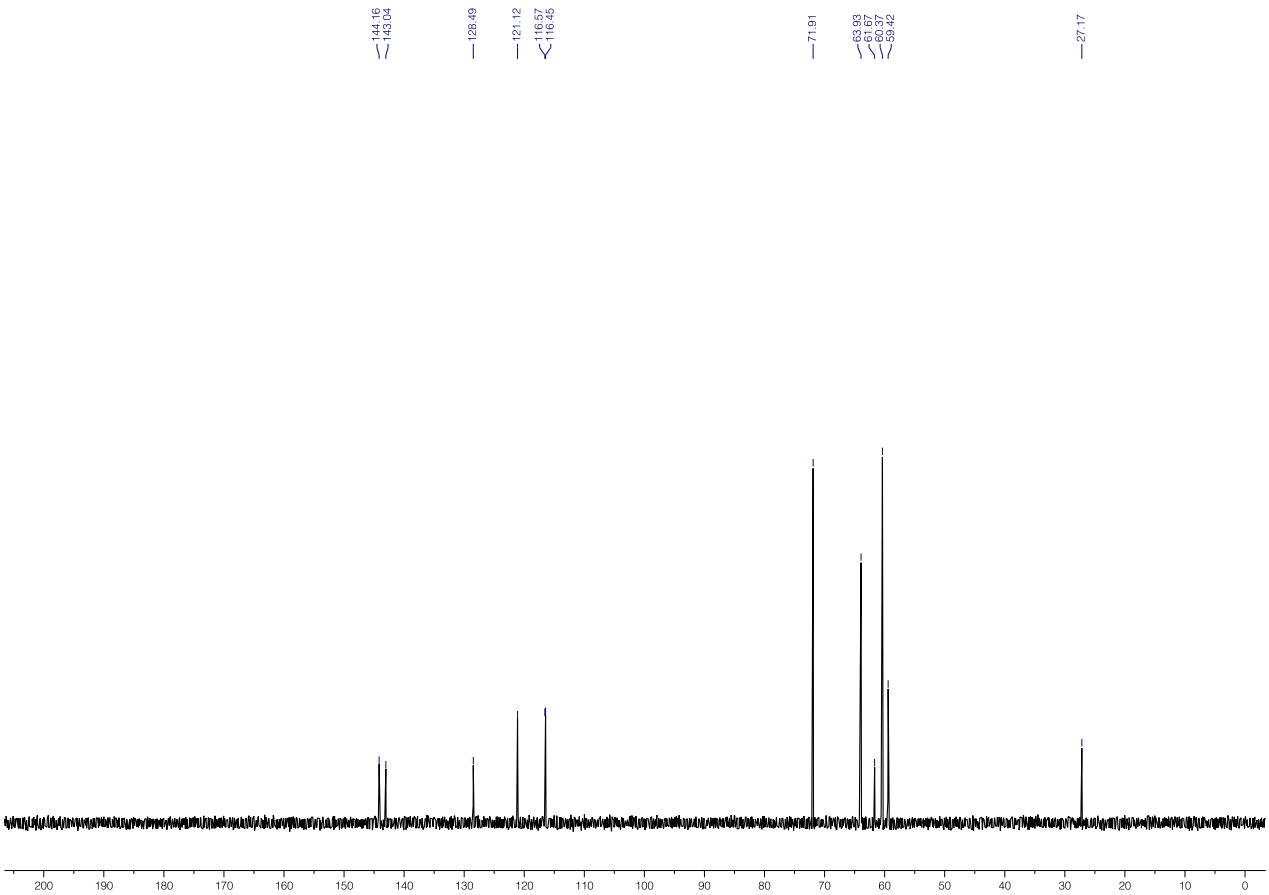

Figure S82. ^{13}C NMR spectrum of **B10** (400 MHz, D_2O).

9.4. Functionalization of 4.0 nm magnetite nanoparticles

Functionalization of magnetite NPs with a mixture of A7 and B10: A solution of 4.0 nm magnetite NPs (3.0 mg) in toluene (2 mL) was mixed with a solution of **A7** in THF (43.1 µL; *c* = 12.8 mM). The resulting solution was degassed by bubbling with argon and it was stirred at 45 °C under argon atmosphere for ten hours. Then, a solution of **B10** in degassed methanol (110 µL; *c* = 20 mM) was added and the mixture was stirred at 45 °C under argon atmosphere for an additional 14 hours. Next, additional aliquots of **A7** (43.1 µL; *c* = 10 mM in degassed THF) and **B10** (110 µL; c = 20 mM in degassed methanol) were introduced and the mixture was stirred at 45 °C under argon atmosphere for an additional six hours (**A7**/**B10**-functionalized Fe_3O_4 NPs precipitated from the solution). The solution was cooled down to room temperature; the solids were collected by centrifugation, dissolved in methanol (100 µL), precipitated with toluene (4 mL), collected by centrifugation, once again dissolved in methanol (100 µL), precipitated with toluene (4 mL), dried with a stream of nitrogen, and finally dissolved in 2 mL of methanol. The surface coverage of azobenzene on the resulting NPs, χ (determined by UV/Vis absorption spectroscopy) corresponded to ~0.10.

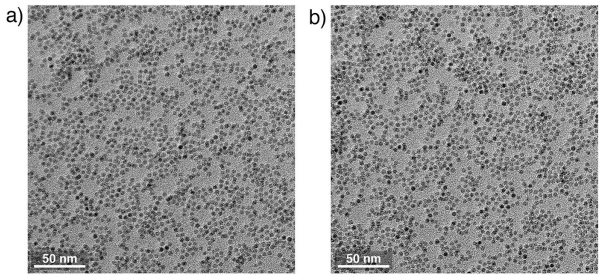

Figure S83. Representative TEM images of (a) 4.0 nm Fe_3O_4 NPs capped with oleic acid and (b) Fe_3O_4 NPs co-functionalized with a mixture of **A7** and **B10** ($\chi \approx 0.10$).

10. Molecular dynamics simulations

A thiolated gold nanoparticle with a diameter of 2.5 nm was modeled as an icosahedron[17-19] decorated with 91 ligands (14 thiolated azobenzenes **A*m*** and 77 background ligands **B*n***). We considered nine systems: *trans*-**A1**/**B1**-, *cis*-**A1**/**B1**-, *trans*-**A1**/**B3**-, *cis*-**A1**/**B3**-, *trans*-**A3**/**B1**-, and *cis*-**A3**/**B1**-, *trans*-**A5**/**B8**-, *cis*-**A5**/**B8**-, and *cis*-**A5**/**B9**-functionalized nanoparticle. The ligands were described by a force field used in our previous studies. Electric charges were calculated from the electrostatic potential fitting in the implicit solvent of water using GAUSSIAN 09.[20] The simulations were performed with NAMD[21] in the NPT ensemble (p = 1 bar and T = 300 K), using Langevin dynamics (γ_{Lang} = 1 ps^{-1}) with a time step of 2.0 fs. Initially, the simulated NPs were placed in water with counterions (in a box of 100×100×100 $Å^3$). The Particle Mesh Ewald (PME)[22] method was used for evaluating long-range Coulombic interactions. After 2,000 steps of minimization, the equilibration of the functionalized NPs lasted for ~10-20 ns. The hydrogen bond numbers were analyzed by VMD[23] with a cutoff distance of 4 Å and an angle of 60°. The distance between the NP center and the N=N moiety was averaged over all the ligands. The local number of water molecules was averaged over the last 5 ns.

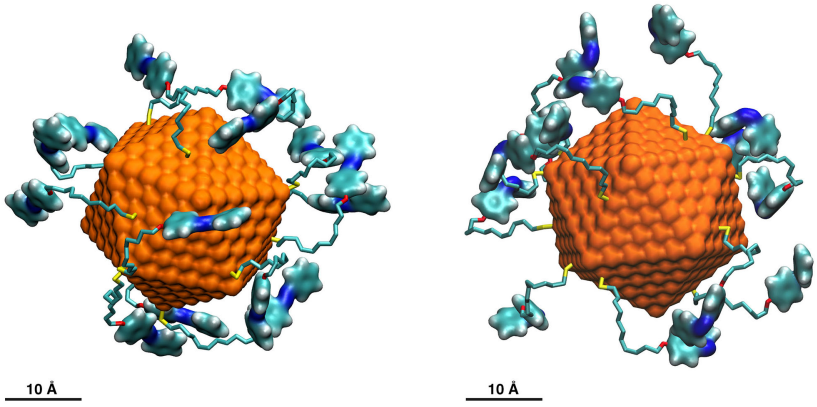

Figure S84. Snapshots from molecular dynamics (MD) simulations of a *trans*-**A1**/**B1**-coated 2.5 nm gold NP (left) and a *cis*-**A1**/**B1**-coated 2.5 nm NP (right) in water. Equilibration time = 20 ns. The images correspond to those shown in the main text's Figures 4a and b, respectively, except that background ligands **B1** were removed for clarity. Color codes: C, cyan; N, blue; O, red; S, yellow.

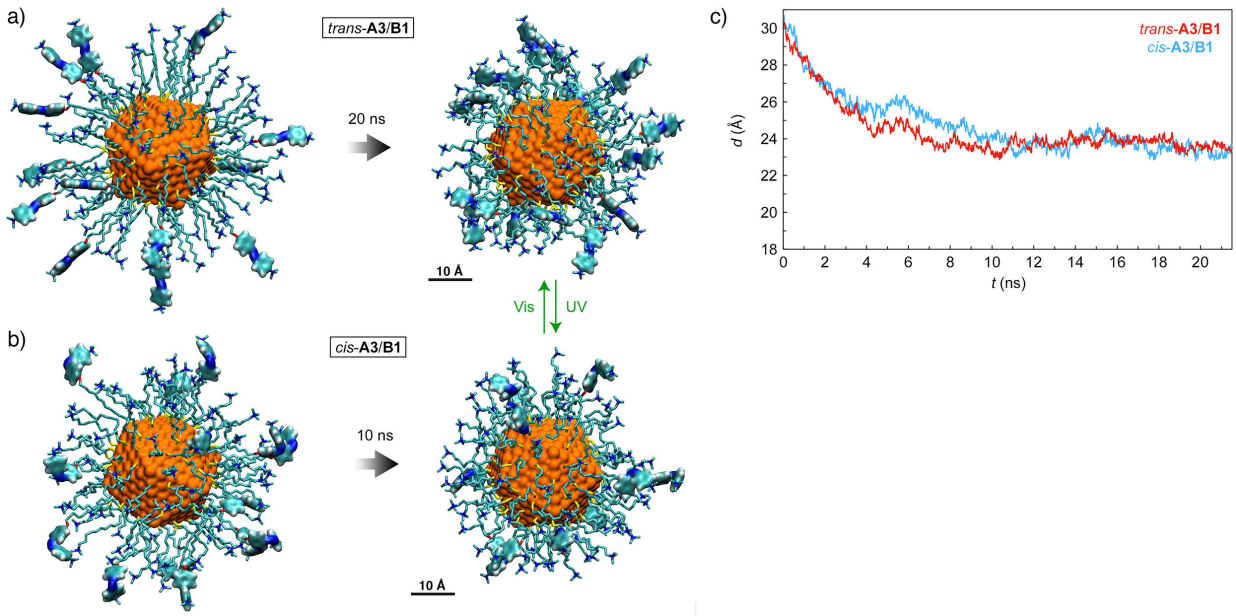

Figure S85. Snapshots from MD simulations of a *trans*-**A3**/**B1**-coated 2.5 nm gold NP (a) and a *cis*-**A3**/**B1**-coated 2.5 nm gold NP (b). (c) Average distance between the center of the NP and the center of mass of the N=N moiety of the *trans* (red) and *cis* (blue) isomer of **A3** as a function of time. Note that over time, the average distance in both cases equilibrates to ~23.5 Å, which is similar to the distance between *cis*-**A1**'s N=N moiety and the NP center, but considerably more than that between *trans*-**A1**'s N=N moiety and the NP center (compare with Figure 4c in the main text).

Analysis of conformational freedom of azobenzene in ligands containing oligo(ethylene glycol) vs. alkyl chains: We found that azobenzene **A2** co-adsorbed with background thiol **B6** undergoes the *cis*→*trans* back-isomerization faster (k = 0.053 h^{-1}) than when co-adsorbed with **B1** (k = 0.024 h^{-1}), which could be explained by the higher conformational flexibility of **B6**'s oligo(ethylene glycol) linker and consequently less congested environment. To substantiate this claim, we performed MD simulations of *cis*-**A2**/**B1**- and *cis*-**A2**/**B6**-functionalized 2.5 nm gold NPs and analyzed the position of the azobenzene group in time. To this end, we defined the root-mean-square deviation (RMSD) of the N=N moiety as,

$$\mathrm{RMSD} = \sqrt{\frac{\sum_{i=1}^{N_{\mathrm{atoms}}} (r_i(t_1) - r_i(t_2))^2}{N_{\mathrm{atoms}}}} \ ,$$

where N_{atoms} is the number of atoms whose positions are being compared (in our case, the two nitrogen atoms of the azo moiety), and $r_i(t)$ is the position of atom i in a three-dimensional space at time t. As t_2, we selected 10 ns as a time, at which equilibrium is most likely reached.

The results (Figure S86) confirm that the azobenzene group moves a larger distance (with respect to the 1-ns reference frame) in the presence of background ligand **B6**.

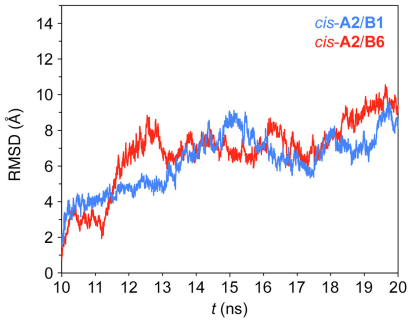

Figure S86. Root-mean-square deviation of the N=N moiety in *cis*-**A2** co-adsorbed on 2.5 nm Au NPs with **B1** (blue) and **B6** (red).

This reasoning is further confirmed by analyzing the distance of the azobenzene group in *cis*-**A2**/**B1**- vs. *cis*-**A2**/**B6**-functionalized 2.5 nm Au NPs from the surface of gold. As Figure S87 shows, the average distance between the center of mass of the N=N moiety and the surface of gold is smaller for **B6**, indicating that this background ligand offers more room for the azobenzene groups.

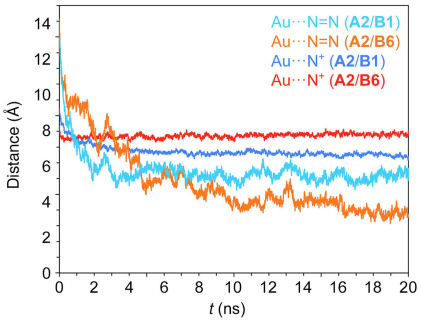

Figure S87. Average distance of the center of mass of **A2**'s N=N moiety from the surface of gold on *cis*-**A2**/**B1**-functionalized 2.5 nm Au NPs (cyan) vs. *cis*-**A2**/**B6**-functionalized 2.5 nm Au NPs (blue). For comparison, average distances between **B1**'s and **B6**'s ammonium N atoms and the gold surface are also plotted.

In Figure S89, we plotted the total number of atoms within an arbitrary distance (we selected 3 Å) of the **A2** ligands. It can be seen that *cis*-**A2** resides in a less congested environment on **A2**/**B6**-functionalized NPs compared with **A2**/**B1**-functionalized NPs.

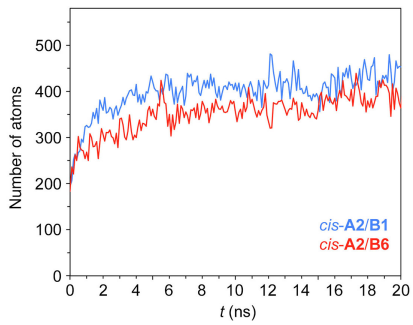

Figure S88. The total number of atoms present within 3 Å of **A2** ligands on an **A2**/**B1**- vs. an **A2**/**B6**-functionalized NP.

To verify that the different kinetics of back-isomerization in *cis*-**A2**/**B1**- and *cis*-**A2**/**B6**-coated Au NPs are not due to the different degrees of azobenzene aggregation, we analyzed the snapshots from the simulations at t = 20 ns (Figure S89). Indeed, we found that the aggregation was negligible in both cases (see also Figure S90).

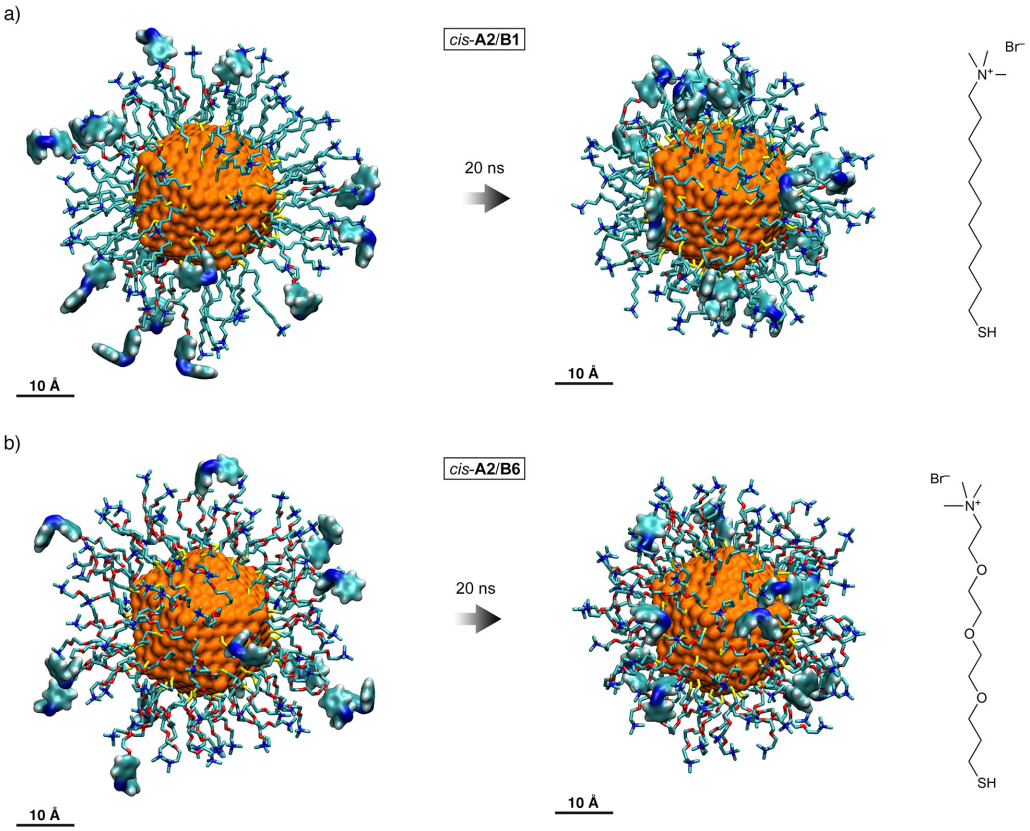

Figure S89. (a) Snapshots from MD simulations of a *cis*-**A2**/**B1**-coated 2.5 nm gold NP. (b) Snapshots from MD simulations of a *cis*-**A2**/**B6**-coated 2.5 nm gold NP.

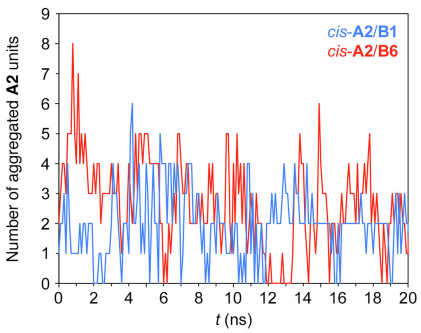

Figure S90. An attempt to quantify the aggregation of *cis*-**A2** on an **A2**/**B1**- vs. an **A2**/**B6**-coated 2.5 nm Au NP. An azobenzene group of an **A2** ligand is considered aggregated when there are at least six atoms of another **A2**'s azobenzene group within a distance of 4 Å.

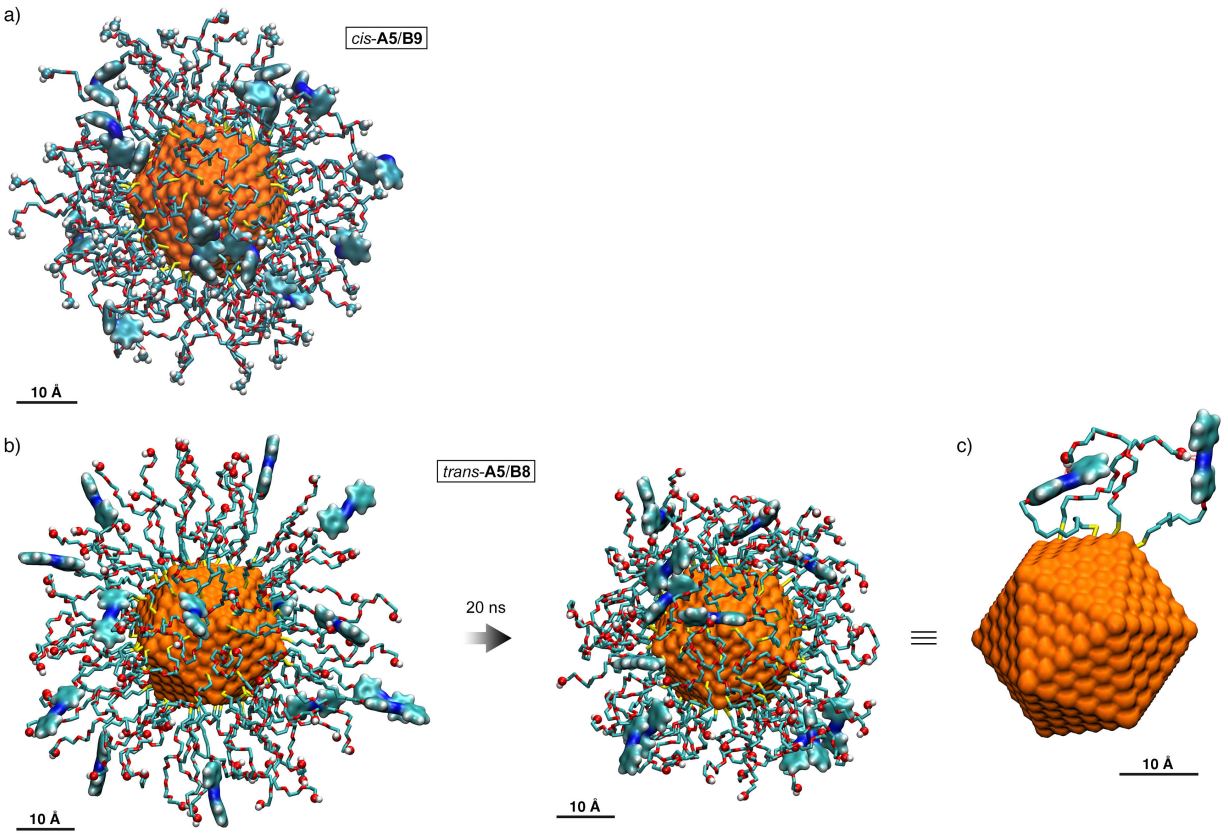

Figure S91. (a) Snapshot from MD simulations of a *cis*-**A5**/**B9**-coated 2.5 nm gold NP. (b), (c) Snapshots from MD simulations of a *trans*-**A5**/**B8**-coated 2.5 nm gold NP.

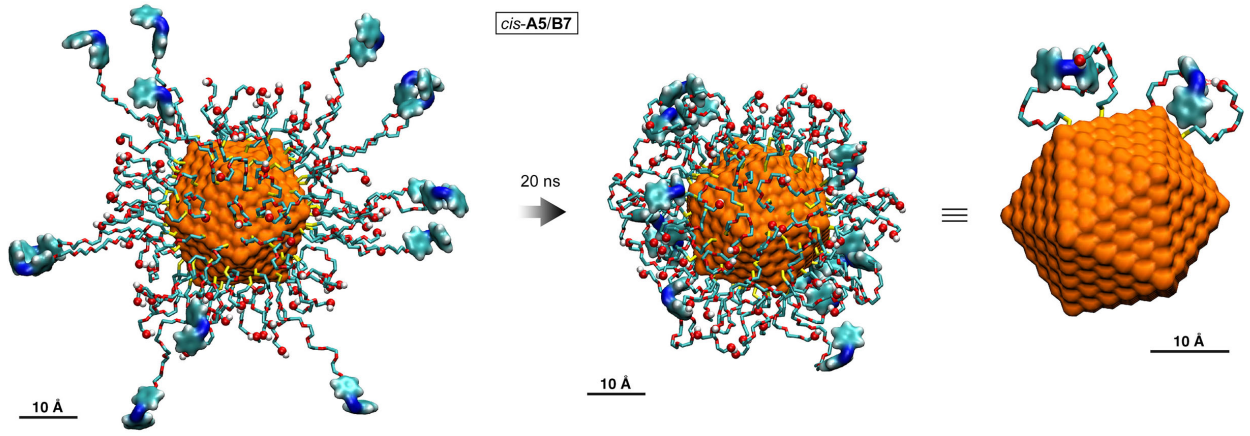

Figure S92. Snapshots from MD simulations of a *cis*-**A5**/**B7**-coated 2.5 nm gold NP.

11. Supporting movie captions

Supporting Movie 1: Simulation of a 5.5 nm gold NP co-functionalized with a densely packed binary monolayer of *trans*-**A1** and **B1** in water. In the first part of the movie, the system was allowed to relax for ca. 20 ns. In the second part of the movie, the relaxed NP is rotated about its vertical axis. In the third part of the movie, background ligands **B1** were removed for clarity.

Supporting Movie 2: Simulation of a 5.5 nm gold NP co-functionalized with a densely packed binary monolayer of *cis*-**A1** and **B1** in water. In the first part of the movie, the system was allowed to relax for ca. 20 ns. In the second part of the movie, the relaxed NP is rotated about its vertical axis. In the third part of the movie, background ligands **B1** were removed for clarity.

Supporting Movie 3: Simulation of a 5.5 nm gold NP co-functionalized with a densely packed binary monolayer of *trans*-**A1** and **B3** in water. In the first part of the movie, the system was allowed to relax for ca. 16 ns. In the second part of the movie, the relaxed NP is rotated about its vertical axis. In the third part of the movie, background ligands **B3** were removed for clarity.

Supporting Movie 4: Simulation of a 5.5 nm gold NP co-functionalized with a densely packed binary monolayer of *cis*-**A1** and **B3** in water. In the first part of the movie, the system was allowed to relax for ca. 16 ns. In the second part of the movie, the relaxed NP is rotated about its vertical axis. In the third part of the movie, background ligands **B3** were removed for clarity.

12. Supporting references

(1) Chovnik, O.; Balgley, R.; Goldman, J. R.; Klajn, R. Dynamically Self-Assembling Carriers Enable Guiding of Diamagnetic Particles by Weak Magnets. *J. Am. Chem. Soc.* **2012**, *134*, 19564–19567.

(2) Zhao, H.; Sen, S.; Udayabhaskararao, T.; Sawczyk, M.; Kučanda, K.; Manna, D.; Kundu, P. K.; Lee, J.-W.; Král, P.; Klajn, R. Reversible Trapping and Reaction Acceleration within Dynamically Self-Assembling Nanoflasks. *Nat. Nanotech.* **2016**, *11*, 82–88.

(3) Manna, D.; Udayabhaskararao, T.; Zhao, H.; Klajn, R. Orthogonal Light-Induced Self-Assembly of Nanoparticles using Differently Substituted Azobenzenes. *Angew. Chem. Int. Ed.* **2015**, *54*, 12394–12397.

(4) Yang, Y.; Velmurugan, B.; Liu, X.; Xing, B. NIR Photoresponsive Crosslinked Upconverting Nanocarriers Toward Selective Intracellular Drug Release. *Small* **2013**, *9*, 2937–2944.

(5) Jong, L. I.; Abbott, N. L. Rate-Dependent Lowering of Surface Tension during Transformations of Water-Soluble Surfactants from Bolaform to Monomeric Structures. *Langmuir* **1998**, *14*, 2235–2237.

(6) Chu, Z.; Han, Y.; Král, P.; Klajn, R. "Precipitation on Nanoparticles": Attractive Intermolecular Interactions Stabilize Specific Ligand Ratios on the Surfaces of Nanoparticles. *Angew. Chem. Int. Ed.* **2018**, *57*, 7023–7027.

(7) Zdobinsky, T.; Maiti, P. S.; Klajn, R. Support Curvature and Conformational Freedom Control Chemical Reactivity of Immobilized Species. *J. Am. Chem. Soc.* **2014**, *136*, 2711–2714.

(8) Strong, L.; Whitesides, G. M. Structures of Self-Assembled Monolayer Films of Organosulfur Compounds Adsorbed on Gold Single Crystals: Electron Diffraction Studies. *Langmuir* **1988**, *4*, 546–558.

(9) Rosales, A. M.; Mabry, K. M.; Nehls, E. M.; Anseth, K. S. Photoresponsive Elastic Properties of Azobenzene-Containing Poly(ethylene-glycol)-Based Hydrogels. *Biomacromolecules* **2015**, *16*, 798–806.

(10) Ruslim, C.; Ichimura, K. Spectroscopic and Thermal Isomerization Characteristics of 3,3'-Dialkoxy and Dialkanoyloxy Azobenzenes. *J. Mater. Chem.* **2000**, *10*, 2704–2707.

(11) Ho, S. F.; Mendoza-Garcia, A.; Guo, S.; He, K.; Su, D.; Liu, S.; Metin, O.; Sun, S. A Facile Route to Monodisperse MPd (M = Co or Cu) Alloy Nanoparticles and their Catalysis for Electrooxidation of Formic Acid. *Nanoscale* **2014**, *6*, 6970–6973.

(12) Sharma, S.; Kim, B.; Lee, D. Water-Soluble Pd Nanoparticles Capped with Glutathione: Synthesis, Characterization, and Magnetic Properties. *Langmuir* **2012**, *28*, 15958–15965.

(13) Ridelman, Y.; Singh, G.; Popovitz-Biro, R.; Wolf, S. G.; Das, S.; Klajn, R. Metallic Nanobowls by Galvanic Replacement Reaction on Heterodimeric Nanoparticles. *Small* **2012**, *8*, 654–660.

(14) Das, S.; Ranjan, P.; Maiti, P. S.; Singh, G.; Leitus, G.; Klajn, R. Dual-Responsive Nanoparticles and their Self-Assembly. *Adv. Mater.* **2013**, *25*, 422–426.

(15) Liu, Z.; Hu, B.; Messersmith, P. B. Acetonide protection of dopamine for the synthesis of highly pure *N*-docosahexaenoyldopamine. *Tetrahedron Lett.* **2010**, *51*, 2403–2405.

(16) Yeo, W.-S.; Min, D.-H.; Hsieh, R. W.; Greene, G. L.; Mrksich, M. Label-free detection of protein-protein interactions on biochips. *Angew. Chem. Int. Ed.* **2005**, *44*, 5480–5483.
(17) Heaven, M. W.; Dass, A.; White, P. S.; Holt, K. M.; Murray, R. W. Crystal Structure of the Gold Nanoparticle $[N(C_8H_{17})_4]$ $[Au_{25}(SCH_2CH_2Ph)_{18}]$. *J. Am. Chem. Soc.* **2008**, *130*, 3754–3755.
(18) Zhu, M.; Lanni, E.; Garg, N.; Bier, M. E.; Jin, R. Kinetically Controlled, High-Yield Synthesis of Au_{25} Clusters. *J. Am. Chem. Soc.* **2008**, *130*, 1138–1139.
(19) Mori, T.; Hegmann, T. Determining the Composition of Gold Nanoparticles: A Compilation of Shapes, Sizes, and Calculations using Geometric Considerations. *J. Nanopart. Res.* **2016**, *18*, 295.
(20) Frisch, M. J.; Trucks, G. W.; Schlegel, H. B.; Scuseria, G. E.; Robb, M. A.; Cheeseman, J. R.; Scalmani, G.; Barone, V.; Mennucci, B.; Petersson, G. A.; Nakatsuji, H.; Caricato, M.; Li, X.; Hratchian, H. P.; Izmaylov, A. F.; Bloino, J.; Zheng, G.; Sonnenberg, J. L.; Hada, M.; Ehara, M.; Toyota, K.; Fukuda, R.; Hasegawa, J.; Ishida, M.; Nakajima, T.; Honda, Y.; Kitao, O.; Nakai, H.; Vreven, T.; Montgomery, J., J. A.; Peralta, J. E.; Ogliaro, F.; Bearpark, M.; Heyd, J. J.; Brothers, E.; Kudin, K. N.; Staroverov, V. N.; Kobayashi, R.; Normand, J.; Raghavachari, K.; Rendell, A.; Burant, J. C.; Iyengar, S. S.; Tomasi, J.; Cossi, M.; Rega, N.; Millam, J. M.; Klene, M.; Knox, J. E.; Cross, J. B.; Bakken, V.; Adamo, C.; Jaramillo, J.; Gomperts, R.; Stratmann, R. E.; Yazyev, O.; Austin, A. J.; Cammi, R.; Pomelli, C.; Ochterski, J. W.; Martin, R. L.; Morokuma, K.; Zakrzewski, V. G.; Voth, G. A.; Salvador, P.; Dannenberg, J. J.; Dapprich, S.; Daniels, A. D.; Farkas, Ö.; Foresman, J. B.; Ortiz, J. V.; Cioslowski, J.; Fox, D. J. *Gaussian, Inc.* Wallingford, CT, 2009.
(21) Phillips, J. C.; Braun, R.; Wang, W.; Gumbart, J.; Tajkhorshid, E.; Villa, E.; Chipot, C.; Skeel, R. D.; Kalé, L.; Schulten, K. Scalable Molecular Dynamics with NAMD. *J. Comput. Chem.* **2005**, *26*, 1781–1802.
(22) Darden, T.; York, D.; Pedersen, L. Particle Mesh Ewald: An N·log(N) Method for Ewald Sums in Large Systems. *J. Chem. Phys.* **1993**, *98*, 10089–10092.
(23) Humphrey, W.; Dalke, A.; Schulten, K. VMD: Visual Molecular Dynamics. *J. Mol. Graph. Model.* **1996**, *14*, 33–38.